STUDIES IN SOLID–SOLID REACTIONS

A THESIS SUBMITTED TO THE

UNIVERSITY OF POONA

FOR THE DEGREE OF

DOCTOR OF PHILOSOPHY

IN CHEMISTRY

BY

SATISH S. TAMHANKAR

M. Sc.

NATIONAL CHEMICAL LABORATORY

POONA - 411 008 (India)

January 1978

ACKNOWLEDGEMENT

I am grateful to Dr. L. K. Doraiswamy, Head of the Chemical Engineering and Process Development Division, National Chemical Laboratory, Poona, for his inspiring guidance and kind encouragement throughout the course of this work.

I am indebted to the Council of Scientific and Industrial Research for the award of a research fellowship and to the Director, National Chemical Laboratory, for permitting me to submit this work in the form of a thesis.

My sincere thanks are due to the Director, Defence Metallurgical Research Laboratory, Hyderabad, for allowing me to use the electron probe microanalyser, and to Mr. R. Natarajan for carrying out the analysis of samples.

Finally, I utilise this opportunity to thank Dr. V. S. Patwardhan for useful discussions and the staff members as well as my colleagues for their cheerful co-operation.

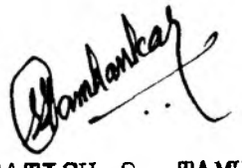

(SATISH S. TAMHANKAR)

JANUARY 1978

SUMMARY

Solid-solid reactions have usually been the domain of physicists and physical chemists. As such, much of the work reported on these reactions has been of a fundamental nature, such as thermodynamic and transport considerations. Theories of diffusion have been especially well developed and established, but relatively little is known about the reaction counterpart. Thus, the physics of the processes has been studied in great detail, but less is understood about the chemical interactions occurring simultaneously. Solid-solid reactor design has therefore tended to remain a totally empirical art.

Solid-solid reactions are of great industrial importance as exemplified by the cement industry and the manufacture of refractories, catalysts, and magnetic and electronic materials. Yet, there are only a few attempts reported in the literature on the analysis of these reactions which can form a rational basis for the design of reactors for carrying out solid-solid reactions.

A major objective of the present work is to bring solid-solid reactions within the overall purview of chemical reaction engineering. Analysis of these reactions has been attempted from this view point. Consequently an analogy

is suggested between solid-solid and gas-solid (noncatalytic) reactions.

This being probably one of the first attempts in this direction, many simplifying assumptions have been made to focus attention on the principal features involved. To start with, the simple case of one-way diffusion is considered. The various assumptions made and their validity are discussed in appropriate places. The following aspects of solid-solid reactions are considered.

(1) Review and appraisal of the literature on solid-solid reactions: Although in recent years a few significant studies have been reported in the literature on solid-solid reactions, no comprehensive article has yet appeared which seeks to cover the various aspects of these reactions with particular emphasis on analysis. Hence, the first chapter is devoted to a critical appraisal of the present state of analysis along with other important aspects of these reactions.

(2) Analysis of pellet-pellet reactions based on a reaction zone model: This is essentially an artificial situation, but has the merit of providing a clear insight into the relative roles of diffusion and reaction. The major purpose of this analysis is to bring out the importance of the reaction zone, in the analysis of which the steady state

assumption has been made. The results have been tested with some of the reported data obtained by electron probe microanalysis (EPMA).

(3) Rigorous analysis of the reaction zone: A more rigorous analysis is attempted in this chapter, taking into consideration the basic unsteady nature of its formation. In addition, no a priori assumption is made regarding zone width which is permitted to extend to the limit of the solid. However, a finite reaction zone has been observed experimentally, an observation which has been used in the preliminary steady state analysis presented in Chapter 2. In the present chapter, while no assumption regarding a finite zone thickness has been made in the solution of the equation, the appearance of a finite zone has been explained on the basis of the limit of detectability of the EPMA instrument. A method has been proposed for the estimation of diffusivity and rate constant, and the well known parabolic growth rate law is discussed.

(4) Experimental studies on the pellet-pellet system CuO-Fe_2O_3: Results are obtained on the pellet-pellet system CuO-Fe_2O_3, and the data are tested with the models developed above.

(5) Analysis of mixed powder reactions: The methodology used in the treatment of pellet-pellet reactions

is extended to formulate a general model for mixed powder reactions. The procedure suggested is tested by analysing some of the reported data on mixed powder reactions.

(6) Experimental studies on an industrially important solid-solid system Si-CuCl: The system is studied under mixed powder conditions. Kinetic studies indicated the autocatalytic nature of this reaction. The data are analysed from this view point, and effects of various parameters discussed.

A brief description is given below of each of the six facets of solid-solid reactions considered in this study.

(1) Solid-solid reactions: review and appraisal

Diffusion in solid-solid systems has been extensively studied. Some of the recent developments also consider diffusion and reaction in solid-solid systems. However, the literature on the analysis of solid-solid reactions is scanty. Hence, in this chapter the relevant literature is critically reviewed and the important aspects have been highlighted. With major emphasis on analysis, the following topics have been discussed: (1) fundamental considerations, (2) experimental techniques, (3) analysis of pellet-pellet reactions, (4) analysis of mixed powder reactions, (5) role of the gas phase, and (6) reactor development. Examples of

industrial applications, important systems studied, and the mathematical models used, are tabulated.

(2) Diffusion and reaction in pellet-pellet systems

To facilitate analysis, solid-solid reactions are studied by carrying out reaction between cylindrical pellets of two reactants kept in surface-to-surface contact. Diffusion in such systems has been extensively studied so far, but relatively little attention has been given to the reaction occurring therein. In the present analysis a reaction zone is postulated within a reactant, wherein the other reactant species diffuses and reacts simultaneously. The steady state mass balance equation for such a case is solved with proper boundary conditions. The final expression obtained for the concentration profile in this zone involves two important parameters: (i) reaction zone thickness and (ii) Thiele modulus, a dimensionless group incorporating diffusivity and the reaction rate constant.

Steady state has been assumed for the sake of simplicity, so that the reaction zone thickness would depend only on the Thiele modulus. An approximate expression has been obtained relating these two parameters, and the concentration profiles predicted have been shown to match with the reported experimental profiles, with a maximum

deviation of 6%. Data obtained by EPMA on the following systems were used for testing the model: $MgO-Cr_2O_3$, $MgO-Fe_2O_3$, and $NiO-Al_2O_3$.

In the above analysis, first-order reaction was considered, and this assumption has been found valid while verifying the model. For the sake of generality, the treatment has been extended to the case of an nth order reaction. An expression correlating the Thiele modulus, reaction zone thickness and order of reaction has been obtained.

(3) An analysis of the reaction zone

With the primary objective of establishing the model, the above analysis pertained to steady state in the reaction zone. Also the treatment provided only predictive equations; knowledge of precise values of diffusivity and rate constant is desirable for a more rigorous test of the model. This is provided by the unsteady state behaviour of the reaction zone considered here. This consideration emerged out of a scrutiny of a few reported studies, wherein reaction zone thickness was found to change slowly with time.

Solution of the problem has been obtained by assuming a concentration profile extending to an infinite distance. The appearance of a finite reaction zone has then

been explained based on the limit of detectability of the EPMA instrument. Thus, after a certain finite distance, the concentration of the species being too low cannot be detected by the instrument, and a finite zone appears.

Based on the above analysis, a method has been formulated for the estimation of diffusivity and rate constant. The estimated values can then be used to predict concentration profiles under a given set of conditions. The method could not be tested, however, due to lack of reported experimental data accessible to such an analysis.

Finally, the well known parabolic growth rate law, often used in solid-solid reactions studies, has been examined in the light of the above development. It has been shown mathematically that under certain conditions this law, formulated on the basis of diffusion control in the product layer, can also be consistent with diffusion-cum-reaction control in the reaction zone considered here. Further, it has been pointed out that the validity of the law can sometimes be a misinterpretation. Thus, the danger in using this law for discerning the controlling mechanism has been highlighted.

(4) Experimental studies on the pellet-pellet system $CuO-Fe_2O_3$

The system copper oxide-iron oxide was studied in the

pellet-pellet form, and analysed using EPMA. Experiments were carried out with sintered pellets of the two kept in contact at 950°C. The reacting couple was taken out at different times and quenched in air. Samples were prepared for EPMA by encapsulating in Araldite moulds, and concentration profiles of Cu and Fe were obtained. The results indicated (i) absence of diffusional resistance in the product layer, and (ii) one-way diffusion, that of Cu.

Using the experimental data obtained, concentration profiles were predicted. These matched well with the experimental profiles. The reaction zone thickness showed variation with time, indicating unsteady state behaviour. The corresponding model could predict concentration profiles that matched better with the experimental profiles. The diffusivity and rate constant values obtained were in the range usually encountered in solid-solid reactions.

(5) Analysis of mixed powder reactions

Analogy between solid-solid and gas-solid (non-catalytic) reactions has been brought out more clearly by introducing the concept of a hypothetical particle. Different controlling regimes are then considered, and a conversion-rate expression has been derived for each of them. A procedure has been outlined for a systematic analysis of

data on mixed powder reactions. This has been tested with data on a few reported systems ($ZnO-Fe_2O_3$, $ZnO-Al_2O_3$, phthalic anhydride-p-nitroaniline).

(6) Studies on an industrially important solid-solid system Si-CuCl

A number of mixed powder reaction studies amongst oxides have so far been reported in the literature. With a view to studying a different but industrially important reaction, the system Si-CuCl was chosen. This appears as an important step in the manufacture of chlorosilanes.

Experiments were carried out with mixed powders of ferrosilicon (the commercial source of silicon) and cuprous chloride under various conditions. The results suggested that this system represents a typical autocatalytic solid-solid reaction. In each case, the rate maximum was observed typically at $\alpha < 0.5$. Necessary rate expressions have been developed based on its autocatalytic nature. Activation energies for the two rate constants, noncatalytic (k_o) and autocatalytic (k''_{ac}), have been obtained. Change in k_o with temperature showed a typical trend, which has been explained based on a shift in the controlling mechanism. The reaction was carried out under conditions of kinetic control.

Effects of various parameters, such as particle size

of ferrosilicon, reactant ratio, and additives, has been discussed. Zinc added in small quantities was found to accelerate the reaction. A similar effect was observed when fresh copper formed in the reaction was added; commercial fine copper powder had no effect.

CONTENTS

CHAPTER 1

SOLID-SOLID REACTIONS: REVIEW AND APPRAISAL

1.1 INTRODUCTION

Solid-solid reactions have been carried out since as early as the beginning of the twentieth century. The manufacture of refractories and ceramics, one of the olden arts, utilises solid-solid reactions extensively. Other industries like cement and electronics also employ solid-solid reactions. The manifold applications of these reactions in the now ever expanding electronics industry are well known. Another important area of application of solid-solid reactions is catalyst development. The various areas of application of solid-solid reactions, along with the mode of application, are summarised in Table 1.1.

One of the first to realise the importance of solid-solid reactions was Pukall (1914) who prepared a number of compounds, which were otherwise not possible to prepare before. His work was followed by that of Hedvall. An extensive list of such compounds along with the raw materials and reaction temperatures has been presented by Singer and Singer (1971).

Though solid-solid reactions were thus practised

TABLE 1.1

Examples of Industrial Applications of Solid-Solid Reactions

No.	Field of application	Nature of application/reaction	Reference(s)
1	2	3	4
1	Ceramics	Manufacture of ceramic and refractory materials; also small quantities of certain compounds, added to improve the properties, react in the solid state.	Kingery (1967) Singer and Singer (1971)
2	Oxide semiconductors and ferrites	Manufacture (and doping).	Sittig (1970)
3	Cement production	In the dry manufacturing process the components react in the solid state. Typically, in the $MO-SiO_2$ and $MO-Al_2O_3$ systems (M=Ca, Mg, etc.), a number of product phases are formed and proper conditions are to be chosen to get desired compositions.	Lea (1970)
4	Catalyst preparation	Mixed oxide catalysts, which are known to be very selective, are some times prepared in the solid-state.	Naidu *et al* (1973) Bleijenberg *et al* (1965) Stork and Pott (1974)

TABLE 1.1 (continued)

1	2	3	4
5	Metallurgy	(i) Preparation of solid solutions and alloys.	Shamsuddin and Prasad (1977)
		(ii) Reduction of ores, e.g. iron ore (hematite) by coke.	Ray (1974)
6	Polymer chemistry	(i) Polymerisation in the solid state	Voigt-Martin (1974)
		(ii) Preparation of large polymer single crystals.	Baughman (1974)
7	Fertilizers	The compounds react in the solid state during processing, as well as when fed to the soil.	Adhya et al (1974) Srinivasa et al (1973)
8	Drugs	If the adjuvents present in the drugs react with the active ingredients, stability of the drug is affected leading to storage problems.	Tarjányi et al (1971)
9	Spacecraft thermal control	Heat sources required in spacecraft most conveniently use solid-solid exothermic reactions.	Riebling (1969)

TABLE 1.1 (continued)

1	2	3	4
10	Organic chemistry	Useful in controlling the rate, isomer distribution and steriochemistry of organic compounds, e.g.	Pimentel (1958) Cohen and Schmidt (1964)
		(i) transcinnamic acid dimerises only in the solid state,	
		(ii) disproportionation reactions (terephthalic acid synthesis)	Gokhale *et al* (1975)
11	Inorganic pigments	A number of inorganic pigments, such as basic silicate, white lead, lead zinc oxides etc. are prepared by solid-solid reaction. The partial conversions desired in certain cases can be achieved by solid-solid reactions only.	Kirk and Othmer (1968)
12	Inorganic complexes	Preparation of some inorganic complexes which could not otherwise be prepared.	Gentile and Mao (1965) Gentile and Campisi (1965) Gentile and Shankoff (1965) Gentile *et al* (1967) Rastogi and Dube (1967)

earlier, modelling of these reactions started much later. Jander (1927) for the first time presented a mathematical analysis of solid-solid reactions. Though it involved a number of assumptions, it had the merit of being the first of its kind. Later, Jander's model was modified and developed further by a number of workers. All these models provide conversion-time relationships for mixed powder systems. Various such models and their applications will be discussed subsequently.

Studies on solid-solid reactions have been carried out either with mixed powders or with pellets of well defined geometries. Although mixed powder reactions are of greater practical interest, for an understanding of these reactions studies on pellet-pellet systems appear to be necessary. These studies are aimed at elucidating transport mechanisms and to gain insight into the phenomenon of coupled diffusion and reaction. This important aspect of solid-solid reactions will be discussed separately.

A few review articles have appeared in the literature from time to time (e.g. Feigl *et al*, 1944; Cohn, 1948; Rose, 1961; Parravano, 1962; Yoganarsimhan, 1970; Rastogi, 1970). The older of these articles are of limited use since recent developments have not been included, while the newer ones tend to be specific and limited in scope.

Solid-state reactions, in general, include reactions in which at least one of the phases is a solid. Thus a variety of reactions, gas-solid, solid-solid, decomposition, transformation, etc., are grouped under the title of solid-state reactions. Solid-solid reactions further consist of three types of reactions : addition, addition by elimination and exchange. The present work is restricted to solid-solid addition reactions; mention of the other types will be made wherever it is felt relevant.

Emphasis will be placed on the analysis of solid-solid reactions; but other aspects of these reactions, such as thermodynamics, diffusion, and experimental techniques, will also be discussed. Finally the progress in reactor development will be briefly surveyed.

1.2 FUNDAMENTAL CONSIDERATIONS

Two approaches can be employed towards the understanding of solid-solid reactions : (i) based on the thermodynamic behaviour of the systems, which is more or less a gross approach; and (ii) based on molecular energy levels, which has received relatively little attention. It should be emphasised that in a solid-solid reaction, the immobile product layer formed may offer a barrier to the progress of the reaction. It is essential that either or both the reactants should diffuse through this layer as well

as through the other reactant and react. This calls for a consideration of diffusion in solids.

1.2.1 Thermodynamic considerations

For any reaction to occur, it has to be favoured thermodynamically. In solid-solid reaction systems, the chemical potentials and activities of the reactants and products are constant throughout the reaction and so is the free energy difference ΔG. Consequently, solid-solid reactions never reach equilibrium. Often such a reaction reaches an apparently constant conversion because of the strong diffusional resistance offered by the immobile product layer formed between the reactants.

A brief reference to certain important aspects of thermodynamic parameters as they apply to solid-solid reactions appears relevant here. The use of these parameters in formulating the kinetics will be brought out in Section 1.4.3.

The free energy change ΔG of a reaction can be expressed as

$$\Delta G = \Delta H - T\Delta S \qquad (1.1)$$

It has been observed that for many solid-solid reaction systems, the entropy contribution to the free energy change

of reaction is very small. This is because most of the reactions consist mainly of lattice rearrangements. Obviously, order-disorder changes contribute little to the reaction, so that

$$\Delta G \approx \Delta H \qquad (1.2)$$

This has been conceptually explained by Duncan and Stewart (1967) who applied statistical mechanics to correlate the disorder entropy with the occurence of the most probable lattice rearrangement. Their calculations of the values of ΔG, ΔH and ΔS from the experimentally observed rate constants also support the assumption in Equation 1.2.

Novrotsky and Kleppa (1968) have in fact found a constant value of $\Delta H \approx -10$ kcal/mole for all the spinel formation reactions on the basis of the experimental investigations on a variety of systems. Since most of the spinel formation reactions are lattice rearrangements, the difference in lattice energies of the products and reactants should also give the enthalpy of formation. Here again a value of $\Delta H \approx -10$ kcal/mole was obtained by Miller (Navrotsky and Kleppa, 1968). There are also instances where ΔH is considerably different from this value. This has been attributed to the structural differences and the site preference characteristics of cations. These differences

also affect the reactivity of compounds (Stone and Tilley, 1965).

Values of different thermodynamic parameters have also been reported by Rastogi *et al* (1963) in their studies on a number of organic solid-solid reactions.

An interesting method of calculating thermodynamic parameters, particularly the free energy of formation, is from the emf measurements at high temperatures of a solid cell consisting of the reactants and a solid electrolyte in the form of pellets (Kröger, 1974; Toropov and Barzakovskii, 1966). This method is now widely used for obtaining the free energy values of solid-solid reactions.

1.2.2 Energetics

The energetics of solid-solid reactions has not so far been studied, a notable exception being the work of Melton (1971) who developed a theory to describe the initiation of chemical reactions in solids.

It is well known that of the four modes of energy, viz. translational, rotational, vibrational and electronic, a solid (being a rigid body) possesses mainly the vibrational energy. Obviously, the initiation of a reaction in a solid is via the excitation of the vibrational energy levels of the

individual molecules. Melton has assumed that lattice vibrations in a solid can be treated as pseudo collisions between the individual molecules in the lattice. Thus, the solid is treated as an ordered dense gas. Chemical reactions in solids are then explained by the collision theory developed for gases. The treatment finally results in the following expression for the rate constant:

$$k = \frac{P_{i \rightarrow f}\ \bar{v}}{\sqrt{2}\ bN_a} \qquad (1.3)$$

where b is the lattice spacing, N_a the number of atoms in the molecule, $P_{i \rightarrow f}$ the probability that one of the collision partners will undergo a transition from the initial to a final state, and $\bar{v}$ the mean molecular velocity. Though the development is remarkable, especially since this particular approach is still quite new, the results are of qualitative interest only. This is mainly because of the mathematical difficulties in calculating $P_{i \rightarrow f}$.

The probabilistic theory developed by Waite (1957a, 1958, 1960) which is described in Section 1.5.1 may be referred to in this connection, wherein the probability of approach of the reaction partners which are randomly distributed is considered and a distance x_o is defined within which they react.

Since in solid-solid reactions the basic problem is that of energy transfer between different modes of vibrations, it may be interesting to study the problem from the view-point of statistical thermodynamics, wherein vibrational energy and partition function are defined based on the fundamental properties of the molecules, and the equilibrium constant for a reaction is then defined in terms of partition functions. This, however, needs an elaborate treatment.

1.2.3 Diffusion

Most of the solid-solid reactions are considered to be diffusion-controlled. Three diffusivities are involved in a solid-solid reacting system: self diffusivity, diffusivity of a reactant through the product layer and its diffusivity in the other reactant.

Self-diffusion has been studied in greater detail, mostly using the well known technique of radioactive tracers. However, a solid-solid reaction is not known to be influenced by self-diffusion. An exceptional case has been reported by Schwab *et al* (1961) who concluded that the exchange reaction,

$$CuO + ZnSO_4 \longrightarrow CuSO_4 + ZnO$$

is self-diffusion controlled. However, as stated earlier, our concern here is mainly with the addition type of solid-solid reactions. As such, self-diffusion studies need not be given much attention.

Since most of the solid-solid reactions are considered diffusion-controlled, the equations derived so far consider only this aspect of the reaction. But surprisingly all such studies have been restricted to diffusion of reactants through the product layer, and only in a very few cases has diffusion of a reactant into the other reactant been given any thought. This point will be pursued in greater detail in Section 1.4.3.

It is worthwhile mentioning a drawback of the diffusivity studies, which can be of vital importance. Diffusivities are generally obtained from separate experiments conducted with one of the reactants and the product both in pellet form, kept in contact. In all such studies, the product is synthesised independently by a known method. This would have its own definite stoichiometry, lattice structure, defect characteristics and impurity concentration. The product formed during reaction, on the other hand, may have very different characteristics. Consequently the diffusivities in the two cases may be different since diffusion in polycrystalline solids is known to be influenced by these factors.

An example illustrating this fact is the difference in the diffusivity values reported by Tomás *et al* (1969) and by Arrowsmith and Smith (1966) for the system, phthalic anhydride + sulphathiazole. The values reported by Arrowsmith and Smith from independent diffusion experiments are of the order of 10^{-7} - 10^{-8} cm^2/sec, whereas those reported by Tomás *et al* from *in situ* evaluation during reaction and analysed by the Serin-Ellickson expression (see section 1.5.1) are of the order of 10^{-11} cm^2/sec.

Moreover, the structure of the product formed between reactant phases is different as exemplified by Schmalzried and Rogalla (1963) for the system,

$$Al_2O_3 \text{ (single crystal)} + NiO \text{ (powder)} \rightarrow NiAl_2O_4$$

The product phase formed between the reactants was polycrystalline on the NiO side but single crystal on the Al_2O_3 side.

Studies on diffusion in solids are thus complicated by many factors, like grain boundaries, electroneutrality conditions, Kirkendall effect of mass flow, sintering, etc.

The principal methods of analysis used in diffusion studies are described below. Only the salient features germane to the purpose are discussed.

Interdiffusion

Interdiffusion studies mainly refer to the diffusion of a reactant in the product layer. But recently such studies have also been extended to diffusion of a reactant into the other reactant. However, reaction occurring simultaneously is neglected in all such studies. This will be brought out more clearly in Section 1.4.3.

In a binary reaction system, when both the cations diffuse in opposite directions, it is impossible to find the individual diffusivities. Hence what is called an interdiffusion coefficient, generally denoted by $\tilde{D}$, is defined. Determination of $\tilde{D}$ is quite difficult because of the complexity introduced by its dependence on concentration. The differential equation involved is

$$\frac{\partial C}{\partial t} = \frac{\partial}{\partial x}\left(D \frac{\partial C}{\partial x}\right) \qquad (1.4)$$

which may be solved by the Boltzmann-Matano method (see Shewmon, 1963). This method has been applied to NiO-MgO and NiO-CaO systems by Apple and Pask (1971).

Wagner (1969) developed a theory for counterdiffusion of cations through the product layer, where he obtained the individual fluxes of the two based on chemical potential

gradient, the respective valencies, activity coefficients and transport numbers. The interdiffusion coefficient $\tilde{D}$ has been defined as

$$\tilde{D} = \frac{\bar{N}_1 \bar{N}_2 (v_1 - v_2)}{\partial \bar{N}_2 / \partial x} \qquad (1.5)$$

where $\bar{N}_1$ and $\bar{N}_2$ are the mole fractions of the two species and v_1 and v_2 their velocities. The final expression obtained is:

$$\tilde{D}(\bar{N}_2^*) = \frac{(\bar{N}_2^+ - \bar{N}_2^-)\, V_m(\bar{N}_2^*)}{2\, t(\partial \bar{N}_2/\partial x)_{x = x^*}} \left[(1-Y^*) \int_{-\infty}^{x^*} \frac{Y}{V_m}\, dx + Y^* \int_{x^*}^{\infty} \frac{1-Y}{V_m}\, dx \right] \qquad (1.6)$$

where

$\bar{N}_2^*$ = mole fraction of cation 2 on the concentration profile at the particular distance x^*

$V_m(\bar{N}_2^*)$ = molar volume of cations at the particular mole fraction of interest, i.e. $\bar{N}_2^*$

t = time of diffusion anneal

$(\partial \bar{N}_2/\partial x)_{x=x^*}$ = tangent to the profile curve at the particular distance x^*

Y = $(\bar{N}_2 - \bar{N}_2^-)$, an auxiliary variable of composition

Y^* = value of Y at $\bar{N}_2 = \bar{N}_2^*$

$\bar{N}_2^+$ and $\bar{N}_2^-$ = mole fractions of B^{3+} in B_2O_3 and in AO respectively.

This method has been applied to the system $MgO-MgAl_2O_4$ by Whitney II and Stubican (1971) who also correlated the $\tilde{D}$ values thus calculated to the individual self-diffusivities.

Greskovich and Stubican (1970) compared the methods of Boltzmann-Matano and Wagner using the system $MgO-Cr_2O_3$ and concluded that the latter analysis yields more correct values. This is so because the experimentally observed change in molar volume is not accounted for in the Boltzmann-Matano analysis.

1.3 EXPERIMENTAL TECHNIQUES

Before proceeding to the analysis of solid-solid reactions, it would be desirable to outline briefly the experimental techniques generally used in these studies. Since a number of phases, crystalline or amorphous, may be present simultaneously in such a system, analysing the extent of reaction and the choice of experimental technique become critical. The techniques used specifically for a variety of systems studied have been included in Table 1.4.

1.3.1 X-ray analysis

X-ray analysis is the most widely used method, particularly in single crystal studies. In polycrystalline mixtures the method presents certain obvious drawbacks. In

this method, the change in intensity of a particular line of the pure component (usually one with maximum intensity) is followed during the course of reaction. But the intensity of the line depends on the crystallinity of the substance. Hence poorly crystalline intermediates hinder the detection of other phases. Moreover, the lower limit of detection is more than 5 to 10% depending on the apparatus used, so that lower conversions are not detectable. Expressions have been derived for mixed powder analysis by X-ray techniques (Klug and Alexander, 1974). X-ray intensity measurement techniques are time consuming and hence are not suitable for kinetic studies. High temperature on-line X-ray analysis has also been employed, which may be a useful technique.

1.3.2 Chemical analysis

Chemical methods are most convenient and quick. Hence whenever possible, such methods are used. The particular method of analysis to be used depends on the system under study. But usually a simple titration is good enough for the purpose (Krishnamurthy *et al*, 1974; Hlaváč, 1961; Tomás *et al*, 1969; Ramachandran *et al*, 1974). Chemical methods are useful for mixed powder systems; but for pellet-pellet systems they are not convenient.

1.3.3 Thermal analysis

This technique is particularly useful when a gaseous product is formed as one of the products, so that loss in weight as a function of time and temperature could be recorded. It can be used for reactions of the following type:

$$A(s)+B(s) \longrightarrow C(s)+D(g)$$; addition by elimination (e.g. Hulbert and Klawitter, 1967)

The loss in weight data can be correlated by the expression derived by Freeman and Carroll (1958) to evaluate the kinetics.

For solid-solid addition reactions, since there is no weight loss, thermogravimetric analysis (TGA) is of no use. But since solid-solid reactions are normally exothermic, differential thermal analysis (DTA) is a possible method. Borchardt and Daniels (1957) have derived expressions for the kinetics of liquid phase reactions. These relations could be used for solid state reactions also (Padmanabhan *et al*, 1960) provided adequate care is taken in carrying out experiments. The main drawbacks of solid systems are low heat conductivity of solids, possibility thereby of presence of temperature gradients, difference in heat capacities and heat transfer coefficients of reference and sample, etc., which may be

taken care of by choosing a small sample size, a dynamic atmosphere, and a product of reaction itself as the reference.

1.3.4 Gravimetric methods

When gaseous products are formed in the reaction, the kinetics can also be followed by measuring the volume or pressure of the gas at various time intervals (McCartney *et al*, 1961; Riemen and Daniels, 1957). Typical examples of this type of reactions are

$$Ag_2SO_4 + CaO \longrightarrow CaSO_4 + 2\,Ag + \tfrac{1}{2}\,O_2$$

$$BaCO_3 + BaTiO_3 \longrightarrow Ba_2TiO_4 + CO_2$$

When the reaction involves more than one step (consecutive reactions) and the final product is of interest, this procedure is of no use for kinetic studies, e.g. reduction of iron ore by coke, where the reduction occurs in steps,

$$Fe_2O_3 \longrightarrow Fe_3O_4 \longrightarrow FeO \longrightarrow Fe$$

1.3.5 Magnetic susceptibility measurements

The magnetic susceptibility measurements are useful

in studies on solid-solid reactions provided the reactants and products have markedly different magnetic susceptibilities. The formation of the spinel $NiFe_2O_4$ has been studied by this technique, since the spinel has higher magnetic susceptibility (Szabó *et al*, 1961).

1.3.6 Electrical conductivity measurements

Copp *et al* (1966) in their studies on reactions between Cr_2O_3 and MO (M = Mg, Ni, Zn, Co) proposed this method of measurement of electrical conductance ($\bar{L}$) or resistance ($1/\bar{L}$) for kinetic studies. Under dynamic conditions log ($1/\bar{L}$) *vs* 1/T data were collected and the results compared with X-ray diffraction analysis. Thus fractional conversion was correlated to conductivity changes.

This method can be useful in certain cases where reactants and products have distinctly different electrical conductivities. This fact has been used by Brandley and Greene (1967) in their studies on reactions between iodides of Ag, K and Rb, where the product (K, Rb) Ag_4I_5 has high electrical conductivity.

The method has certain obvious drawbacks: the electrical conductivity of polycrystalline materials is determined by the conductivity of surface layers and intergranular contacts; hence changes in electrical

conductivity may occur before any new phase has been formed. Moreover, metastable intermediates, if formed, will hinder the true conductivity change measurements. As such, even before X-rays could detect any new phase, there would be considerable changes in electrical conductivity. These, and some other important points, have been discussed by Deren and Haber (1966). Since metals are highly conducting, these studies will not be applicable to metallic systems.

1.3.7 Visual techniques

When a coloured product is formed, the course of reaction can be followed by measuring the product layer thickness by a moving microscope. This technique was introduced by Rastogi *et al* (1962), but certain factors restrict its use. Surface diffusion and vapour phase diffusion are well-known in many systems. Particularly in organic solids many compounds are known to sublime and to have high vapour pressures. The measurement of the thickness could be deceptive then as the product might form on the surface, whereas throughout the cross section it might be absent. In systems in which thicknesses are of the order of a few hundred microns such measurements cannot be used.

1.3.8 Electron probe microanalysis (EPMA)

This recent technique is found to be very precise and accurate. So far small concentrations were difficult to analyse; also concentration changes over a very small length were impossible to determine. Both these problems have now been overcome by this method.

The instrument uses an electron beam which can be focused sharply at a point. The bombardment of atoms with the electrons causes knocking out of the electrons of the atom in different energy levels. As a result there are transitions of electrons in the higher energy levels to the lower ones, and corresponding characteristic X-rays of different frequencies are emitted. These X-ray photons are counted by Geiger-Müller type counters or are detected by photocells. By an attached computer, the data could be converted finally to an X-Y plot of concentration *vs* distance.

Yamaguchi and Tokuda (1967) studied a number of oxide systems and obtained concentration profiles of the different components in a system. There are also a few more instances (Pettit *et al*, 1966; Whitney and Stubican, 1971; Minford and Stubican, 1974) where electron microprobe analysis has been used for obtaining concentration profiles.

The penetration depth of an electron beam is small, of the order of 10^{-4} cm, so that only surface concentration is recorded. In pellet-pellet systems, some times due to vapour phase or surface diffusion contributions, reaction occurs only on the surface. Hence the samples should be cut along the axis and then the method employed, so that likely erroneous results are avoided.

Apart from the methods described above, a variety of other methods can be used depending on the particular system under investigation. Thus use of IR, NMR, mass spectroscopy, reflectance spectroscopy, etc., may be made in the analysis of solid-solid reactions. Newer techniques like low energy electron diffraction (LEED), electron spectrometric chemical analysis (ESCA), X-ray electron photospectroscopy, etc., are coming up.

1.4 ANALYSIS OF PELLET-PELLET REACTIONS

Studies in pellet-pellet systems are mainly aimed at elucidating the transport mechanism in detail and to gain insight into the phenomenon of coupled diffusion and reaction. The second aspect, which is important from the engineering point of view, has received relatively little attention.

The changes occurring in a mixed powder system have

a complex time dependence. Also, the geometries of individual particles are not well defined. Though often particles are assumed to be spherical, in actual practice all kinds of shapes (flakes, plates, cylinders, needles, etc.) are encountered simultaneously. Moreover, size distribution is also a factor. Hence studies on mixed powder systems, though more important from the practical view-point, are inadequate for the elucidation of the detailed mechanism of the process.

The obvious method of overcoming these difficulties is to take a system with a fixed geometry and hence a well defined contact surface area. This can most conveniently be achieved by taking cylindrical pellets of the reactants in contact. Such studies have helped considerably in understanding the mass transfer phenomena in solid-solid systems mainly by marker movement experiments.

1.4.1 The role of diffusion

In a pellet-pellet system, once the product layer has formed by the phase boundary processes, for the reaction to proceed one or both of the reactants should diffuse through this product layer and react. Depending on whether the diffusion is one-sided or counterdiffusion is involved, the product growth will occur on only one side or both sides

of the original interface. In systems in which ionic diffusion occurs, the condition of electroneutrality restricts the diffusion process and consequently the product growth on the two sides of the original interface. For example, in oxide systems which are often encountered in practice, different situations can be encountered as represented in Figure 1.1. Consequently, the product growth on the two sides of the original interface will be in the ratio 1:3 in case (c) and 1:2 in case (d).

A number of systems have been studied to investigate the mode of diffusion. Most of them make use of the marker experiments to follow the interface movement. The markers used are normally inert platinum wires which are originally placed at the interface. But as pointed out correctly by Pettit *et al* (1966), these markers may not be really inert in high temperature studies. Also, slippage and breakage of markers may take place due to the uneven stresses developed at the interface. Hence, it has been suggested (Yamaguchi and Tokuda, 1967) that texture composition, which is found to be different in the two parts in case of counter-diffusion, can serve as a natural marker. Also, because of faster diffusion of one of the cations, vacancies are created which are visible under a microscope as pores. This layer of pores can be treated as a marker (Carter, 1961 a; Hardel, 1972). Kooy (1965) has suggested a method of

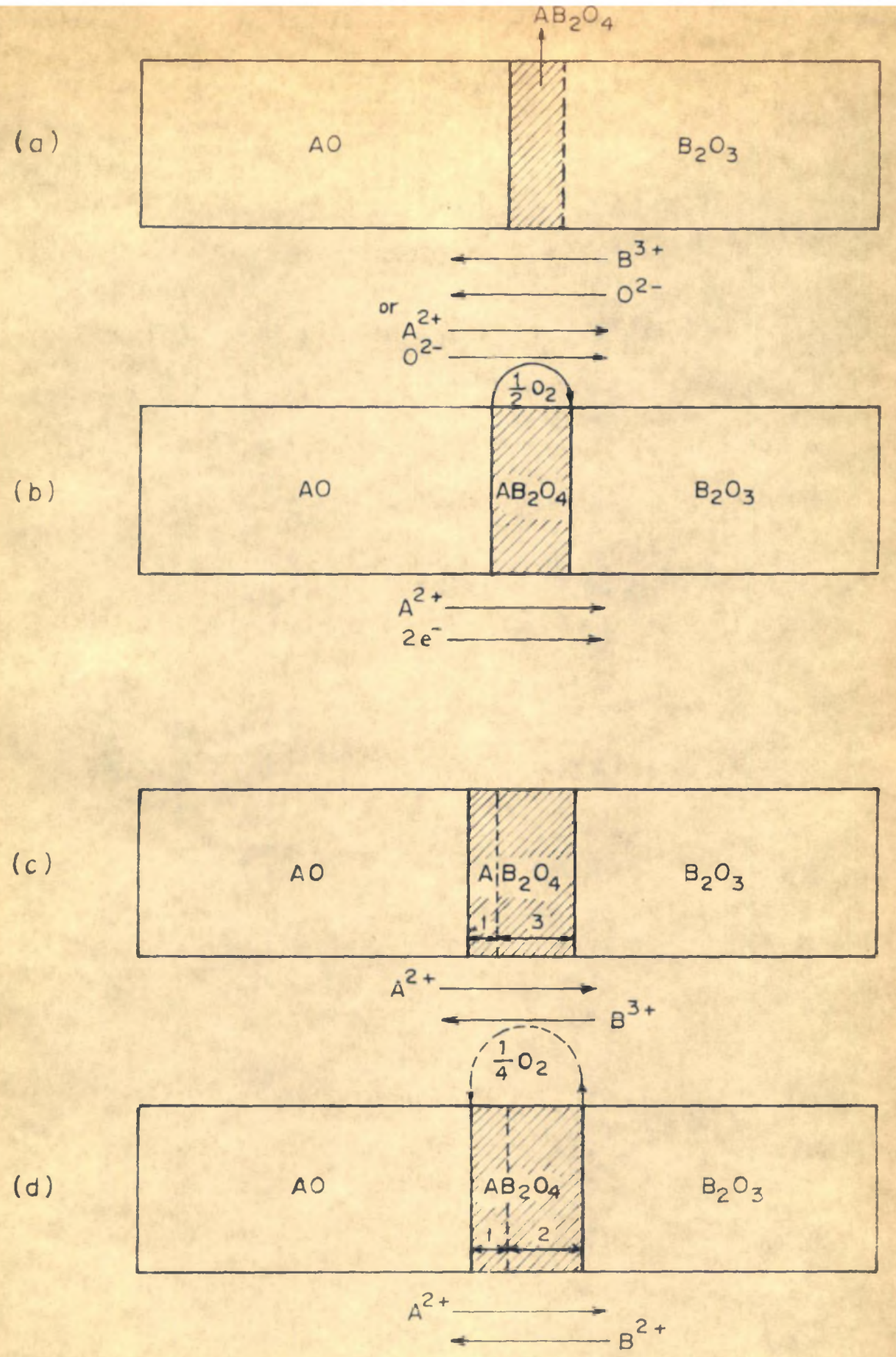

DIFFERENT MODES OF DIFFUSION

FIGURE 1·1

restricted contact, so that depending on diffusion rates uneven product growth as well as swelling and contraction on two sides can be observed (see Figure 1.2).

1.4.2 Sintering

Kuczynski and coworkers (Kuczynski, 1965) have extensively studied the phenomenon of sintering and have developed mathematical expressions of the form $(r^{\bullet})^{n} = kt$, where $r^{\bullet}$ is the neck radius and n takes different values depending on the mechanism of sintering. They extended these studies to the problem of sintering and reaction. Thus, Kuczynski (1965) studied the systems $NiO-Fe_2O_3$ and $MgO-Fe_2O_3$, with spheres of one in contact with plates of the other. Due to fast diffusion of MgO, swelling on the Fe_2O_3 side was observed. But some Fe_2O_3 was also found to have diffused in MgO, which was neglected in previous studies. From the shape and large radii of necks, it is evident that neck growth is not controlled by vacancy gradient due to surface tension as in a purely sintering process. In fact the time dependence of neck growth was found to be in accord with the relation

$$r^{\bullet} \alpha t^{1/2} \qquad (1.7)$$

and not

$$r^{\bullet} \alpha t^{1/5} \qquad (1.8)$$

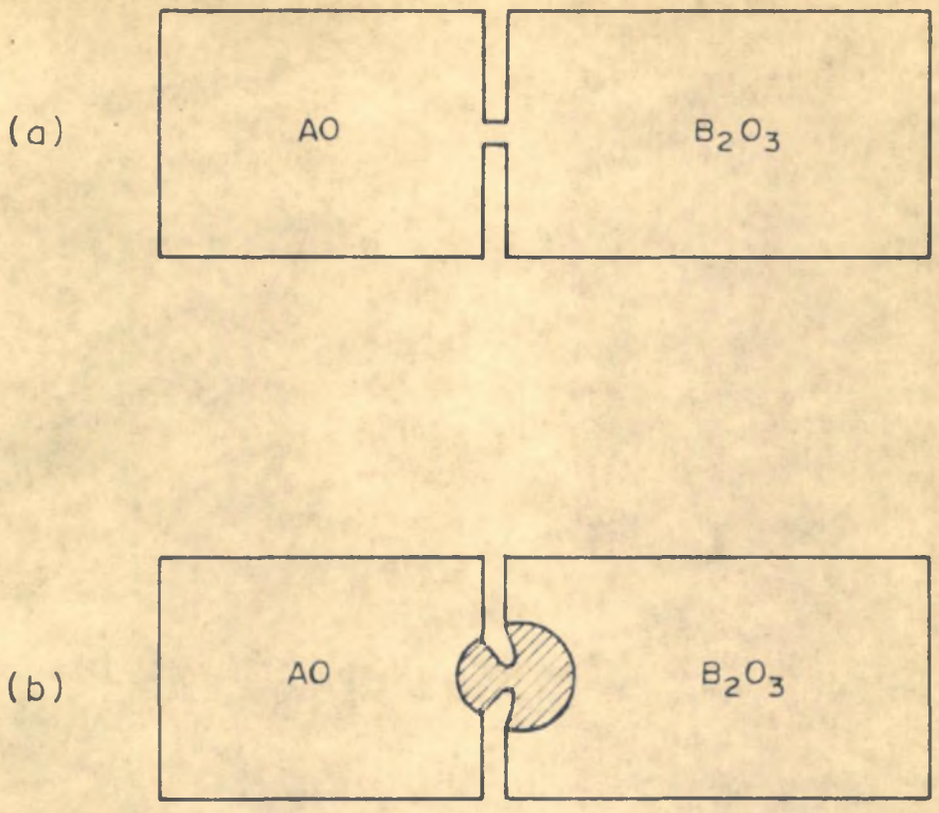

UNEVEN SWELLING DUE TO COUNTER DIFFUSION

(KOOY, 1965)

FIGURE 1·2

Similar observations have been made by Kooy (1965).

1.4.3 Reaction models

Studying solid-solid reactions by keeping the pellets of the reactants in contact is advantageous in understanding the nature of mass transport and the mechanism operative. A system in the pellet-pellet form is also attractive for the mathematical analysis of the coupled diffusion and reaction problem; more so because it retains the structures and concentration profiles in a clearly distinguishable pattern after the reaction is quenched.

Earlier studies mainly used the parabolic law of Tammann (1920) to follow the overall rate of reaction. According to this law, the square of the product zone thickness is directly proportional to time:

$$(\Delta x)^2 = Kt \qquad (1.9)$$

The expression is more or less an empirical one and is based on the assumption that the diffusion of the reacting species through the product layer is the controlling step, so that

$$\frac{d(\Delta x)}{dt} \alpha D, \text{ the diffusivity}$$

$$\alpha \frac{1}{\Delta x}$$

$$\alpha A, \text{ the cross-sectional area}$$

or

$$\frac{d(\Delta x)}{dt} = \frac{c A D}{\Delta x} \qquad (1.10)$$

where c is a proportionality constant ($1/cm^2$). Integration of the above expression yields Equation 1.9, the parabolic rate law, where K is the overall rate constant.

Because of the simplicity of the expression, and the easily obtainable product layer thickness (PLT) values, the parabolic rate law has been in use for long. In a number of studies parabolic rate constants have been obtained and hence the activation energies and other thermodynamic parameters. Typical examples of PLT studies are presented in Table 1.2. However, the validity of the parabolic rate law may not necessarily mean that diffusion in the product layer controls.

A rigorous model, considering diffusion in the product layer as the controlling step, is due to Wagner (1936). In his treatment, Wagner considered only the counterdiffusion of cations in the product layer. The rate

TABLE 1.2

Examples of Systems for which the Kinetics have been Studied by Pellet-Pellet Experiments

No.	System	Rate law	Reference
1	2	3	4
1	$NiO-Al_2O_3$	$(\Delta x)^2 = Kt$	Pettit *et al* (1966)
2	$NiO-Al_2O_3$	$(\Delta x)^2 = Kt$	Minford and Stubican (1974)
3	$NiO-Cr_2O_3$	$(\Delta x)^2 = Kt$	Greskovich (1970)
4	$MgO-Cr_2O_3$	$(\Delta x)^2 = Kt$	Greskovich and Stubican (1969,1970)
5	$MgO-Al_2O_3$	$(\Delta x)^2 = Kt$	Whitney and Stubican (1971)
6	$SrO-WO_3$	$(\Delta x)^2 = Kt$	Flor *et al* (1974)
7	$CaO-WO_3$	$(\Delta x)^2 = Kt$	Flor *et al* (1977)
8	$CoO-Ga_2O_3$	$(\Delta x)^2 = Kt$	Laqua (1976)

TABLE 1.2 (continued)

1	2	3	4
9	AgI-TlI	$(\Delta x)^2 = Kt$	Flor *et al* (1975)
10	AgI-(K, Rb)I Initial :	$\Delta x = Kt$	
	Later :	$(\Delta x)^2 = Kt$	Brandley and Greene (1967)
11	Hg_2Cl_2-I_2	$(\Delta x)^2 = 2Kt \exp(-q\Delta x)$	Rastogi and Dube (1967)
	Hg_2Br_2-I_2	$(\Delta x)^2 = Kt$	
	Hg_2I_2-I_2		
12	Picric acid with hydrocarbons	$(\Delta x)^2 = 2Kt \exp(-q\Delta x)$	Rastogi *et al* (1963)
13	Picric acid with naphthols	$(\Delta x)^2 = 2Kt \exp(-q\Delta x)$	Rastogi and Singh (1966)
14	p-Dimethylaminobenzaldehyde-diphenylamine hydrochloride	$(\Delta x)^3 = K't$	Qureshi *et al* (1975)

of consumption of reactants was equated to the diffusional flux, the expression for which was derived considering the fundamental properties of ions, such as charge, mobility, chemical potential, etc. Thus, for the reaction scheme, $AX + BX \longrightarrow ABX_2$, the diffusional flux is given by

$$j(x) = \frac{\partial C_A}{\partial t} = \frac{-\partial C_B}{\partial t} = \frac{-(C_A + C_B)}{1 + \dfrac{z_B' C_B v_B}{z_A' C_A v_A}} z_B' C_B v_B \frac{d\mu_o(AX)}{dx} \qquad (1.11)$$

Integrating over the product layer thickness Δx, the expression for j_{total} was obtained:

$$j_{total} = -\int_I^{II} \frac{C_A + C_B}{1 + \dfrac{z_B' C_B v_B}{z_A' C_A v_A}} \frac{z_B'}{\Delta x} v_B C_B d\mu_o(AX) \qquad (1.12)$$

where z' is the charge, C the concentration, v the velocity (mobility) and μ_o the chemical potential, and I and II indicate the boundaries of the product layer. Koch and Wagner (1936) applied this theory to obtain the reaction rate constant $\bar{k}$ using the expression

$$\bar{k} = j_{total} \Delta x \qquad (1.13)$$

This value of $\bar{k}$ was found to be in good agreement with the

experimental value. But certain observations were not explained by the theory.

Schmalzried (1962, 1965) further developed the theory, considering all the three possible mechanisms of diffusion for the reaction

$$AO + B_2O_3 \rightarrow AB_2O_4$$

He defined the flux for an i^{th} species as

$$j_i = - \frac{C_i D_i}{RT} \text{ grad } \eta_i \qquad (1.14)$$

where η_i is the electrochemical potential, C_i the concentration of the i^{th} species and D_i its diffusivity. Integrating the flux equation over the product layer thickness and assuming parabolic rate law, an expression for the rate constant K was obtained as follows:

$$K = \frac{\epsilon z_i' C_i D_i^o}{m_o \Delta G_{AB_2O_4}} \left[1 - \exp \left\{ \frac{m_o \Delta G^o_{AB_2O_4}}{RT} \right\} \right] V \qquad (1.15)$$

where

D_i^o = self diffusion coefficient of the rate determining ion, when a'_{AO}, the activity = 1

ϵ = a numerical factor of the order of one

m_o = coefficient reflecting the defect type of the reaction product

$\Delta G^{o}_{AB_2O_4}$ = Gibbs energy of formation for AB_2O_4 and

V = increase of the product volume due to the transport of one equivalent of ions through the reaction layer.

Rastogi and coworkers (see Rastogi, 1970), in their studies on a number of organic solid-solid reactions, used the modified form of the parabolic rate law given by

$$(\Delta x)^2 = 2 K t \exp(-q \Delta x) \qquad (1.16)$$

where q is a constant for a given system. As such, the expression is an empirical one, but theoretical justification based on probabilistic considerations has been provided by Rastogi and Singh (1966). Equation 1.16 above has been reported earlier by Cohn (1948) who obtained it by modifying the parabolic rate law considering the effect of exothermicity on the reaction rate.

As can be inferred from the above discussion, much attention has been given so far to diffusion in the product zone. The interactions taking place at the phase boundaries have been relatively neglected. Schmalzried

first recognised this fact, and in a recent article (Schmalzried, 1974) has considered the phase boundary reactions as cation rearrangements. These rearrangements, predicted to be occurring in a narrow zone, yield the product and the rate of rearrangement determines the reaction rate.

Schmalzried defined the relaxation time t_r for the cation rearrangement. Then, for the reaction

$$AO + B_2O_3 \rightarrow AB_2O_4$$

the advancement of the phase boundary is a function of the mobility of B-ions in AO and of t_r. Thus,

$$\frac{d(\Delta x)}{dt} = f\{D_B^{(AO)}, t_r\} \qquad (1.17)$$

As zeroth approximation, it is set to be

$$\frac{d(\Delta x)}{dt} = \frac{\gamma \Delta x_r}{t_r} \qquad (1.18)$$

where Δx_r, the reaction zone thickness, is given by

$$\Delta x_r = \{2 D_B^{(AO)} t_r\}^{1/2} \qquad (1.19)$$

γ is a numerical factor indicating the fraction transformed into the product in time t_r.

The recent technique of electron probe micro analysis (EPMA), when used in studying solid-solid reactions, has clearly indicated the existence of such a reaction zone. Greskovich and Stubican (1969) studied the system $MgO-Cr_2O_3$ using the EPMA technique. They obtained concentration profiles of Cr^{3+} in MgO, forming a reaction zone. The analysis was attempted by considering only the diffusion of Cr^{3+} in the reaction zone. The diffusivity was assumed to be directly proportional to the concentration. Referring to Figure 1.3

$$D' = D_{C=C'} = D_o \frac{C'}{C_o} \qquad (1.20)$$

where

$$C = C' \text{ at } x = x' \qquad (1.21)$$

The unsteady state diffusion equation

$$\frac{\partial C}{\partial t} = \frac{\partial}{\partial x} \left(D \frac{\partial C}{\partial x} \right) \qquad (1.22)$$

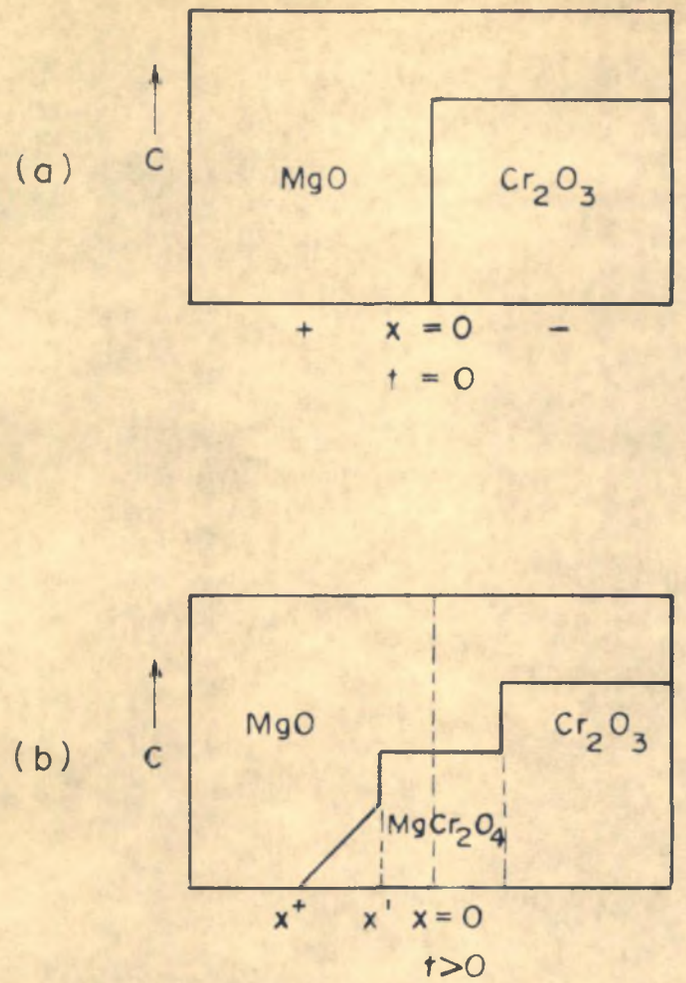

SCHEMATIC REPRESENTATION OF CONCENTRATION PROFILES

(GRESKOVICH AND STUBICAN, 1969)

FIGURE 1·3.

was then solved for the boundary conditions

$$C = C' \quad , \quad x = x'$$
$$C = 0 \quad , \quad x = x^{+} \tag{1.23}$$

The final expression obtained was

$$C/C' = (1.23)^2 \, x^{+} \, (x^{+} - x)/4 \, D't \tag{1.24}$$

Actually, it is not only the diffusion but also the reaction of Cr^{3+} in the reaction zone that should be considered.

Arrowsmith and Smith (1966) attempted an analysis in which they considered simultaneous diffusion and reaction in an organic pellet-pellet system. In their analysis, an irreversible second order reaction has been assumed ($A + B \rightarrow C$). Mass balances have been written in the form

$$\frac{\partial C_A}{\partial t} = D \frac{\partial^2 C_A}{\partial x^2} - k'' C_A C_B \tag{1.25}$$

and

$$\frac{\partial C_B}{\partial t} = D \frac{\partial^2 C_B}{\partial x^2} - k'' C_A C_B \tag{1.26}$$

with the initial and boundary conditions,

$$\left.\begin{aligned} C_A &= C_{Ao},\ C_B = C_C = 0,\ x < 0 \\ C_A &= C_C = 0,\ C_B = C_{Bo},\ x > 0 \end{aligned}\right\} t = o \qquad (1.27)$$

$$\left.\begin{aligned} C_A &= C_{Ao},\ C_B = C_C = 0,\ x = -\infty \\ C_A &= C_C = 0,\ C_B = C_{Bo},\ x = +\infty \end{aligned}\right\} t > o \qquad (1.28)$$

The density has been assumed constant, so that

$$\rho = C_A M_A + C_B M_B + C_C M_C \qquad (1.29)$$

The nonlinear Equations 1.25 and 1.26 were then converted into dimensionless form and solved numerically, Thus ω $(= C/C_{Ao})$ **vs** z $(= x\sqrt{C_{Ao}k''/D})$ plots have been prepared for different values of θ' $(= C_{Ao}k''t)$; a typical plot is reproduced in Figure 1.4 for $\theta' = 0.1, 0.5, 1.0$, and 2.0. Using these plots and the diffusivity values determined independently, rate constants were evaluated.

1.4.4 Multiphase product layer formation

This is an important field of research in solid-solid reaction studies. Multiphase product layer appears in the

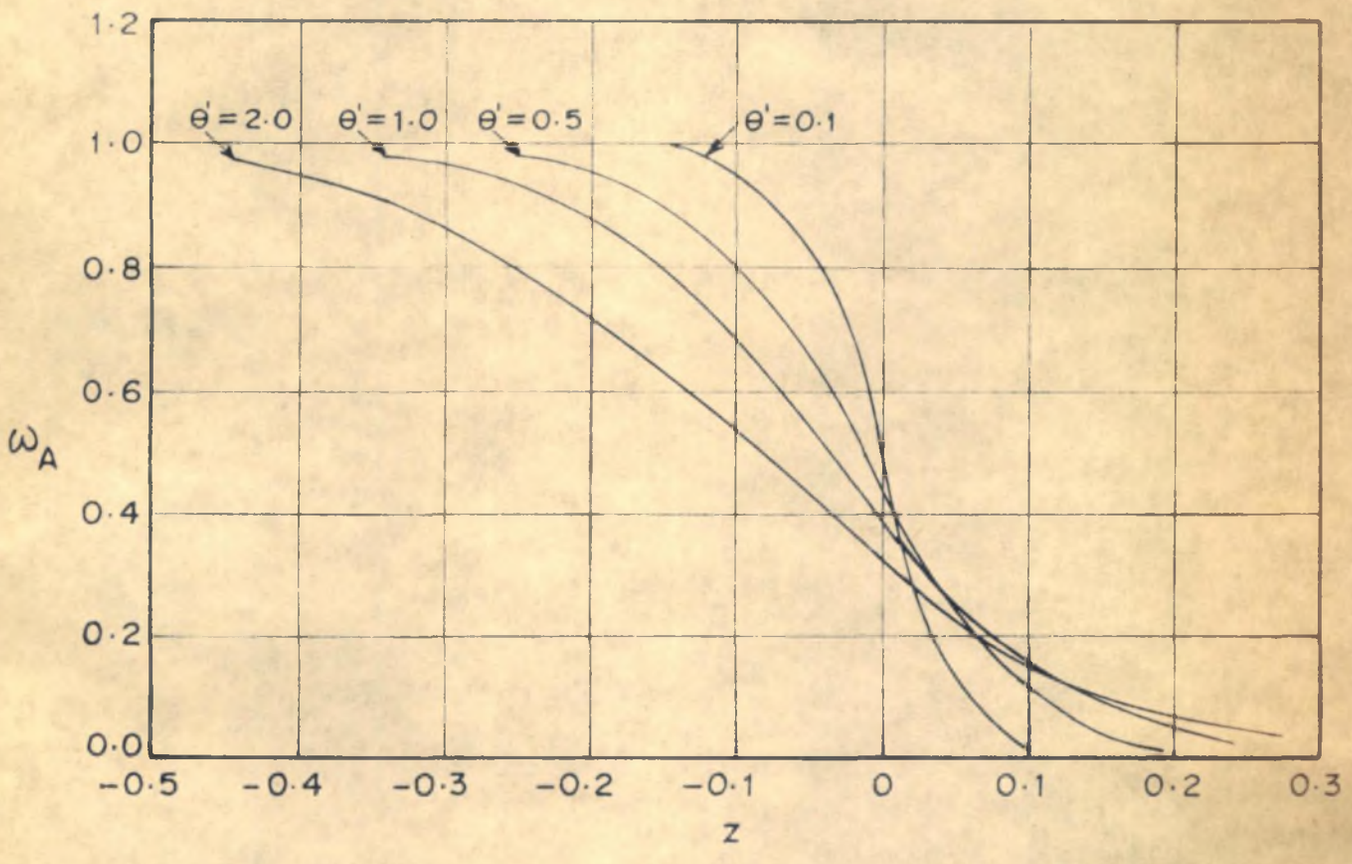

VARIATION OF ω_A WITH z AND θ' FOR $C_{Ao}=C_{Bo}$

(ARROWSMITH AND SMITH, 1966)

FIGURE 1·4

case of silicates and some aluminates, which are important components of cement. As such, kinetic studies in these cases play a significant role in cement production. Titanates, which are important in semiconductors, also exhibit multiphase product formation.

In spite of its importance, this aspect of solid-solid reactions has received scant attention. There have been, however, a few attempts to study these reactions experimentally. One reason for the lack of any theoretical attempt is the mathematical complexity involved in the analysis.

Kohatsu and Brindley (1968) and Brindley and Hayami (1965) studied the systems $CaO-\alpha-Al_2O_3$ and $MgO-SiO_2$ respectively. The following sequence of phases was observed in the product layer (for the former):

$$CaO/C_3A/C_{12}A_7 \quad \text{or} \quad C_{12}A_7H/CA/CA_2/CA_6/Al_2O_3$$

where

$$C = CaO \quad \text{and} \quad A = Al_2O_3$$

The thicknesses of different phases were measured and corresponding rate constants were calculated applying the parabolic rate law to the growth of each phase. Phases were

identified using X-ray and EPMA techniques. Thus,

$$\frac{d(\Delta x)}{dt} = \frac{K}{\Delta x} \qquad (1.30)$$

or

$$(\Delta x)^2 = Kt \qquad (1.31)$$

K is given by the expression:

$$K = \frac{A}{V} \frac{a'b'}{a' + b'} \frac{\Delta \mu}{RT} \qquad (1.32)$$

where

A = cross-sectional area

V = volume growth of reaction product per equivalent

$a' = z'_M C_M D_M$, $b' = z'_X C_X D_X$

(for cation) (for anion)

and

$\Delta \mu$ = difference in chemical potentials across the product layer.

When diffusion of only one kind of ion dominates ($a'b'/a' + b'$) can be approximated to $z' C D$ for the slow moving ion. (z' = ionic valence, C = concentration in equivalents per unit volume, and D = diffusivity).

Different rates were observed for different phases (in a given system). These rates were correlated to the melting point and oxygen packing density of the corresponding phases. Thus, low melting point and low density will facilitate diffusion and thereby growth. In certain cases, exceptions to the rule were observed, e.g. growth of CA_6, in which case the behaviour was explained to be due to the possible contribution of surface diffusion.

Sockel (1972) studied the system $PbO-SiO_2$ and observed the sequence to be

$$PbO/4\ PbO.SiO_2/2\ PbO.SiO_2/PbO.SiO_2/SiO_2$$

Again the parabolic rate law was applied for individual phase growths. Also an expression has been derived relating the parabolic rate constant for a given phase in multiphase growth to that in a single phase growth.

It is usually difficult to assign a precise mechanism of mass transport in such systems. Yamaguchi and Tokuda (1967) have reported EPMA profiles for a few silicate and titanate systems. The nature of these profiles reflects the complexity involved in the analysis.

A detailed mathematical analysis of multiphase product growth considering diffusion as well as chemical

reactions at the interfaces has been reported recently by Zmii and Seryugina (1971 a, 1971 b). Solutions have been obtained for short and long times and the theory has been modified (Zmii and Seryugina, 1976) for the calculation of diffusion and kinetic rate constants. They have also obtained an expression for the time for establishment of quasi-stationary equilibrium.

1.5 ANALYSIS OF MIXED POWDER REACTIONS

As pointed out in the previous section, analysis of mixed powder reactions is complicated. But due to the practical importance of mixed powder systems, they have received greater attention. In the previous section the mechanism of transport and the phenomenon of diffusion and reaction in solid-solid systems were discussed. In this section we discuss the various models proposed for mixed powder reactions.

In essence, in any mixed powder system, the solid particles of reactants should contact one another and at least one of them must then diffuse through an increasing product shell, after the initial surface reaction. This situation gives rise to several possibilities:

1. product growth controlled by diffusion of reactants through a continuous product layer;

2. product growth controlled by phase boundary reactions;

3. product growth controlled by kinetic equations based on the concept of an order of reaction;

4. product growth controlled by nuclei growth.

In the following the basic features of the different models proposed for these as controlling mechanisms will be briefly outlined. The effect of particle size distribution and that of additives will then be considered.

1.5.1 Reaction models

(a) Product layer diffusion control

Models based on this mechanism involve three basic assumptions:

(i) reactant particles are spheres;

(ii) surface diffusion rapidly covers reactant particles with a continuous product layer during the initial stages of the reaction; and

(iii) further reaction takes place by bulk diffusion of mobile reactant species through this product layer, which is the rate controlling step.

Jander (1927) was probably the first to treat a solid-solid reaction mathematically. In addition to the above mentioned assumptions he also made the rather drastic assumption of a constant cross sectional area and an

unchanging volume or density during the progress of a reaction. He derived the following expression for the fractional conversion α :

$$\{1 - (1 - \alpha)^{1/3}\}^2 = Kt \qquad (1.33)$$

where K = rate constant given by

$$K = \frac{2\ c\ DA}{r^2} \qquad (1.34)$$

One assumption that cannot be experimentally realised in a mixed powder system is that of constant reaction cross-section, since the surface area of the unreacted particle changes continuously as the reaction progresses.

Serin and Ellickson (1941) attempted to modify the rate expression of Jander by eliminating the assumption of constant reaction cross-section. A number of other rate expressions have also been derived based on different approaches. These are summarised in Table 1.3.

In the Valensi-Carter model, change in volume due to reaction is accounted for by introducing a parameter Z in the expression. This and the first two (Jander and Serin-Ellickson) are the most widely used models in mixed powder reaction rate studies.

TABLE 1.3

Models for Mixed Powder Reactions

No.	Reaction model	Mathematical expression	Reference (s)
1	2	3	4
1	Product layer diffusion control:		
	(i) Jander	$Kt = \{1-(1-\alpha)^{1/3}\}^2$	Jander (1927)
	(ii) Serin-Ellickson	$(1-\alpha) = \frac{6}{\pi^2} \sum_{n\ \text{odd}} (\frac{1}{n^2}) \exp(-n^2\ ^2Dt/r^2)$	Serin and Ellickson (194]
	(iii) Kröger-Ziegler	$K \ln t = \{1-(1-\alpha)^{1/3}\}^2$	Kröger and Ziegler (1954)
	(iv) Zhuravlev-Lesokhin-Temple'man	$Kt = \{\frac{1}{(1-\alpha)^{1/3}} - 1\}^2$	Zuravlev et al (1948)
	(v) Ginstling-Brounstein	$Kt = 1-2/3\ \alpha - (1-\alpha)^{2/3}$	Ginstling and Brounstein (1950)

TABLE 1.3 (Continued)

1	2	3	4
	(vi) Dünwald-Wagner	$Kt = \frac{6}{\ln \pi^2 (1-\alpha)}$	Dünwald and Wagner (1934
	(vii) Valensi-Carter	$Kt = \frac{Z-\{1+(Z-1)\alpha\}^{2/3}-(Z-1)(1-\alpha)^{2/3}}{(Z-1)}$	Valensi (1936) Carter (1961 b)
2	Nuclei growth control	$(kt)^m = -\ln(1-\alpha)$	Avrami (1939,1940,1941)
3	Phase boundary reaction control:		
	(i) Sphere reacting from the surface inwards	$kt = 1-(1-\alpha)^{1/3}$	Jach (1963)
	(ii) Circular disk reacting from edge inwards or a cylinder	$kt = 1-(1-\alpha)^{1/2}$	"
	(iii) Contracting cube	$\alpha = 8k^3t^3 - 12k^2t^2 + 6kt$	Sharp et al (1966)

TABLE 1.3 (Continued)

1	2	3	4
4	Based on the concept of an order of reaction	$kt = \frac{1}{n-1}\left\{\frac{1}{(1-\alpha)^{n-1}} - 1\right\}$	
5	Based on the concept of an index of reaction	$\frac{d\alpha}{d(t^m)} = k'(1-n\alpha)^i$	Taplin (1974)
6	Empirical:		
	(i) Blum and Li	$\frac{d\alpha}{dt} = \frac{a-\alpha}{t}$	Blum and Li (1961)
	(ii) Patai *et al*	$\frac{d\alpha}{dt} = \frac{k''(a-\alpha)^m}{\alpha^n}$	Patai *et al* (1961)
		$\frac{d\alpha}{dt} = k''(a_1-\alpha)(a_2-0.5\alpha)$	Patai *et al* (1962)
7	Stochastic: Waite	$k''t^{1/2} + I = \left(\frac{\alpha}{1-\alpha}\right)\frac{1}{a\ t^{1/2}}$	Wen *et al* (1974)

The Jander and Valensi-Carter models have been modified by a number of workers to account for particle size, shape and distribution. These modifications will be discussed subsequently.

(b) Nuclei growth control

This approach considers the nucleation of product phase at active sites and the rate at which the nuclated particles grow. The general form of the equation is

$$\ln (1 - \alpha) = -(kt)^m \qquad (1.35)$$

The parameter m accounts for (i) reaction mechanism, (ii) number of nuclei present, (iii) composition of parent and product phases, and (iv) geometry of the nuclei.

If a reaction is represented by this model, a plot of $\ln \ln \frac{1}{1-\alpha}$ *vs* $\ln t$ should give a straight line, with slope m and intercept m ln k. The nuclei growth model has been applied successfully to a number of decomposition reactions (where a gas phase is involved), but its applications to solid-solid reaction systems are rare (see Table 1.4).

(c) Phase boundary reactions control

When the diffusion of the reactant species through the product layer is fast compared to reaction, the kinetics is controlled by phase boundary reactions.

Models have been developed for different geometries and corresponding boundary conditions. Thus, for a sphere reacting from the surface inwards the fractional reaction completed α and time t are related by the expression,

$$kt = 1 - (1 - \alpha)^{1/3} \qquad (1.36)$$

which is identical with the expression derived for gas-solid (noncatalytic) reactions (Levenspiel, 1974). For a circular disk, reacting from the edge inwards, or for a cylinder, the relation is

$$kt = 1 - (1 - \alpha)^{1/2} \qquad (1.37)$$

and for a contracting cube

$$\alpha = 8k^3t^3 - 12k^2t^2 + 6kt \qquad (1.38)$$

In all these models, it is assumed that reaction is

slow compared to diffusion, but fast enough to occur in a very short thickness near the interface. However, simultaneous diffusion and reaction of the diffusing species A in the bulk of the solid B is not given any consideration.

(d) Kinetic equations based on the concent of an order of reaction

The general rate equation for an n^{th} order reaction is represented by

$$\frac{1}{n-1}\left[\frac{1}{(1-\alpha)^{n-1}} - 1\right] = kt \qquad (1.39)$$

Vant Hoff's differential analysis can be used to determine whether a reaction could be classified by a reaction order.

Thus, Kutty and Murthy (1974) have applied first order kinetics to the reaction between urea nitrate and tricalcium phosphate in an ensemble of fine particles. They have attributed this to slow nucleation of one of the products and fast spreading of it further, because of negligible diffusion resistance. Branson (1965) observed that for the reaction between ZnO and Al_2O_3, the Valensi model is applicable only at high temperatures ($> 1000^{o}C$),

whereas below 1000°C the rate constant k is time dependent. This was predicted to be due to the possibility of phase boundary controlled kinetics in the early stages of the reaction. Hence, the data were correlated by the second order kinetic equation,

$$k'' t = \frac{1}{a}\left(\frac{\alpha}{a-\alpha}\right) \qquad (1.40)$$

To explain this, two possible mechanisms suggested by him are:

(i) diffusion through the product layer is so rapid that no reaction is possible at spinel-alumina interface; or

(ii) nucleation from a supersaturated solid solution of ZnO in Al_2O_3.

The first mechanism suggests that reaction does not occur at the phase boundary but in the bulk of the solid, whereas the second suggests the possibility of nuclei growth control. However, this has not been verified.

(e) Generalised approach

The rate equations mentioned above and grouped under different controlling mechanisms can all be represented by a single expression,

$$F(\alpha) = kt \qquad (1.41)$$

$F(\alpha)$ for $\alpha = 0.5$ and hence the ratio $t/t_{0.5}$ may be determined, where $t_{0.5}$ is the time required for 50% conversion. Sharp et al (1966) have prepared numerical tables which give the values of $F(\alpha)$ and $t/t_{0.5}$ for values of α between 0 and 1. Taplin (1974) has suggested a unified treatment for most kinetic expressions used for the reaction of powdered materials by writing the rate equation in the generalised form

$$\frac{d\alpha}{d(t^m)} = k'(1 - n\alpha)^i \qquad (1.42)$$

The exponent of time m depends on the kinetic regime. i has been named by him as "index of reaction", which in many of the previous studies was misinterpreted as the order of reaction. By numerical values and different plots, the expression has been shown to be appropriate with different values of m, n and i depending on the kinetics. Thus, for linear kinetics where the reaction rate varies as the area of the reaction interface, the equation is shown to be valid for different particle shapes, with m and n values of 1 and indices of reaction (i) values of 2/3, 1/2 and 0 respectively for sphere, elongated cylinder and thin disk.

Because of particle size distribution, values of i other than those mentioned for individual particles are obtained. Thus, values of i as high as 1.5 have been reported. However, the shape of a real particle is usually irregular, and generalisation can be achieved by considering a right rectangular prism of variable dimensions. In similar fashion, other types of kinetics, such as parabolic kinetics, nucleation-based kinetics, limited-extent kinetics, etc. are shown to be generalised by Equation 1.42 with different values assigned to m, n and i.

Remarkably, coupling between linear and parabolic processes leading to joint kinetics has also been approximated by the index-of-reaction equation with m = 2/3 (Taplin, 1973 a). Except for this, however, almost in all other studies it has been assumed that only one type of kinetics prevails for the entire reaction, which is obviously not the case; different regimes could be operative in a single reaction during its progress. This has been pointed out by Taplin (1973 b).

(f) Empirical equations

Apart from the different models presented above, a number of authors have proposed different empirical equations

to describe the kinetics of a mixed powder reaction. Thus, Blum and Li (1961) found that the rate equation

$$\frac{d\alpha}{dt} = \frac{a-\alpha}{t} \qquad (1.43)$$

describes the kinetics of nickel ferrite formation from the observation of a straight line plot obtained for αt *vs* t. The equation was found to hold for all ferrite formation reactions.

Patai *et al* (1961, 1962) in their studies on the oxidation of p-divinyl benzene (p-DVB) and carbon black by $KClO_4$, have used the empirical rate expressions:

$$\frac{d\alpha}{dt} = \frac{k''(a-\alpha)^m}{\alpha^n} \qquad (1.44)$$

and

$$\frac{d\alpha}{dt} = k'' (a_1 - \alpha) (a_2 - 0.5\ \alpha) \qquad (1.45)$$

where the values of the empirical constants m and n were found to be 1 and 2/3 respectively; a_1 and a_2 are the initial concentrations of the reactants. The

equations represent different forms of kinetic rate expression, with different values of the order of reaction.

(g) A stochastic model

From the discussion presented above it is seen that the nature of solid-solid reactions is statistical, because of the inhomogeneity of mixing and other factors. Hence, a stochastic model would be more realistic in describing the course of a solid-solid reaction. Such a model has been developed by Waite (1957a, 1958, 1960) in which a probabilistic distribution of pairs of A and B particles is considered, and different probability densities are calculated. The total change in the pair probability density with time ($\partial P_{ij}/\partial t$) is considered to be due to diffusion and chemical reaction. Thus

$$\frac{\partial P_{ij}}{\partial t} = \left(\frac{\partial P_{ij}}{\partial t}\right)_{Chem} + \left(\frac{\partial P_{ij}}{\partial t}\right)_{diffusion} \qquad (1.46)$$

$(\partial P_{ij}/\partial t)_{diffusion}$ was calculated by considering a six-dimensional hyperspace and applying the theory of stochastic processes, whereas $(\partial P_{ij}/\partial t)_{chem}$ was obtained by defining a hypothetical distance of separation x_o between the A and B particles within which they react. Finally, an

expression for the probability density of AB pairs (ρ_{AB}) as a function of x and t is obtained, which is solved for two types of boundary conditions, viz. (i) Smoluchowski boundary conditions, and (ii) Collins' or radiation boundary conditions. The final form of the expression obtained using Smoluchowski boundary conditions is (Wen et al, 1974):

$$\left(\frac{\alpha}{1-\alpha}\right) \frac{1}{a\, t^{1/2}} = k'' t^{1/2} + I \qquad (1.47)$$

which reduces to the ordinary second order rate equation with I = 0.

Waite (1957 b) has applied his theory to the problem of radiation damage. The theory has also been applied by Wen et al (1974) in their studies. No attempt to apply this theory to solid-solid reactions has been made hithertofore. It would be particularly interesting if the data for different particle sizes is analysed using Equation 1.47 in terms of an effectiveness factor (similar to that for other heterogeneous reactions), since the diffusional resistance is separated here in the factor I.

In spite of the drawbacks in some of the models, and

the empiricism in the others, they have been used to analyse a number of solid-solid mixed powder reactions. In many of these studies the equations used fitted the data reasonably well. Some times, the fit was achieved by adjusting the experimental conditions to match the assumptions made in the theoretical development; at other times the deviations observed were explained on the basis of experimental errors and other factors. The different systems studied and the models used for analysis are summarised in Table 1.4.

1.5.2 Effect of particle size distribution

Particle size distribution encountered in practice can have important effects on kinetics. The smaller particles in the ensemble will be consumed in a short period of time, when bigger particles are still reacting. Hence, reaction rate per unit volume, which is based on the radius of an individual particle, will be affected; in the areas comprising smaller particles, reaction would already be over and the region dead with respect to progress of reaction.

Sasaki (1964) first attempted to account for the effect of particle size distribution on kinetics. The basic rate expression assumed was the one developed by Carter (1961 b). Saski considered groups of different size

TABLE 1.4

Examples of Systems for which Mixed Powder Models have been Used

No.	Systems	Model	Experimental technique	Reference
1	2	3	4	5
1	$MgO-Fe_2O_3$	Jander	X-ray diffraction	Fresh and Dooling (1966)
2	$MgO-Al_2O_3$	Serin-Ellickson	Chemical analysis of unreacted MgO	Hlaváč (1961)
3	$NiO-Fe_2O_3$	Empirical	Saturated magnetisation measurements	Blum and Li (1961)
4	$NiO-Fe_2O_3$	Jander		Economos and Clevenger (1960)
5	$NiO-Al_2O_3$	Serin-Ellickson	Chemical analysis of unreacted NiO by EDTA titration	Stone and Tilley (1965)
6	$ZnO-Fe_2O_3$	Jander (for T 1000°C)	(i) X-ray diffraction (ii) Chemical analysis	Duncan and Stewart (1967)
7	$ZnO-Fe_2O_3$	Jander	Chemical analysis of unreacted ZnO	Krishnamurthy et al (1974)
8	$ZnO-Al_2O_3$	(i) Second order kinetic (ii) Valensi-Carter (T 1000°C)	X-ray diffraction	Branson (1965)

TABLE 1.4 (Continued)

1	2	3	4	5
9	$ZnO-BaCO_3$	Nuclei growth	Thermogravimetric analysis	Hulbert and Klawitter (1967)
10	$Fe_2O_3-BaCO_3$	Jander	Chemical and gravimetric analysis	Ward and Struthers (1937)
11	$Fe_2O_3-Li_2CO_3$	Ginstling-Brounstein	Thermogravimetric analysis	Johnson and Gallaghar (1975)
12	Fe_2O_3-NiO Fe_2O_3-ZnO Fe_2O_3-CdO	Reduced time plot of Sharp et al	Mössbauer spectroscopy	Eiss et al (1976)
13	$Fe_2O_3-Bi_2O_3$	Second order kinetic (for simultaneous reactions)	X-ray diffraction	Mukherjee and Wang (1971)
14	$PbO-ZrO_2$	Valensi-Carter	(i) X-ray diffraction (ii) Chemical analysis of unreacted PbO	Sasaki (1964)

TABLE 1.4 (Continued)

1	2	3	4	5
15	SiO_2-graphite	(i) Linear rate law (for low temperature and/or short time) (ii) Nuclei growth (for high temperature and/or long time)	Measurement of CO gas formed	Klinger *et al* (1966)
16	SiO_2-ZrO_2	Second order kinetic	X-ray diffraction	Ramani *et al* (1969)
17	CaO-Ag_2SO_4	Serin-Ellickson	Weight loss measurements	Riemen and Daniels (1957)
18	UO_2-graphite	Carter	Optical microscopy	Lindemer *et al* (1969)
19	WO_3-$SrCO_3$	Serin-Ellickson	Thermogravimetric analysis	Flor *et al* (1974)
20	Phthalic anhydride-sulphathiazole	Serin-Ellickson	Chemical analysis	Tomás *et al* (1969)
21	Phthalic anhydride-p-nitroaniline	Jander	Chemical analysis	Ramachandran *et al* (1974)

TABLE 1.4 (Continued)

1	2	3	4	5
22	Urea nitrate–tricalcium phosphate	(i) First order (fine particles) (ii) Parabolic (coarse particles)	(i) Electrical conductivity (ii) Chemical analysis	Kutty and Murthy (1974)
23	p-Divinyl benzene–$KClO_4$	Empirical	Volhard method of chloride analysis	Patai *et al* (1961)

particles designated by mean radius ($_ir_o$) for i^{th} group, fraction of component A in i^{th} group (f_i) and reacted fraction of i^{th} group (α_i).

Carter's expression was then applied to obtain for the i^{th} group an expression:

$$\frac{Z-\{1+(Z-1)\ \alpha_i\}^{2/3} - (Z-1)\ (1-\alpha_i)^{2/3}}{2\ (Z-1)} = \frac{k}{a_o^{2(i-1)}\ {}_ir_o^2}\ t \qquad (1.48)$$

where $_ir_o = a^{i-1}\ {}_1r_o$ and a_o is the ratio of the mean radii of adjascent groups. Hence summing up for all the groups, an expression for overall conversion was obtained. But, in this treatment, it was assumed <u>a priori</u> that the Valensi-Carter model fits with $Z = 2$, where Z is the volume of the product formed per unit volume of the reactants consumed. This was overcome in another modification of the same expression by Kapur (1973) who considered the integrated function of the fraction reaction completed $\alpha(t)$ with r_n and r_u respectively as the radii of the smallest and the largest particles in the ensamble. He obtained

$$\alpha(t) = \int_{r'}^{r_u} M(r)\ \alpha\ (r,kt)\ dr + \int_{r_n}^{r'} M(r)\ dr \qquad (1.49)$$

for $t = t_c(r') > t_c(r_n)$

and

$$\alpha(t) = \int_{r_n}^{r_u} M(r)\, \alpha\,(r,kt)\, dr \qquad (1.50)$$

for $t < t_c\,(r_n)$

since particles of radius $< r'$ react completely in time $t_c(r')$. Here, $M(r)\,dr$ is the mass fraction of the reacting particles in the size range r to $r+dr$. Thus, the effect of completion of reaction in smaller particles in a short time interval has been taken care of. Sasaki's data have been tested for the fit and it has been shown that the model fits the data well with $Z = 2$ (without *a priori* assumption).

Taplin (1974) in his discussion on the generalised rate expression, has used log-normal distribution of particle sizes, in describing linear kinetics.

1.5.3 Effect of additives

Both catalytic and inhibitory effects are found to be exhibited by additives in a solid-solid mixed powder system. These may be due to a number of different

interactions of the additives with the reaction system. Thus, they may affect the crystal structure of a solid by increasing or decreasing the number of defects in the lattice, thereby creating or diminishing vacancy concentration. Such effects are well known in solid state chemistry, particularly in connection with the semiconducting properties of a solid. In fact 'doping' is a well known and very important technique in semiconductor technology. The conductivity of a sample can be increased or decreased. as desired, by addition of the dopents. This has also an important application in catalysis. in view of similar dopent effects. These effects depend on the ionic radii of the dopent and the host cation and also on the site preference characteristics of the cations. Thus, in NiO, addition of Li^{+} increases the conductivity whereas same in ZnO, decreases the conductivity. On the other hand, Ga^{3+} ions have exactly opposite effects on the two.

Additives may also promote sintering on the surface, facilitating material transport, and they may promote reaction by acting as oxygen-transfer agents. They may inhibit the reaction physically by acting as a barrier between reactants, or in some cases chemically by trapping the active intermediates. Elucidation of the correct mechanism of promotion or inhibition requires detailed studies. Patai et al (1961, 1962) have made observations on

the effect of certain additives such as $LiCO_3$, PbO and Zn on the solid phase oxidation of p-DVB and carbon by $KClO_4$.

Schwab and Rau (1958) studied the exchange reaction $ZnO + CuSO_4$. Reaction rate was found to be accelerated by the addition of Li^+ to ZnO and retarded by the addition of Ga^{3+} to it. On the other hand, in the reaction $NiO + MoO_3 \longrightarrow NiMoO_4$, addition of Cr^{3+} to NiO enhanced the rate, while that of Li^+ retarded it.

An interesting observation is reported by Szabó et al (1961) in their studies on the reaction between pure NiO and Fe_2O_3. The activation energy for the reaction was found to be 95 kcal/mole; addition of 1% Cr_2O_3 to the NiO reduced it to 59 kcal/mole, whereas addition of 1% TiO_2 to the Fe_2O_3 raised it to 132 kcal/mole.

1.5.4 The concept of effective contact

Solid-solid reactions differ from other types of heterogeneous reactions (gas-solid, gas-liquid, etc.) mainly in the nature of contact between the reactant partners. Whereas in other cases at least one of the reactants is in a flow pattern, in solid-solid systems both the reactants are stagnant, unless one of them (or part of it) is transported as a gas. Obviously, therefore, the progress of

a solid-solid mixed powder reaction depends to a significant extent on the initial contact between the reactants. The initial contact has to be achieved through proper mixing.

Apart from mixing, other factors like relative particle sizes of the two, particle size distribution, particle shapes, sintering characteristics, etc., also affect the contact between the reactants. Sintering can some times introduce complexity in the analysis since it may change this contact area during the course of a reaction, as a result of contraction or expansion and neck growth. (For detailed discussion on sintering, see Coble and Burke, 1961; Kuczynski and Stablein, 1961).

Goodison and White (1961) studied sintering in the system $MgO-Fe_2O_3$, and found the rate of densification to depend on the ratio of coarse to fine particles; most pronounced contraction was observed in samples with 90% fine MgO mixed with 10% coarse Fe_2O_3, whereas greatest expansion was observed with 10% coarse MgO with 90% coarse Fe_2O_3 particles. Henrich (1954) for the system $CdO-Cr_2O_3$ and Jáky *et al* (1965) for the system $CdO-Fe_2O_3$ observed that the reaction started earlier in compacted tablets than in the uncompacted powder mixtures, but later the rates were slower in tablets than in the uncompacted samples. According to Jáky *et al*, this is due to the reformation of

the CdO/Fe_2O_3 contacts, which can be achieved more easily in uncompacted samples than in the tablets. The observations may be better explained as being due to possible vapour phase diffusion of one of the reactants, since in that case obviously an uncompacted sample will facilitate the diffusion; also it will provide more surface area for reaction. The initial higher rates in tablets could be due to the initial surface reaction, the rate of which will be lower in uncompacted samples, because of less contact area.

Patai *et al* (1961, 1962) considered the effect of contact surface area on the rate constants in their studies on the oxidation of p-divinylbenzene (p-DVB) and carbon by $KClO_4$. The observed rate constants (k) obtained by fitting the data with empirical rate equations were found to depend on the surface areas of the two. New rate constants were obtained using the following expressions:

$$k_1 = k(S_A/S_B) \qquad \text{for } S_A > S_B \qquad (1.51)$$

and

$$k_2 = kr^2(S_A/S_B) \qquad \text{for } S_A < S_B \qquad (1.52)$$

where S_A and S_B are the surface areas of $KClO_4$ and

p-DVB or carbon, respectively and r is the radius of a $KClO_4$ particle. The absolute surface area of the oxidant ($KClO_4$) was found to be more important. The effect of compounding pressure on the k values was also studied. Generally the contact area between two spheres is proportional to $p^{2/3}$. Here the correlation obtained was:

$$k_3 = \frac{k}{p^{1/2}} \qquad (1.53)$$

This is probably due to the irregular shapes of the particles. Increase in contact area and thereby modification of the kinetics has been considered by Tomás et al (1969) who studied the sintering of one of the reactants by dilatometry and correlated it to the overall kinetics.

Recently Johnson and Gallagher (1975) have reported the effect of surface area of the Fe_2O_3 powder on the rate constant in the system Fe_2O_3-Li_2CO_3. They did experiments with Fe_2O_3 powders of different known surface areas to obtain rate constants. Hence an empirical relation for the rate constant was established:

$$k = \frac{c}{r^2} \qquad (1.54)$$

where r is the radius of equidimensioned spheres and c a constant.

An interesting development in the above work was that the surface area of the Fe_2O_3 was assumed to be made up of contributions from equidimensioned spheres. Hence, surface area

$$S = \frac{3}{\rho r} \tag{1.55}$$

where ρ is the density of Fe_2O_3. Combining (1.54) and (1.55)

$$S = \frac{3}{\rho \sqrt{c}} \sqrt{k} \tag{1.56}$$

Equation 1.56 was verified by a logarithmic plot, the slope of which was found to be $1/2$ as expected.

Though the importance of the contact area was realised no attempt was made to treat the problem theoretically. Komatsu (1965) has reported probably the first rigorous attempt based on the number of contact points. The model considered by him for the packing of spherical particles of A and B is represented in Figure 1.5. By simple geometrical considerations, he expressed the number of

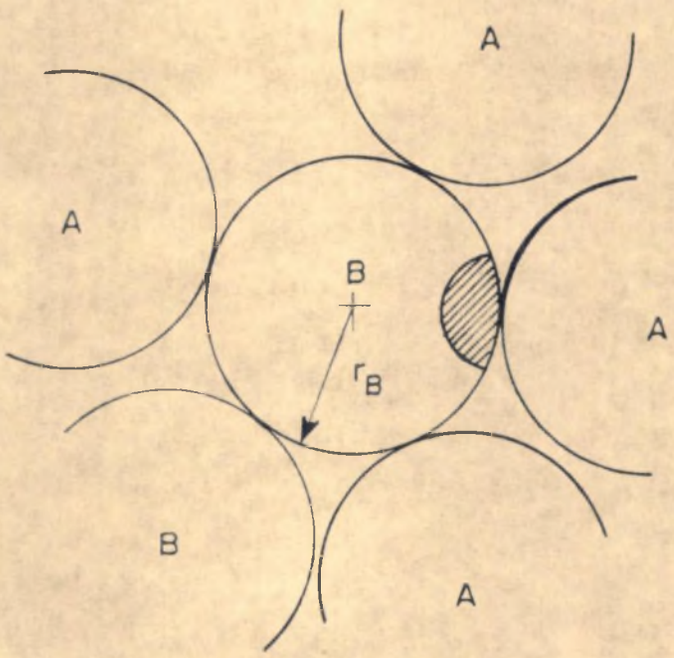

THE MODEL OF THE PACKING

(KOMATSU, 1965)

FIGURE 1·5

contact points between one central B particle and the surrounding A particles in an ideal system by an expression

$$N^{o}(A/B) = N_{B}^{o} \left[\frac{s\,\bar{w}}{1 + s\,\bar{w}} \right] \qquad (1.57)$$

where N_{B}^{o} is the total number of particles of A and B surrounding the central B particle, $\bar{w}$ is the weight ratio of the components (W_A/W_B), and s is given by Equation 1.58:

$$s = \frac{r_B^3\,\rho_B}{r_A^3\,\rho_A} \qquad (1.58)$$

where r_A, r_B and ρ_A, ρ_B are the radii and densities of the components A and B, respectively.

In real systems irregular shapes are encountered; also the packing is not perfect. As such, the actual number N(A/B) would be less than $N^{o}(A/B)$ and is given by

$$N(A/B) = N_{B} \left[\frac{s\,\bar{w}}{1 + s\,\bar{w}} \right]^{g}, \quad g > 1 \qquad (1.59)$$

where the parameter g is introduced to account for the

difference in packing state. He applied his theory to modify the Jander equation and obtained the following expression for the rate constant of the Jander equation:

$$K(T, s, \bar{w}) = K^{o}(T) \left[\frac{s \bar{w}}{1 + s \bar{w}} \right]^{g} \qquad (1.60)$$

The theory was successfully applied to the systems $CaCO_3$-MoO_3, $BaCO_3$-SiO_2, CuCl-Si and $PbCl_2$-Si (Komatsu, 1965). Komatsu and Uemura (1970) have extended the theory to account for counterdiffusion.

Haber and Ziolkowski (1972) have applied the Komatsu model to the system Co_3O_4-MoO_3. They considered the following relations:

$$K = K_o \left[\frac{s \bar{w}}{1 + s \bar{w}} \right]^{g} , \quad r_A/r_B > 1 \qquad (1.61)$$

and

$$K = K_o \left[\frac{1}{1 + s \bar{w}} \right]^{g} , \quad r_A/r_B < 1 \qquad (1.62)$$

From logarithmic plots they obtained the values of the parameter g. Thus g was found to be 13.6 for $r_A/r_B > 1$

and 3.74 for $r_A/r_B < 1$.

The same authors calculated the rate constant k for unit surface area of Mn_2O_3 in the system Mn_2O_3-MoO_3 and found that this k was constant with composition.

1.5.5 Multicomponent systems

In some cases, e.g. in the cement industry, one has to deal with multicomponent solid-solid reactions. Even when one goes from a binary to a ternary system, the phase diagram, if available, reveals the complexity in the system. An additional composition term is involved, and the behaviour of the system depends on the region of the phase diagram in which one is operating. If the additional third component is in a minute quantity ($< 1\%$), it can be treated as a dopent which affects the system in a particular fashion. This has been discussed in Section 1.5.3. When all the three components are in comparable proportions, a variety of new compounds may be formed. Systems consisting of more than three components will obviously be considerably more complex.

So far, only a few phase equilibrium studies have been reported in the literature. Thus, Reijnen (1965) has studied the system MgO-FeO-Fe_2O_3; Winkler (1965) has

reported structure studies in the systems $BaO-MeO-Fe_2O_3$ (Me = Co, Ni, Cu, Zn, Mn, Mg). Analysis of diffusion and reaction in such systems has not yet been attempted.

1.6 ROLE OF THE GAS PHASE

The gas phase has always played an important role in solid-solid reaction studies. Some time back it was a major subject of controversy amongst the workers in the field. In fact, a group of Russian investigators claimed that all the mixed oxide solid-solid reactions occur via gas phase diffusion, the first step being the dissociation of one of the reactants. This conclusion was based on the fact that contact area between particles presents too small a cross-section for rapid diffusion.

1.6.1 Contribution of vapour phase diffusion

The larger chemical reactivity of small particles is often accounted for by Thomson's relation (Parravano, 1962):

$$\ln \frac{p}{p^o} = \frac{M}{RT} \frac{2r}{\rho 2} \qquad (1.63)$$

which gives the vapour pressure over the surface of a solid with a radius of curvature r, solid density ρ and

molecular weight M, as a function of the pressure in equilibrium over a flat surface. Clearly, with decreasing particle size, the vapour pressure increases tremendously. This also corresponds to an increase in free energy of the surface. In fact the driving force for subsequent sintering in the compacts arises from the excess surface free energy of the pressed compact over that of the final sintered body (Clarke and Williams, 1961).

Many organic substances are known to sublime or to have considerable vapour pressure. Certain inorganic oxides such as NiO, ZnO and PbO (Pettit et al, 1966; Duckwitz and Schmalzried, 1971; Harris and Cook, 1968) are also known to be transported via the vapour phase, as shown by experiments with nonporous materials or with the reactants kept apart.

Konoyuk and Vashuk (1974) treated the kinetics of solid phase reactions whose rate is limited by the sublimation of one of the reactants. They also applied Thompson's relation in the form

$$\frac{dp}{dr} = \frac{RT\,j}{4\pi r^2 D}\left(1 - \frac{p}{p^o}\right) \qquad (1.64)$$

where p_o = total pressure, p = partial pressure and

j = flux of the substance evaporating from a unit surface of a spherical body with radius r and at temperature T. The final expression obtained was shown to be the same as that of Ginstling and Brounshtein (see Table 1.3) under certain conditions.

Apart from sublimation, the other process that contributes to gas phase diffusion is dissociation. Thus, in many oxide systems, oxygen pressure is shown to affect the kinetics greatly since transport of oxygen in the gas-phase occurs along with the cation diffusion.

Certain solid-solid reactions of industrial importance are known to proceed via gaseous intermediates. Thus in the reaction between silica and graphite, Klinger et al (1966) have shown that the reaction proceeds through the dissociation of silica :

$$SiO_2 \longrightarrow SiO + \frac{1}{2} O_2$$

$$SiO + C \longrightarrow SiC + \frac{1}{2} O_2$$

The reduction of iron ore (e.g. hematite) by the solid reductant coke (carbon) proceeds via intermediate carbon monoxide formation except for the initial stage. Thus,

$$Fe_gO_h(s) + CO(g) \longrightarrow Fe_gO_{h-1} + CO_2(g)$$

and

$$C(s) + CO_2(g) \longrightarrow 2\ CO(g)$$

This reaction has been treated mathematically in detail by Rao (1971), Rao and Chuang (1974) and Sohn and Szekely (1973). The second reaction is taken to be controlling, so that a treatment based on first order gas-solid reaction is followed.

Ginstling and coworkers (Ginstling, 1951; Ginstling and Fradkina, 1952; Pozin *et al*, 1954) carried out several experiments by heating the reactants kept some distance apart and concluded that the reaction proceeds via gas phase diffusion. Yet, this should not rule out the possibility of other mechanisms being operative under mixed powder conditions. *In situ* elucidation of mechanism was attempted by Borchardt (1959). He derived an expression for the maximum reaction rate for the gas phase diffusion mechanism by considering a dissociation step. The maximum reaction rate was given by

$$\bar{R} = \frac{265\ M_s p}{\rho_s n d (M_g T)^{1/2}} \qquad (1.65)$$

where M_g and M_s are the molecular weights of the gas and

the dissociating solid respectively, p is the dissociation pressure, ρ_s the density of dissociating solid, d the particle diameter, and n the number of moles of gas evolved per mole of solid. Further, using the thermodynamic relationship

$$\ln p = \frac{-\Delta H^{o}}{RT} + \frac{\Delta S^{o}}{R} \qquad (1.66)$$

he derived an expression for the lowest temperature of dissociation at which at least 1% conversion should occur. Applying this to the reactions between U_2O_8 and Fe, Cr, Nb and Ni it was positively concluded that for some systems at least (e.g. U_3O_8-Fe and U_3O_8-Nb) gas phase diffusion is absent, since reaction occurred even below the lowest dissociation temperature calculated.

Gluzman and Mil'ner (1960) studied some organic solid-solid reactions with a view to investigating the role of the gas phase in them. In their experiments they separated the two reactants with a fine copper wire mesh so that minimum contact is allowed between particles of the two. They analysed the samples of the two for product formation and concluded that there is little contribution of gas phase diffusion to the reaction, though it was not completely ruled out.

Recent studies by Rastogi and coworkers (Rastogi, 1970; Rastogi et al, 1962; Rastogi and Singh, 1966) show considerable reaction occurring via gas phase diffusion. The experimental technique was one in which two reactants were filled in a capillary with a known distance of separation. The kinetics was followed using the equation:

$$(\Delta x)^2 = 2 K_1 t \exp(-q \Delta x) \tag{1.67}$$

or with the parabolic rate equation

$$(\Delta x)^2 = K_2 t \tag{1.68}$$

depending on the fit of the model.

They also correlated the distance of separation to the kinetics applying the expressions:

$$K_1 = c_1 e^{q_1/x' + c_2} \tag{1.69}$$

and

$$K_2 = c_3 e^{-q_2 x'} \tag{1.70}$$

where x' is the distance of separation and c_1, c_2, c_3, q_1

and q_2 are constants.

In Equation 1.69, as $x' \rightarrow 0$, K_1 attains the value obtained when reactants are in contact, thereby supporting the gas phase diffusion mechanism; whereas in the case of Equation 1.70 since $K_2 \rightarrow 0$ as $x' \rightarrow 0$, it indicates that some other mechanism contributes along with the gas phase diffusion, possibly the surface migration.

1.6.2 Effect of added gases

Forestier and Kiehl (1949, 1950) extensively studied the effect of different gases present on the reaction rates at lower temperatures. They studied the effect of different gases on the nickel ferrite formation reaction. Clear dependence of the rate of formation of the spinel on the liquifaction point of the gas was observed (Figure 1.6). From these studies Forestier concluded (Forestier, 1956): (i) the rate of reaction increases symbatically with the liquification point of the gas used and consequently depends on the amount of adsorbed gas; and (ii) for the same gas, reaction rate is a linear function of the logarithm of the gas pressure and the rate tends to zero as the pressure falls to zero. Thus the effects were mainly attributed to the adsorption of gases.

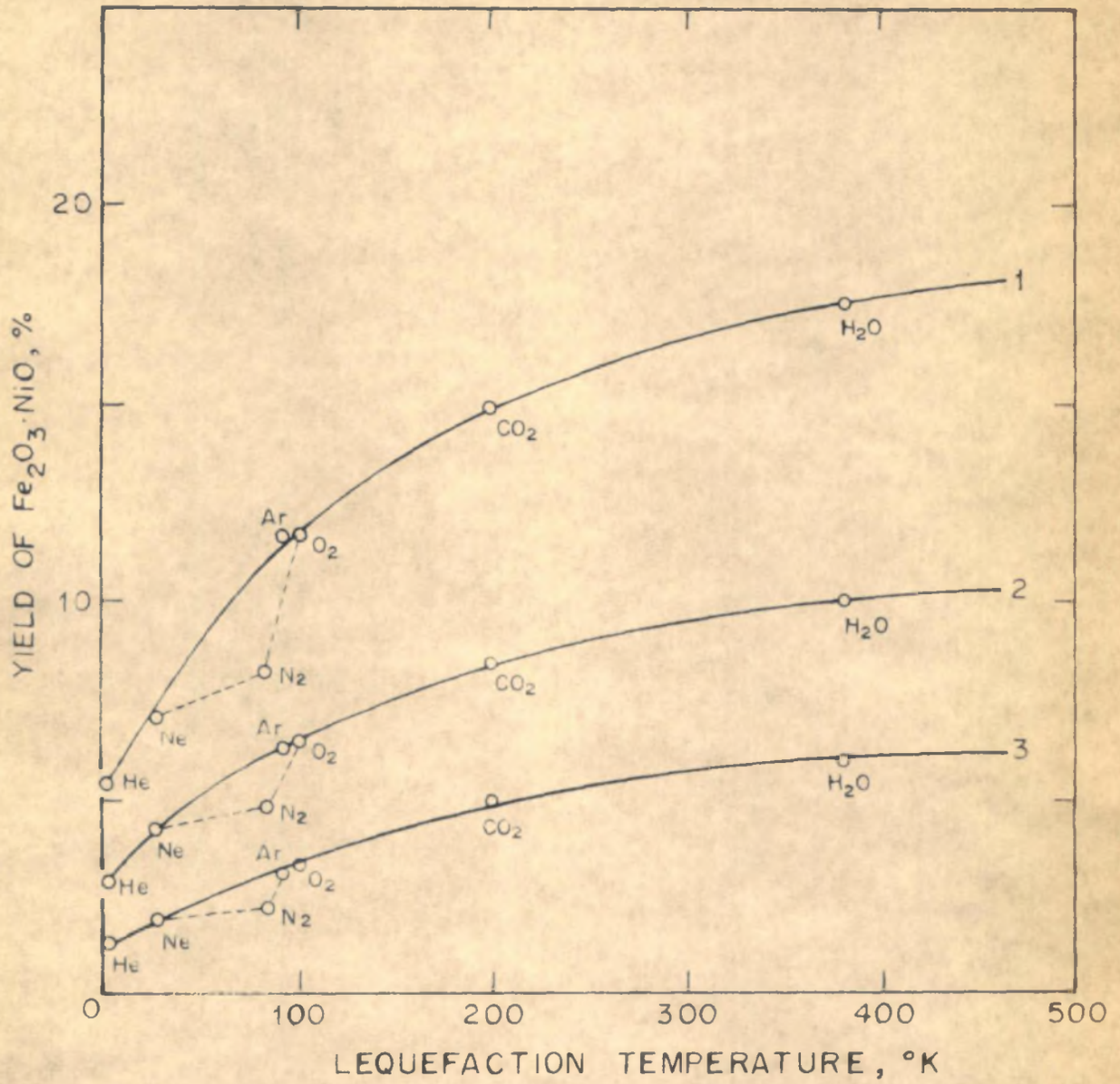

RELATION OF THE YIELD OF NICKEL FERRITE IN ATMOSPHERES OF VARIOUS GASES

(1) 700; (2) 650; (3) 600 °C. HEATING TIME 15 min

(FORESTIER AND KIEHL, 1950)

FIGURE 1·6

Weyl (1956) found that gases adsorbed on the surface of a crystal, even chemically inactive gases such as N_2 or the inert gases, modify the electronic structure of the surface atoms and thus have a considerable effect on the chemical bonds in the solids. Trambouze and Silvent (1961) studied the reaction

$$NiO + MoO_3 \longrightarrow NiMoO_4$$

in presence of various gases. It was observed that inert gases caused higher rates than in vacuum. Reactive gases, such as O_2, H_2, CO_2, had more effect, water vapour having the maximum. They explained the effect to be due to the chemisorption of gases on NiO and considered the controlling process to be surface diffusion. Leonov (1961) observed that in the reaction between MgO and Al_2O_3, the amount of spinal formed in 80 minutes at 1150°C in air was 11.8% and in hydrogen 41.0%. Similarly, for the reaction $ZnO + Al_2O_3 \longrightarrow ZnAl_2O_4$, he observed that in purified argon the reaction proceeded much more rapidly than in argon containing 0.4% O_2 (Leonov, 1960). Leonov thus concluded that reactions between oxides proceeded more rapidly when the partial pressure of O_2 in the gas phase is commensurate with the dissociation pressure of the oxides. The chemical stability of oxides is therefore determined by their dissociation pressure (Toropov and Barzakovskii, 1966) and not by the

melting point as proposed by Tammann who introduced the concept of "reaction temperature" (Tammann, 1925).

Gas phase diffusion is faster than solid phase diffusion, since it occurs through contact areas (which itself may be faster) as well as through pores. This fact could be utilised in synthesising certain materials by deliberately introducing a gas phase into the system. Shäfer (1971) has suggested some interesting synthetic routes. Accordingly, the reaction

$$2CaO + SnO_2 \xrightarrow{900^{\circ}C} Ca_2SnO_4$$

can be accelerated by adding CO or H_2 to the system, since

$$SnO_2(s) + CO \longrightarrow SnO(g) + CO_2$$

and SnO(g) can further react more easily with CaO. Also, in the reaction,

$$NiO + Cr_2O_3 \xrightarrow{1100^{\circ}C} NiCr_2O_4$$

If O_2 is introduced, we have

$$Cr_2O_3 + \frac{3}{2} O_2 \longrightarrow 2\ CrO_3(g)$$

and $CrO_3(g)$ can further react to give the desired product $NiCr_2O_4$.

1.7 REACTOR DEVELOPMENT

1.7.1 Basic design considerations

Standard design procedures have not so far been developed for solid-solid reactors. In most cases, the conventional ceramic technique is used for manufacturing purposes. In this, the finely powdered reactants are first intimately mixed, usually in a ball mill, the powder mixture is pelletised if necessary and heated at the desired temperature for a predetermined time interval. Often the material thus obtained is reground, pelletised and heated again. The procedure is repeated two or three times to ensure complete conversion.

The main difficulties in solid-solid reactions are the requirement of complete mixing (and hence initial ideal contact between reactant particles) and continuous removal of the product layer formed in order to promote better contact between yet unreacted phases. Sintering, as mentioned earlier, presents additional complexity. In the conventional ceramic technique, these difficulties are

overcome by the repeat cycle procedure.

Unlike in other heterogeneous processes, here none of the reactants can be in a flow pattern; contact between unreacted phases can be achieved only through solid state diffusion, which is known to be extremely slow. It can be remedied either by having a device in which the processes of mixing, grinding and heating can be carried out simultaneously (e.g. a rotating furnace-cum-ball mill), or by deliberately introducing a gas phase in the reaction as suggested by Schäfer (1964) (see Section 1.6). The work of Fiegl *et al* (1944) is worth noting in this connection; he carried out solid-solid reactions even at high temperatures with constant stirring using a platinum stirrer.

The contact between solid particles can also be improved by applying pressure. In fact, acceleration of reaction rates by applied pressure is made use of in modifying the ceramic technique; the process is known as pressure sintering or hot pressing. The process normally consists of applying pressure to the ceramic, in powder or cold pressed compact form, in a refractory mould which is heated to an optimum temperature for densification. The pressures employed are of the order of 1000 to 10,000 psi; and temperatures upto 2500^{o}C are used.

An obvious advantage of the process is a lower temperature requirement. In addition, it also helps in achieving microstructural control, enhanced densification, composite fabrication and pressure bonding. As such, it is increasingly used as a fabrication process, especially in the ceramic industry. A detailed review has been presented by Vasilos and Spriggs (1966).

1.7.2 Mechanical design

Information on mechanical design is scanty. There are no standard design procedures; most of the commercial plants are designed from experience and on the basis of empirical expressions. The industries in which this problem is encountered are: ceramics. ferrites, semiconductors, metals and cement. Reactors are either batch type or continuous.

Of these, the ceramic, the ferrites and the semiconductor industries mostly use batch type reactors, following the procedure as described above. The problem of reactor design, therefore, reduces to one of designing a furnace and a mixer for the initial mixing stage. This is done mostly from experience.

In the metal industry, one is concerned with the

reduction of ores (e.g. hematite reduction by coke) wherein solid-solid reactions are encountered. In the cement industry, solid-solid reaction is a major step since the important constituents are all present as solids and react in the solid state. In both the cases, a rotary kiln is used as a reactor. As such, the process is normally a continuous one; the reaction mixture is fed in at one end of the kiln, and discharged at the other end. A gas is also some times introduced in cocurrent or countercurrent flow.

The rotating kilns used in the cement industry are very long (length of the order of 200 to 500 feet and diameter upto 20 to 30 feet); they are positioned slightly inclined to the horizontal (Pollitt, 1964). The entire length is divided into zones for drying, reaction and cooling. The residence time of the cement raw mix in such kilns is typically 2.5 hours in a 200 feet long kiln and 6 hours in a 450 feet long kiln.

Equations have been developed for calculating the length and diameter; for example for a dry process the length required is given by (Martin, 1932):

$$L_k = 20(d_k-1.5) + 0.2\ (d_k-1.5)^2 \qquad (1.71)$$

For design purposes, much depends on the heat requirements in different zones, and as such on the heat capacities of the reactants and products. Calculations are thus made on the basic data available and what is known as a "heat treatment schedule" is prepared.

Verticle tube reactors are also in use in the cement industry. The heights in this case are of the same order as the length of the rotary kiln. Air is passed from the bottom and the raw mix fed at the top. This somewhat resembles a fluidised bed reactor; the air flow is used to adjust the residence time of the raw mix in the reactor.

1.7.3 Recent developments

From the above discussion it may be seen that there is need to develop newer and better processes for the manufacture of mixed oxides. The conventional ceramic technique has obvious drawbacks; also the steps involved being slow, it cannot be adapted to continuous production.

Novel processes have recently been developed, particularly for the manufacture of ceramic nuclear fuels. These can be readily adapted in other industries. The processes developed are: (a) sol-gel process, (b) gel precipitation, and (c) spray processes (pyrogel process and

flame reactor). All of these essentially start with an aqueous phase containing the metal ions in the desired proportions. The main advantages are: (i) lower temperature requirement, (ii) shorter time of contact needed for conversion, and (iii) control over particle size. A brief account of the processes is presented below (Dell, 1972).

(a) Sol-gel process

In essence, this involves forming a concentrated colloidal sol to a semi-rigid gel by a convenient method. The gelation stage is important since it determines the particle shape and size of the final product. The gel is then dried and calcined to obtain the desired product. The process is best suited to the preparation of coarse products.

(b) Gel precipitation

This process combines the advantages of the sol-gel process with those of the well known coprecipitation technique used especially in catalyst preparation. In precipitation often the filtration of hydroxides presents problems since the precipitates are gelatinous. This difficulty is overcome by adding an organic gelling agent, thereby converting the precipitate into a granular form.

(c) Spray processes

The general principle involved here is atomisation of the solution to form a fine spray of droplets which are thermally decomposed in a high temperature environment. This is known as flash hydrolysis. During the short residence time (1-5 seconds) of material in the reactor, the solution evaporates, solidifies, decomposes and undergoes solid state reaction. In this the particle size can be precisely controlled by adjusting the spray parameters. Two types of reactors are used for the purpose; in one the solution is sprayed into a tube heated externally (pyrogel process), and in the other the solution is sprayed directly into a high temperature flame (flame reactor).

Spray processes can also be adapted to alloy preparation by subsequent reduction of the mixed oxides obtained. These are particularly attractive from the chemical engineering view-point, since they can be utilised for continuous production. Further efforts are needed to exploit this novel technique.

CHAPTER 2

DIFFUSION AND REACTION IN PELLET-PELLET SYSTEMS

2.1 INTRODUCTION

The role of diffusion in solid-solid reactions is far more significant than in any other reacting system, such as gas-liquid, gas-solid, etc. As the actual three-dimensional geometry of solid-solid systems is quite complex, no simple mathematical analysis seems possible. To facilitate mathematical analysis, however, pellet-pellet experiments may be carried out. The basic advantage in these experiments is that, the contact surface area being constant, reaction rates can be determined by direct measurement of the product layer thickness.

In such studies, as pointed out in Chapter 1 (Section 1.4.3), it is almost always assumed that the rate is controlled by the diffusion of the reactant species in the product layer. The diffusion and reaction of one of the reactants in the other (resulting in a reaction zone) is often neglected. In the present analysis, assuming first-order kinetics, a model is developed in which the role of the reaction zone is explicitly brought out; and using reported data (obtained by EPMA), the proposed model is verified. The treatment is extended to an n^{th} order reaction

and a procedure indicated for obtaining the order and the concentration profiles in the reaction zone. Considering the assumptions made in the development, the model should only be regarded as providing a predictive equation for pellet-pellet reactions.

2.2 THEORETICAL DEVELOPMENT

2.2.1 The nature of the problem

Let us consider the general class of reactions between two metal oxides AO and B_2O_3:

$$AO + B_2O_3 \longrightarrow AB_2O_4$$

Among the industrially important reactions belonging to this class are reactions between an oxide of a transition metal (Cu, Co, Ni, Mg, Zn, etc.) and Fe_2O_3, Al_2O_3 and Cr_2O_3 to give respectively ferrites, aluminates and chromites. The important mechanisms of mass transport in these reactions are: (i) one-way diffusion of either A^{2+} and O^{2-} or $2B^{3+}$ and $3O^{2-}$, (ii) counter-diffusion of $3A^{2+}$ and $2B^{3+}$, and (iii) one-way diffusion of A^{2+} and $2e^-$ and of oxygen as gas (O_2). In cases (i) and (iii) product growth is restricted to one side of the original interface, whereas for case (ii) it occurs on both sides. In all the cases the slower

moving species will be rate controlling, and different expressions for diffusivities are involved, as explained in the general treatment of Wagner and the later developments of Schmalzried (1974).

As in the case of gas-solid (catalytic) reactions, several modes of diffusion are possible in solid-solid systems as well. The more important among these are: (i) vacancy mechanism, (ii) interstitial mechanism, (iii) surface diffusion, (iv) grain-boundary diffusion, and (v) vapour phase diffusion.

In systems where polycrystalline materials are involved, all or some of the above mechanisms may be operative simultaneously, and separate diffusivities for each mechanism cannot be determined. Hence an overall effective diffusivity D_e may be used as in the case of gas-solid systems. If, however, single crystals are involved, a single mode of diffusion (viz. volume diffusion mainly by vacancy mechanism) should be adequate to define the transport process. In the gross approach using an effective diffusivity D_e, one can apply Fick's laws of diffusion, as in the case of solid catalysts.

From the three important mechanisms of mass transport in such reactions, it can be readily seen that all involve

moving boundaries. In cases (i) and (iii) there would be only one moving boundary, whereas in case (ii) both the boundaries of the product layer would be moving, since product growth occurs on both sides. In addition, in a few instances, a different mechanism may be observed. Thus in certain ferrite formation reactions Fe^{3+} is transported as Fe^{2+} and is again oxidised to Fe^{3+} which reacts to form the ferrite spinel; simultaneously oxygen from Fe_2O_3 is transported in the same direction, while A^{2+} from AO is transported in the opposite direction (Kooy, 1964; Krishnamurthy *et al*, 1974). This situation is similar to the case (iii) described above. In general, in reactions between oxides, case (iii) is more commonly encountered. Hence in the following treatment, this case is chiefly considered. However, to generalise the treatment, the reference axis may be fixed on one of the boundaries and the relative movement of the other boundary followed. Thus in all the three cases there will now be only one moving boundary.

Fortunately, since in all inorganic systems ionic species are involved in the diffusion process, the individual diffusivities are interrelated due to the condition of electroneutrality to be maintained. Hence, even in the case of counter-diffusion of A^{2+} and B^{3+}, an interdiffusion

coefficient $\tilde{D}$ has been defined based on the mole fraction and activity of one of the compounds, usually of AO (Wagner, 1969).

Thus the concentration profile of only one of the species may be followed to monitor the rates. In the case of counter-diffusion, for example, $3A^{2+}$ diffuse and result in three molecules of AB_2O_4, whereas at the same time for charge balance $2B^{3+}$ diffuse and form one molecule of AB_2O_4 at the other boundary. Hence, if we follow only the concentration profile of say A^{2+}, the actual rate of product layer growth will be 4/3 times higher, which will be automatically taken care of by the rate constant of the process, since the reference axis is fixed on one of the boundaries. However, in this case more than one moving boundaries are involved; also basically four different diffusivities and two rate constants are involved. As such mathematical analysis of the process becomes extremely complicated. The present treatment is therefore restricted to a case of one-way diffusion only.

2.2.2 Reaction modelling

Using the concept of an effective diffusivity, a model is now developed for solid-solid reactions based essentially on the moving zone theory for gas-solid reactions

developed earlier by Tudoze (1970) and Mantri et al (1976). In fact Schmalzried (1974) has postulated an effective reaction zone for phase boundary controlled reactions in solid-solid systems also. An analysis of such a zone has been presented by Greskovich and Stubican (1969) wherein they have considered only the diffusion in this zone.

Mention should be made at this stage of a model proposed by Arrowsmith and Smith (1966). This represents perhaps the first attempt to present a quantitative analysis of solid-solid reactions. Two semi-infinite solid rods are considered and boundary conditions at infinity are used. In the zone model developed below, on the other hand, boundary conditions at finite distances are used. This is particularly important when spherical geometry is considered, since the infinite boundary conditions lead to a source or a sink at infinity. Further, here a first-order reaction is assumed as against a second-order reaction assumed by Arrowsmith and Smith.

According to the moving zone concept, reaction in a gas-solid system occurs in three stages: zone formation, zone travel, and zone collapse. Mantri et al have formulated mathematical equations for the three zones and have also derived an expression for the zone thickness for a first order reaction.

Experimental studies on solid-solid reactions using the EPMA technique give the concentration history of one of the solid reactants in the second reactant as the reaction progresses. Typical concentration profiles have been reported for a few systems (Yamaguchi and Tokuda, 1967; Minford and Stubican, 1974; Whitney II and Stubican, 1971). An inspection of these profiles reveals some interesting facts, which point to a similarity in behaviour with the zone model for gas-solid reactions mentioned above. Hence a model is first formulated using the concept of a moving reaction zone, and then a quantitative verification of the model using reported EPMA concentration profiles is presented.

The system can be most appropriately described in terms of two zones: (i) the product zone and (ii) the reaction zone. At time $t = 0$, the two solids are brought together, and kept in contact under isothermal conditions. The reaction is initiated at the phase boundary and progresses inwards, forming a reaction zone of finite width. On completion, this zone starts moving as a whole, leaving behind the product zone formed as a result of the reaction occurring in the reaction zone. Further, the product zone formed may offer a diffusional resistance, thereby decreasing the concentration available for reaction at the interface

between the two zones. This new concentration at the interface may then be maintained at its value by unsteady state diffusion or may continue to decrease depending on the system properties. A few typical stages in the model are illustrated in Figure 2.1. The zone designated here as the reaction zone is referred to as the solid solution region in the EPMA studies.

The situation visualised above involves a moving boundary problem which is normally solved by assuming a pseudo-steady state. This assumption is valid in the case of gas-solid (noncatalytic) reactions, since the rate of transport of gas to the moving boundary is much faster ($\sim$ 1000 times) than the rate of movement of the boundary, which arises because of the large density difference between a gas and a solid. This is obviously not the case in solid-solid systems. Hence, in the following treatment, unsteady state behaviour has been considered.

An analysis of the system at an intermediate stage is attempted. The equations obtained can be adapted to any particular stage by applying the proper boundary conditions. The two zones, viz. the product zone and the reaction zone, are considered separately and the mass balance equations for the two are solved with the corresponding boundary

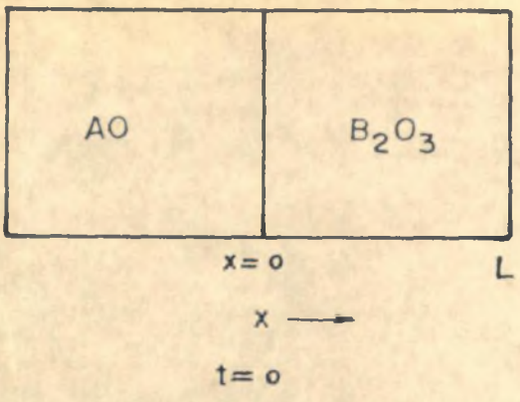

NO REACTION

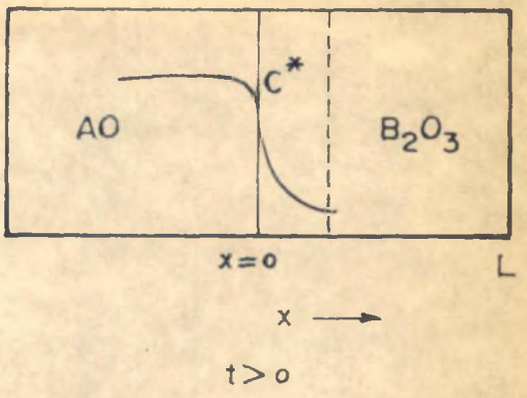

REACTION ZONE FORMATION WITH NO PRODUCT LAYER

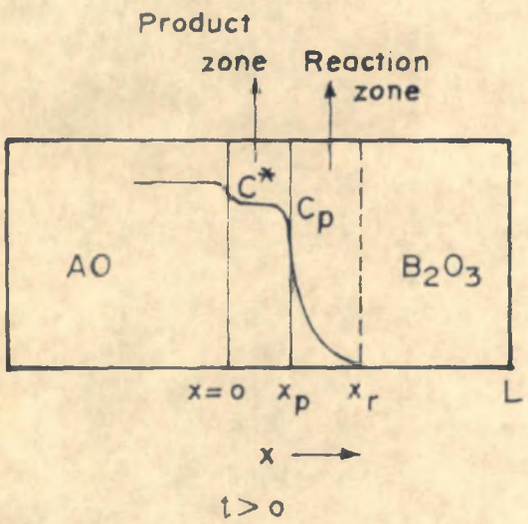

REACTION ZONE ALONG WITH A PRODUCT LAYER WITH NO DIFFUSION RESISTANCE

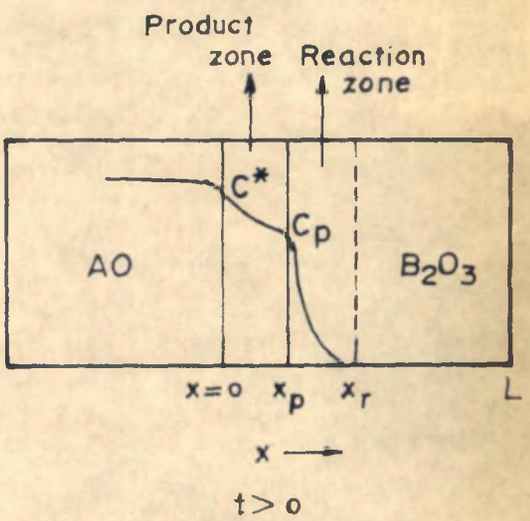

REACTION ZONE ALONG WITH A PRODUCT LAYER WITH A FINITE DIFFUSION RESISTANCE

STAGES IN THE REACTION BETWEEN THE SOLIDS AO AND B_2O_3 IN THE REACTION ZONE MODEL

FIGURE 2·1

conditions; but attention is mainly focused on the reaction zone.

(1) Product zone

As mentioned earlier, the diffusivity is assumed independent of concentration. The governing differential equation can be written as:

$$\frac{\partial C}{\partial t} = D_p \frac{\partial^2 C}{\partial x^2} \tag{2.1}$$

where D_p is the diffusivity of the species under consideration in the product zone (the subscript e indicating effective values being dropped). The initial and boundary conditions are:

$$\left.\begin{aligned} C &= C^o \quad x < 0 \\ C &= 0 \quad x > 0 \end{aligned}\right\} \quad t = 0 \tag{2.2}$$

$$\left.\begin{aligned} C &= C^*, \quad x = 0 \\ C &= C_p, \quad x = x_p \end{aligned}\right\} \quad t > 0 \tag{2.3}$$

The profile is assumed to be extended to infinity, with the additional boundary condition,

$$C = 0, \quad x = \infty, \quad t \geq 0 \tag{2.4}$$

The solution satisfying initial conditions (2.2) and boundary conditions (2.3) and (2.4) is given by Crank (1975) as

$$C = C^* \text{ erfc } \frac{x}{2(D_p t)^{1/2}} \tag{2.5}$$

This solution, derived for a semi-infinite system, is also valid for a region bounded by one or two x-planes (Danckwerts, 1950), if concentrations are the same at the same points in the two cases.

New variables are now defined to convert the expression given by Equation 2.5 into a dimensionless form:

$$\omega = \frac{C}{C^*}, \quad z = \frac{x}{L} \text{ and } \theta = \frac{D_p t}{L^2} \tag{2.6}$$

With these new defined variables, Equation 2.5 becomes

$$\omega = \text{erfc } \frac{z}{2\theta^{1/2}} \tag{2.7}$$

The dimensionless concentration at the end of the

product zone ω_p can be obtained as

$$\omega_p = \text{erfc} \frac{z_p}{2\theta^{1/2}} = 1 - \text{erf} \frac{z_p}{2\theta^{1/2}} \qquad (2.8)$$

(2) Reaction zone

As a first approximation, we shall assume the reaction zone to be of constant thickness. This assumption will be verified later.

Since the time dependence will be implicit in one of the boundary conditions, viz. the boundary condition at the interface between the two zones, the governing differential equation for the reaction zone (with D_r as the diffusivity in this zone) can be written as

$$D_r \frac{\partial^2 C}{\partial x^2} - kC = 0 \qquad (2.9)$$

With initial conditions given by Equation 2.2 and boundary conditions

$$\left.\begin{aligned} C &= C_p, \quad x = x_p \\ \text{and} \quad C &= 0, \quad x = x_r \end{aligned}\right\} \quad t > 0 \qquad (2.10)$$

where the second term accounts for the first-order reaction rate. Here, in addition to the dimensionless variables defined by Equation 2.6, a Thiele modulus is defined as

$$\phi_r = L\left[\frac{k}{D_r}\right]^{1/2} \tag{2.11}$$

Using Equations 2.6 and 2.11, (2.9) becomes

$$\frac{d^2\omega}{dz^2} - \phi_r^2\omega = 0 \tag{2.12}$$

with the boundary conditions

$$\left.\begin{aligned} \omega &= \omega_p, \quad z = z_p \\ \omega &= 0, \quad z = z_r \end{aligned}\right\} \quad t > 0 \tag{2.13}$$

The solution of Equation 2.12 is straightforward and is given by

$$\omega = \omega_p \frac{\sinh\{\phi_r(z_r - z)\}}{\sinh(\phi_r \Delta z)} \tag{2.14}$$

where

$$\Delta z = z_r - z_p \tag{2.15}$$

represents the reaction zone thickness. Substituting Equation 2.8 in (2.14), we get

$$\omega = \left(\text{erfc}\ \frac{z_p}{2\theta^{1/2}}\right) \frac{\sinh\{\phi_r(z_r - z)\}}{\sinh(\phi_r \Delta z)} \qquad (2.16)$$

Recent experimental results point to the essential constancy of ω_p. For example, the EPMA results of Whitney II and Stubican (1971) on the system MgO - Al_2O_3 at 1695°C clearly show that the interface concentration is constant and invariant with time. Thus, in the present treatment the analysis is restricted to ω_p = constant. Although in theory ω_p can have a value of unity, it would appear from reported experimental studies (Yamaguchi and Tokuda, 1967; Minford and Stubican, 1974; Whitney II and Stubican, 1971) that ω_p is practically always less than unity because of the interfacial resistance. No explanation seems possible at present for the observed constancy of ω_p; however, the constancy indicates that thermodynamic equilibrium between the phases has been established at the interface.

The most useful aspect of this analysis of solid-solid reactions is that an expression can be obtained for the reaction zone thickness Δz in terms of the Thiele modulus ϕ_r from Equation 2.14. Such an equation can be

readily developed and is identical with that given by Mantri *et al* for a first-order reaction:

$$\Delta z = \frac{1}{\phi_r} \ln \{\phi_r + (\phi_r^2 + 1)^{1/2}\} \qquad (2.17)$$

A comparison of this model with that for gas-solid reactions reveals certain interesting points:

(i) There is no counterpart to the gas film resistance in solid-solid reactions. In fact, the product itself moves in a direction opposite to that of diffusion, even in the case of one-way diffusion.

(ii) Solid-solid reactions are essentially lattice rearrangements, and will always occur in a finite zone thickness, since diffusion and reaction rates are comparable.

2.3 VERIFICATION OF MODEL

The model developed above will now be tested using the reported EPMA results for three distinct systems (involving a ferrite, an aluminate and a chromite) at different temperatures. The steps involved in the procedure used for testing are:

1. Obtain the precise value of the zone thickness for a given system from the reported EPMA data.

2. Using the value of the zone thickness thus obtained and assuming first-order kinetics, calculate the Thiele modulus from Equation 2.17.

3. From Equation 2.14 calculate the concentration at different positions in the reaction zone, using the values of Δz and ϕ_r determined in steps (1) and (2) and employing the value of ω_p obtained from EPMA studies.

4. Prepare a plot of ω vs position in the reaction zone using the values calculated as above and compare with the experimental concentration profile obtained from EPMA measurements.

The profile obtained by EPMA measurements for the system $MgO - Cr_2O_3$ at 1400°C after 20 hours is reproduced in Figure 2.2 (Yamaguchi and Tokuda, 1967). From this the following precise values were obtained:

(i) Δz the reaction zone thickness, as calculated by normalising the actual value Δx (by an arbitrarily chosen value of 1000 μ at which EPMA results indicate no reaction):

$$\Delta z = 0.1$$

(ii) ω_p the dimensionless concentration at the

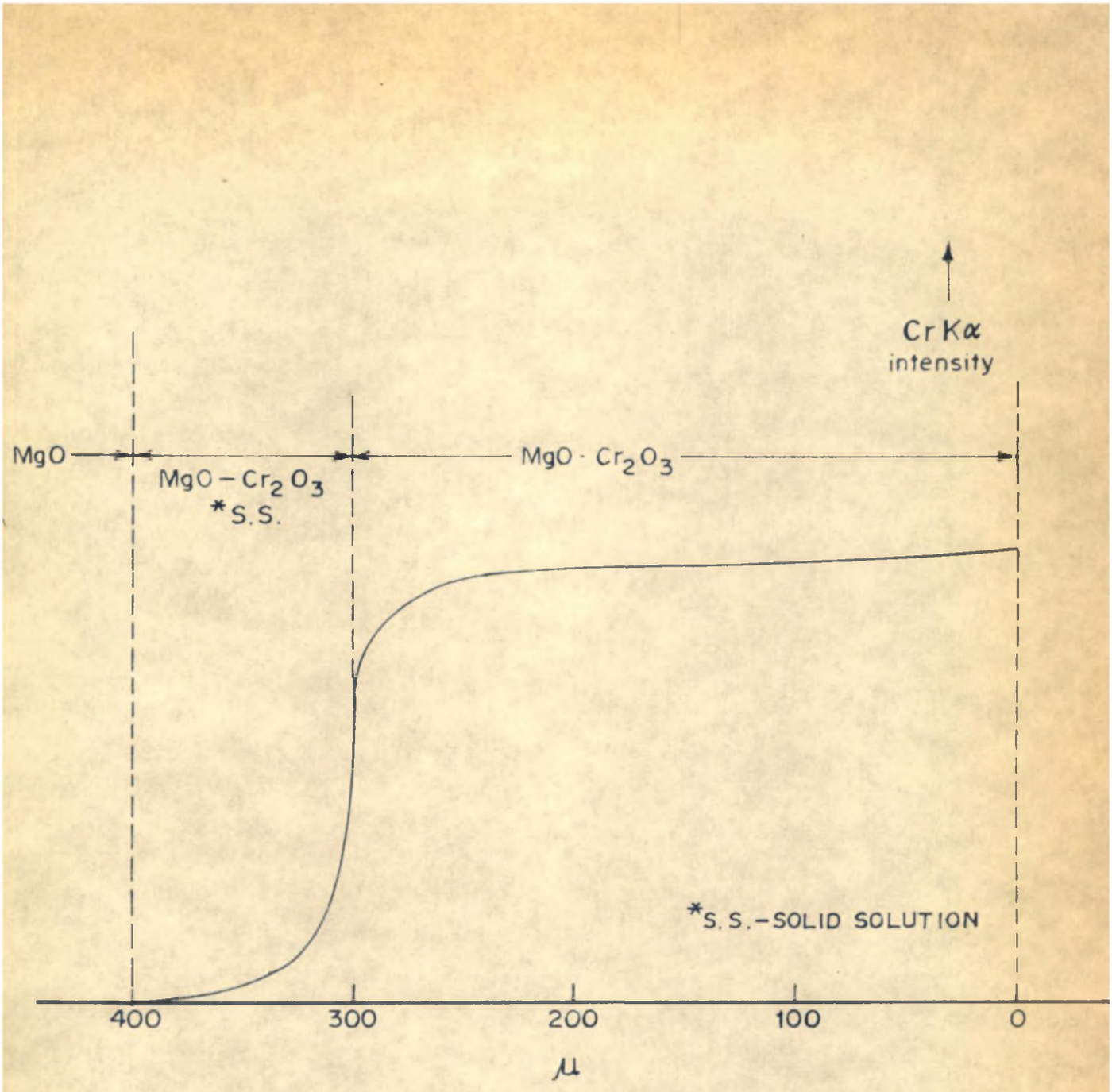

ELECTRON MICROPROBE SCANNING FIGURE FOR THE SYSTEM $MgO-Cr_2O_3$

(YAMAGUCHI AND TOKUDA, 1967)

FIGURE 2·2

start of the reaction zone:

$$\omega_p = 0.5$$

The normalising value of concentration was taken as that at the beginning of the product zone where this value was available, as for the present system, $MgO-Cr_2O_3$. In cases where this value was not available (as for the system $NiO-Al_2O_3$) the value at the end of the product zone was considered so that ω_p at this plane becomes 1. This is brought out in Figure 2.5 for the system $NiO-Al_2O_3$.

(iii) The Δz value obtained from the experimental profile was used to determine the Thiele modulus ϕ_r for the system using Equation 2.17.

$$\phi_r = 45.6$$

(iv) Using the values of Δz, ϕ_r and ω_p in (2.14), the dimensionless concentration ω was calculated at different positions, and the resulting plot of ω vs z is shown in Figure 2.3. The corresponding experimental profile is also reproduced in the same figure. The comparison shows remarkably good match.

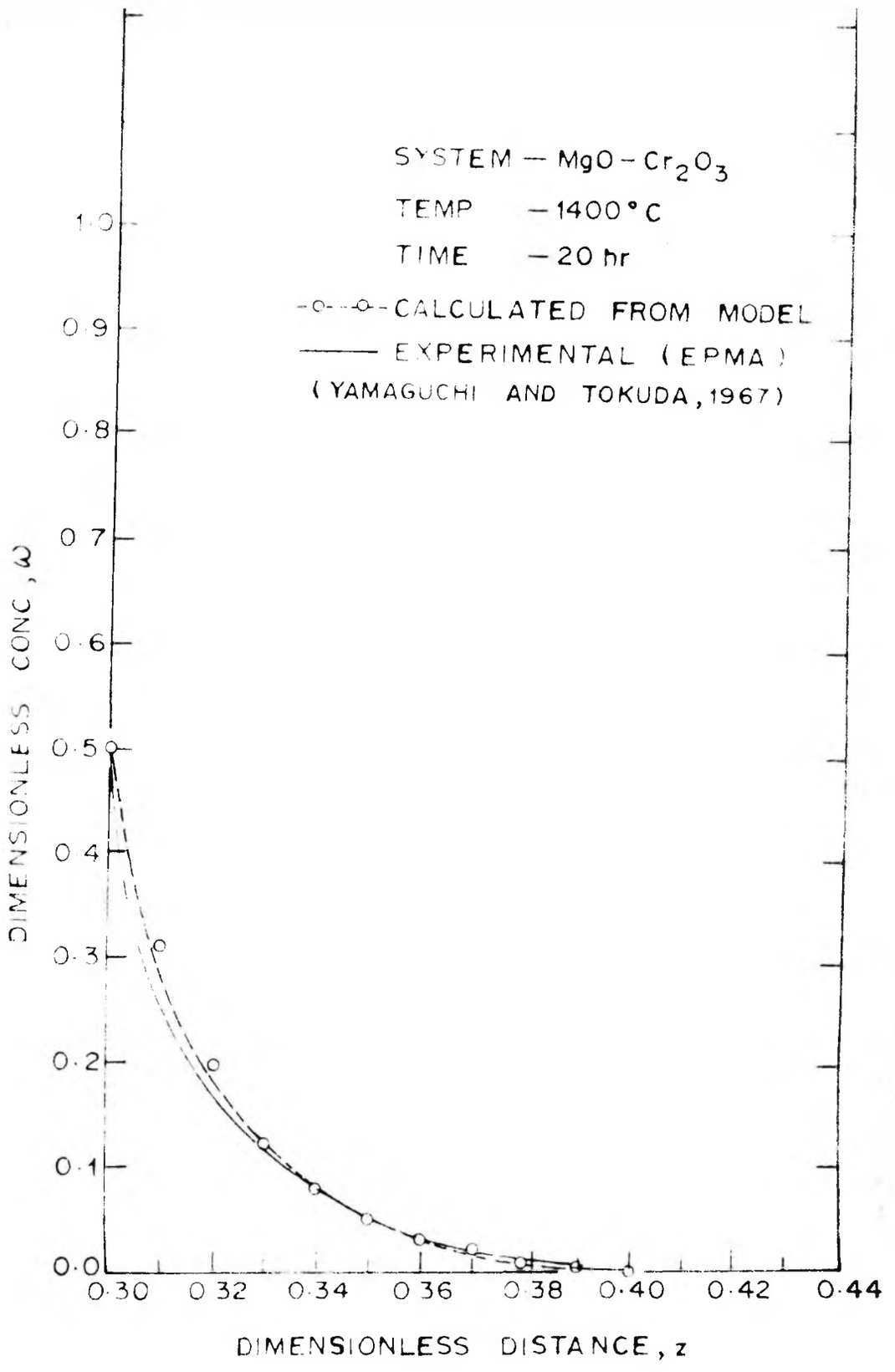

COMPARISON OF THE THEORETICAL PROFILE CALCULATED FROM THE MODEL WITH THE EXPERIMENTAL PROFILE OBTAINED FROM EPMA STUDIES

FIGURE 2·3

Similar calculations were made for: (i) the system $MgO-Fe_2O_3$ at 1250°C from the data of Yamaguchi and Tokuda (1967) and the results are reproduced in Figure 2.4, and (ii) the system $NiO-Al_2O_3$ at 1437°, 1540° and 1630°C from the data of Minford and Stubican (1974) and the results are reproduced in Figure 2.5. In all the cases the profiles prepared based on the model practically coincide with the experimental profiles, the average deviations being: $MgO-Cr_2O_3$, 5.6%, $MgO-Fe_2O_3$, 9.7%; and $NiO-Al_2O_3$, 3.0% (for all the 3 temperatures).

It would appear that the concept of an order of reaction, not explicitly brought out so far, is meaningful even in solid-solid reactions, and can perhaps replace the concept of an index of reaction (Taplin, 1974). However, it should be noted that the present model does not necessarily validate the first-order assumption in view of the other assumptions also involved. It should be regarded as providing a predictive equation which represents the reported data satisfactorily on the assumption of first-order kinetics.

2.4 THE GENERAL ORDER CASE

In case first-order kinetics is not obeyed in a particular system, a general n^{th} order reaction has to be

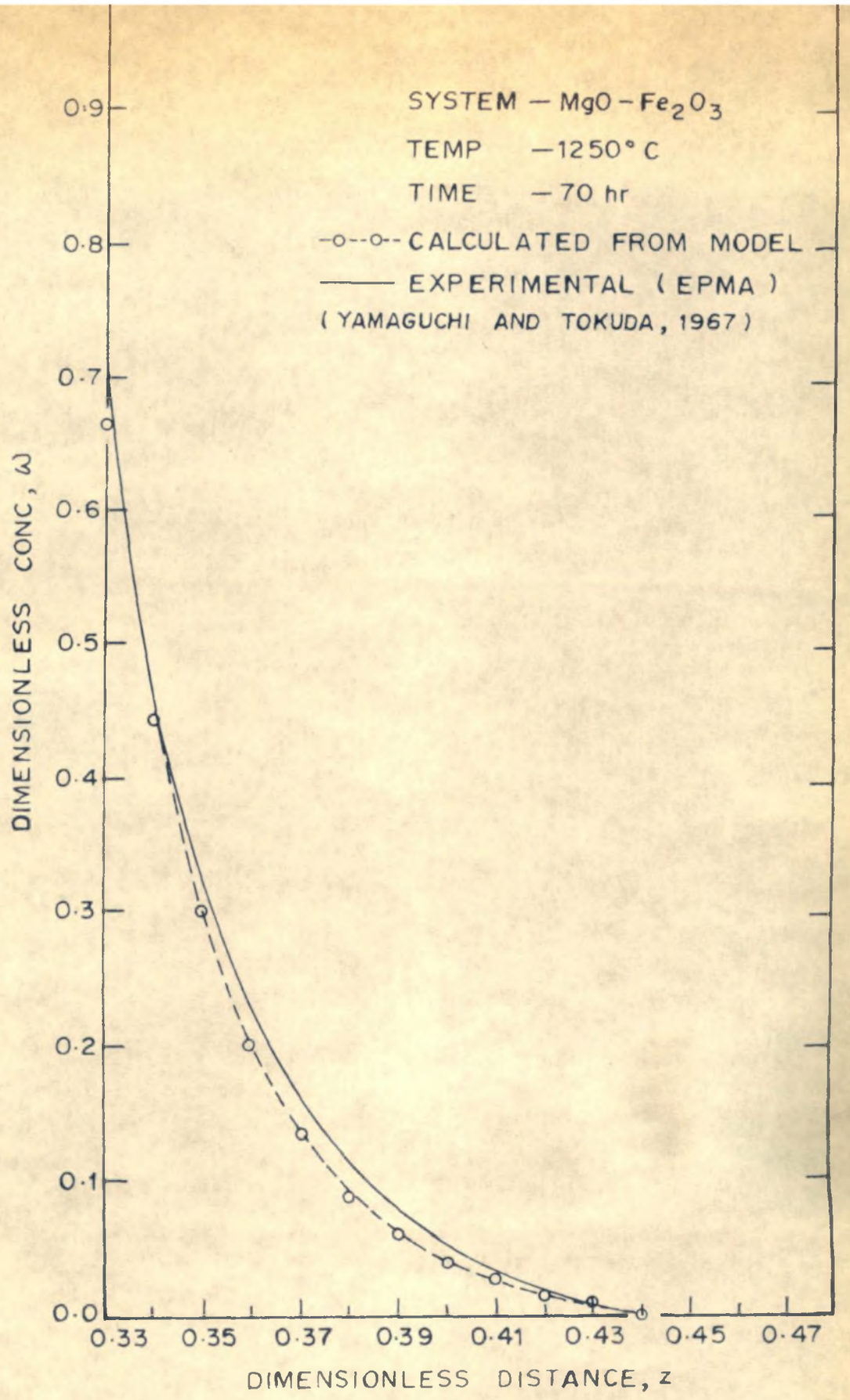

COMPARISON OF THE THEORETICAL PROFILE CALCULATED FROM THE MODEL WITH THE EXPERIMENTAL PROFILE OBTAINED FROM EPMA STUDIES

FIGURE 2·4

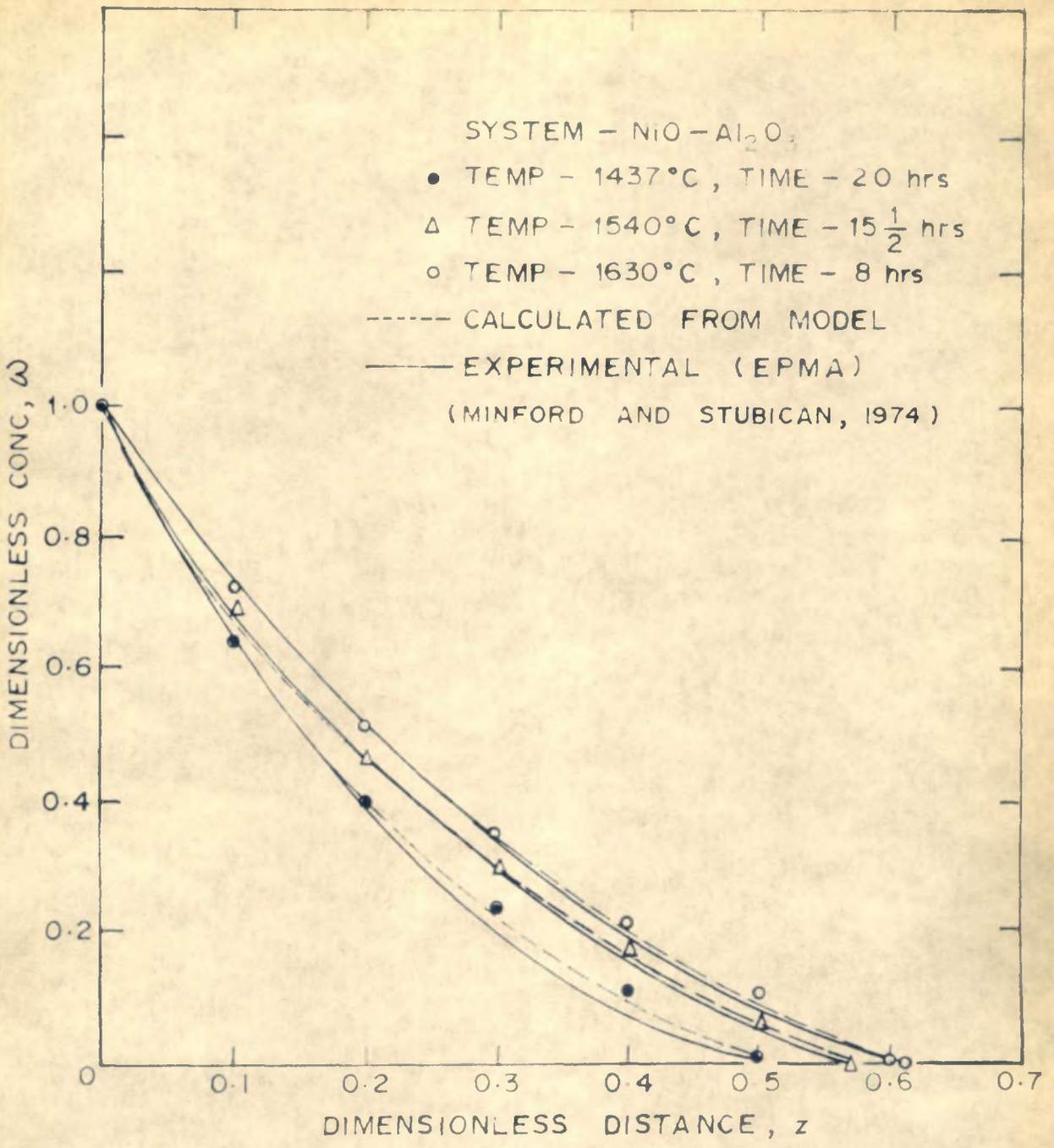

COMPARISON OF THE THEORETICAL PROFILE CALCULATED FROM THE MODEL WITH THE EXPERIMENTAL PROFILE OBTAINED FROM EPMA STUDIES

FIGURE 2·5

considered. Extending the treatment now to an n^{th} order chemical reaction, the continuity equation for the reaction zone can be written in dimensionless form as

$$\frac{d^2\omega}{dz^2} - \phi_r^2 \omega^n = 0 \tag{2.18}$$

where the Thiele modulus ϕ_r now becomes

$$\phi_r = L \left[\frac{kC^{*(n-1)}}{D_r} \right]^{1/2} \tag{2.19}$$

The following solution to Equation 2.18 can be obtained with boundary conditions (2.13):

$$\omega = \left[\frac{n-1}{2} \right]^{\frac{-2}{n-1}} \left[\left[\frac{2}{n+1} \right]^{1/2} \phi_r (z - z_p) + \frac{2}{n-1} (\omega_p)^{\frac{-(n-1)}{2}} \right]^{\frac{-2}{n-1}} \tag{2.20}$$

for $n \neq 1$

Rewriting this equation for the end of the reaction zone, i.e. for

$$\omega = 0, \quad z = z_r \tag{2.21}$$

we obtain

$$\left[\frac{2}{n+1}\right]^{1/2} \phi_r \Delta z + \frac{2}{n-1} (\omega_p)^{\frac{-(n-1)}{2}} = 0 \qquad (2.22)$$

or

$$\phi_r \Delta z = \left[\frac{n+1}{2}\right]^{1/2} \frac{2}{1-n} (\omega_p)^{\frac{1-n}{2}} \qquad (2.23)$$

If now concentration is normalised with respect to the value at the beginning of the zone, then $\omega_p = 1$ and we have

$$\phi_r = \left[\left[\frac{n+1}{2}\right]^{1/2} \frac{2}{1-n}\right] \frac{1}{\Delta z} \qquad (2.24)$$

Plots of log ϕ_r <u>vs</u> log Δz for different values of n can thus be prepared.

An interesting feature of Equation 2.24 is that it gives unrealistic values of ϕ_r for $n > 1$. No conclusion can be drawn from this however, since there is no apparent physical reason for invalidating higher orders.

Clearly, the EPMA profile for at least one experimental condition is necessary for obtaining the values

of n and ϕ_r. Once the reaction order is known, the concentration profiles for other sets of conditions can be predicted from experimental diffusivities (to give ϕ_r).

2.5 CONCLUSIONS

A mathematical analysis of coupled diffusion and reaction in solid-solid systems (in the form of pellets) is presented considering two zones: a product zone, and a reaction zone. Continuity equations for the two are solved to obtain the concentration profiles. Based on these a relation between reaction zone thickness and the Thiele modulus is obtained.

Reported experimental EPMA results are used to verify the predictive equation provided by the model on the assumption, among others, of first-order kinetics. A comparison of the theoretical and experimental profiles shows good agreement. The treatment is then extended to the general n^{th} order case.

The chief assumptions made in the development (in addition to first-order kinetics) pertain basically to the absence of external porosity in solids pelleted and sintered at sufficiently high temperatures and the applicability of the concept of effective diffusivity.

It would have been instructive to compare the values of the Thiele modulus (and possibly of the effective diffusivity) obtained from the model with those reported. Unfortunately this is not possible since values of D_e and k from which ϕ_r can be calculated are not available for the systems tested. However the value of $\phi_r = 45.6$, estimated in Section 2.3 for the system $MgO-Cr_2O_3$ at 1400°C, is based on the experimentally observed zone width, and is clearly well within the range for the existence of a reaction zone in gas-solid reactions (Mantri *et al*, 1976; Tudose, 1970). This is also true for the other two systems tested. Thus, while the value of ϕ_r is physically meaningful and the model does provide an acceptable predictive equation, experimental data on D_e and k for solid-solid reactions are desirable for a more rigorous test of the model.

CHAPTER 3

AN ANALYSIS OF THE REACTION ZONE

3.1 INTRODUCTION

In Chapter 2 a zone model was developed for diffusion and reaction in pellet-pellet systems. Consequently the importance of a reaction zone, as a result of diffusion and reaction of one of the reactants in the other, has been brought out. For the purpose of establishing the model, the simplifying assumption of steady state and hence a constant reaction zone thickness was made. Moreover, concentration profiles at a constant temperature and at different times are not reported in most of the studies. However, such profiles have been obtained in a few cases (Greskovich and Stubican, 1969; Whitney II and Stubican, 1971), which indicate that the reaction zone thickness changes with time and that it takes a long time to establish a steady concentration profile.

An analysis of such a situation is attempted here to obtain the unsteady state concentration profiles in the reaction zone. The solution of the basic equation is obtained using the boundary condition at infinity. However, the existence of a finite reaction zone observed experimentally is explained on the basis of an instrument factor, and its

variation with time predicted. A method is then proposed for obtaining the diffusivity (D) and the rate constant (k). Finally, using the unsteady state analysis, it is shown that the parabolic growth rate law, often used in pellet-pellet studies, can also be consistent with the present model. It is also pointed out that in many cases the applicability of the parabolic rate law could be a misinterpretation.

3.2 THEORETICAL DEVELOPMENT

3.2.1 Solution of the problem

The treatment here is mainly restricted to reactions of the type

$$AO + B_2O_3 \longrightarrow AB_2O_4$$

Further, only one-way diffusion is considered. The model may however be adapted to other situations.

Consider the pellets of AO and B_2O_3 kept with their faces in contact with each other. Reaction between the two will result in a product layer. Further, for the case of one-way diffusion, the species under consideration diffuses through the product layer to reach the other boundary, and then diffuses and reacts within the other reactant. Assuming

no diffusional resistance in the product layer, the concentration profile as obtained by EPMA can be represented as shown in Figure 3.1(a). The absence of diffusional resistance in the product layer is discussed in Section 3.4. Considering only the reaction zone, the profiles obtained as a function of time are represented in Figure 3.1(b). It may be noted that even beyond x_r, the hypothetical boundary of the reaction zone, C_A can be greater than zero; but it is not detected. This will be explained subsequently.

Now, the mass balance equation for the species A in the reaction zone can be written as

$$\frac{\partial C_A}{\partial t} = D \frac{\partial^2 C_A}{\partial x^2} - kC_A \qquad (3.1)$$

As mentioned in Chapter 2, here also a first-order reaction has been assumed. The initial and boundary conditions are:

$$C_A = 0 , \quad x > 0 \quad t = 0 \qquad (3.2)$$

$$C_A = C_A^* , \quad x = 0 \quad t > 0 \qquad (3.3)$$

$$C_A = 0 , \quad x = x_r(t) \quad t > 0 \qquad (3.4)$$

Even if the time dependence appearing in the

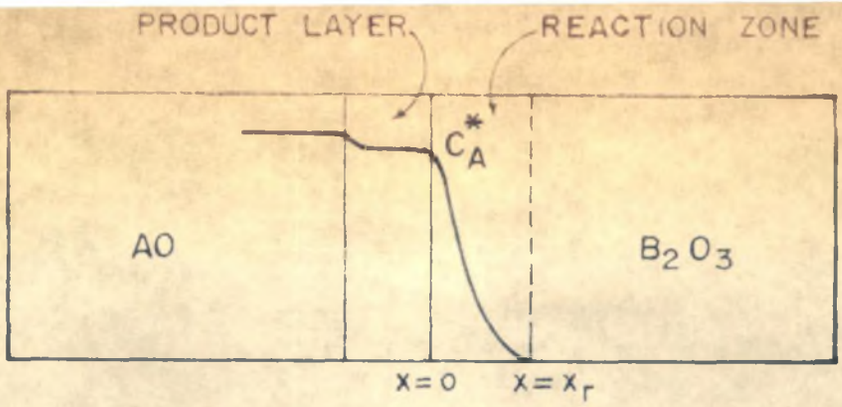

(a) A REPRESENTATIVE CONCENTRATION PROFILE OF SPECIES A, AS OBTAINED BY EPMA ASSUMING NO DIFFUSIONAL RESISTANCE IN THE PRODUCT LAYER

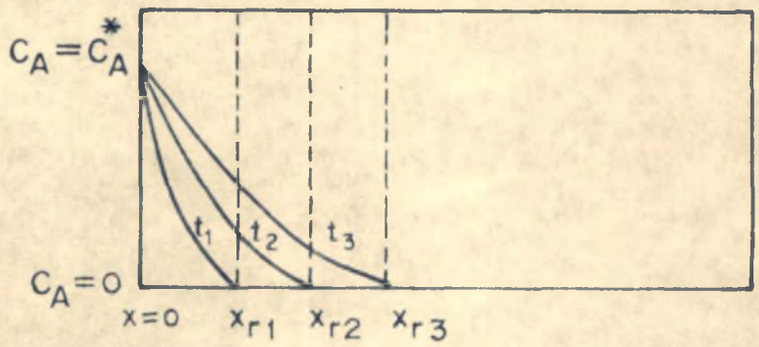

(b) CONCENTRATION PROFILES OBTAINED BY EPMA AS A FUNCTION OF TIME

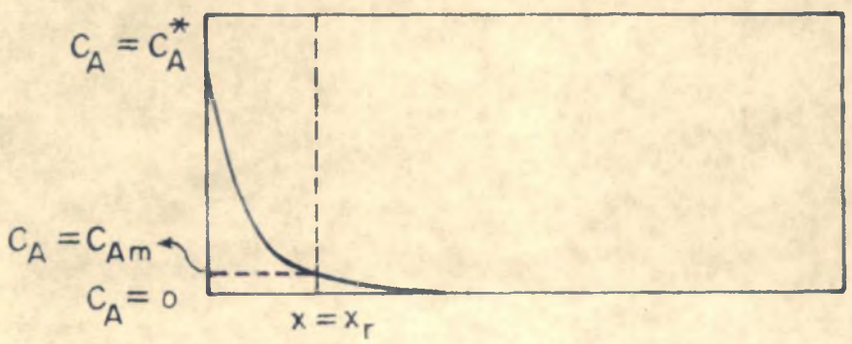

(c) THE APPEARANCE OF A FINITE REACTION ZONE DUE TO THE LIMIT OF DETECTABILITY OF AN INSTRUMENT C_{Am}

boundary condition (3.4) is precisely known, Equation 3.1 cannot be solved analytically. The boundary condition (3.4) implies a finite reaction zone thickness which changes with time. However, the concept of a finite zone is based on the concentration profiles obtained by EPMA. The appearance of such a finite zone could be due to a lower limit of detectability of an instrument; in reality the profile may be considered to be extending to infinity. This phenomenon is illustrated in Figure 3.1(c).

In view of the discussion above, the boundary condition (3.4) can be replaced by a new boundary condition

$$C_A = 0, \qquad x = \infty \qquad t \geqslant 0 \qquad (3.5)$$

Now, Equation 3.1 can be solved for the initial and boundary conditions (3.2), (3.3) and (3.5). A similar problem in gas-liquid reactions has been solved by Danckwerts (1970). The solution is given as

$$\omega = C_A/C_A^* = \frac{1}{2} \exp\left(-x\sqrt{k/D}\right) \operatorname{erfc}\left(\frac{x}{2\sqrt{Dt}} - \sqrt{kt}\right)$$

$$+ \frac{1}{2} \exp\left(x\sqrt{k/D}\right) \operatorname{erfc}\left(\frac{x}{2\sqrt{Dt}} + \sqrt{kt}\right) \qquad (3.6)$$

The same solution holds for the situation under consideration.

3.2.2 Reaction zone thickness

As mentioned above, the instrument has a certain lower limit of detectability; all concentrations of A below this limit are not detected at all. Consequently the value of x at which this lower limit is reached is considered as the end of the reaction zone and the corresponding value of $x(x_r)$ is then the reaction zone thickness. Thus,

$$\omega_m = C_{Am}/C_A^* = \frac{1}{2}\exp\left(-x_r\sqrt{k/D}\right)\ \operatorname{erfc}\left(\frac{x_r}{2\sqrt{Dt}} - \sqrt{kt}\right) + \frac{1}{2}\exp\left(x_r\sqrt{k/D}\right)\ \operatorname{erfc}\left(\frac{x_r}{2\sqrt{Dt}} + \sqrt{kt}\right) \quad (3.7)$$

where C_{Am} denotes the lowest concentration measurable by the instrument and x_r denotes the reaction zone thickness.

Now, defining the following parameters:

$$\left.\begin{aligned} m_1 &= x\sqrt{k/D} \\ m_2 &= \frac{x}{\sqrt{Dt}} \\ m_3 &= \sqrt{kt} \end{aligned}\right\} \quad (3.8)$$

Equation (3.7) becomes

$$\omega_m = \frac{1}{2} \exp(-m_1) \operatorname{erfc}\left(\frac{m_2}{2} - m_3\right) + \frac{1}{2} \exp(m_1) \operatorname{erfc}\left(\frac{m_2}{2} + m_3\right) \tag{3.9}$$

The parameter m_1, as defined above, is similar to a Thiele modulus normally defined in such problems of simultaneous diffusion and reaction. However, here it varies with time due to the variation of x_r with time.

3.2.3 Variation of the reaction zone thickness with time

The variation of reaction zone thickness x_r with time t can be monitored through the variation of m_1 with m_3. Now, since

$$m_1 = m_2 m_3 \tag{3.10}$$

Equation 3.9 can be written in terms of any two of the parameters m_1, m_2 and m_3. A convenient form is obtained by writing Equation 3.9 in terms of m_2 and m_3. Thus,

$$\omega_m = \frac{1}{2} \exp(-m_2 m_3) \operatorname{erfc}\left(\frac{m_2}{2} - m_3\right) + \frac{1}{2} \exp(m_2 m_3) \operatorname{erfc}\left(\frac{m_2}{2} + m_3\right) \tag{3.11}$$

The lower limit of detectability of an instrument for a given system fixes the value of ω_m. Once this value is fixed, giving values to say m_3. corresponding values of m_2 can be calculated from Equation 3.11. The normal range of lower limit for an EPMA instrument is 100-500 ppm. With this, the value of ω_m is calculated to be approximately between 1×10^{-3} and 5×10^{-3}. The value of ω_m depends on the instrument as well as on the system.

To demonstrate the present method, an arbitrary value of 1×10^{-3} is chosen for ω_m. Corresponding values of m_2 and m_3 are then calculated from Equation 3.11 by trial-and-error procedure; m_3 values in the range 0 to 1 are used for these calculations. A plot of m_2 *vs* m_3 is thus prepared for $\omega_m = 1 \times 10^{-3}$ and is presented in Figure 3.2. Using Equation 3.10 a plot of m_1 *vs* m_3 is readily obtained as shown in Figure 3.3.

Figure 3.3 shows almost a straight line plot indicating that the slope (m_2) is almost constant. From the definition of the parameters m_1 and m_3 (Equation 3.8)

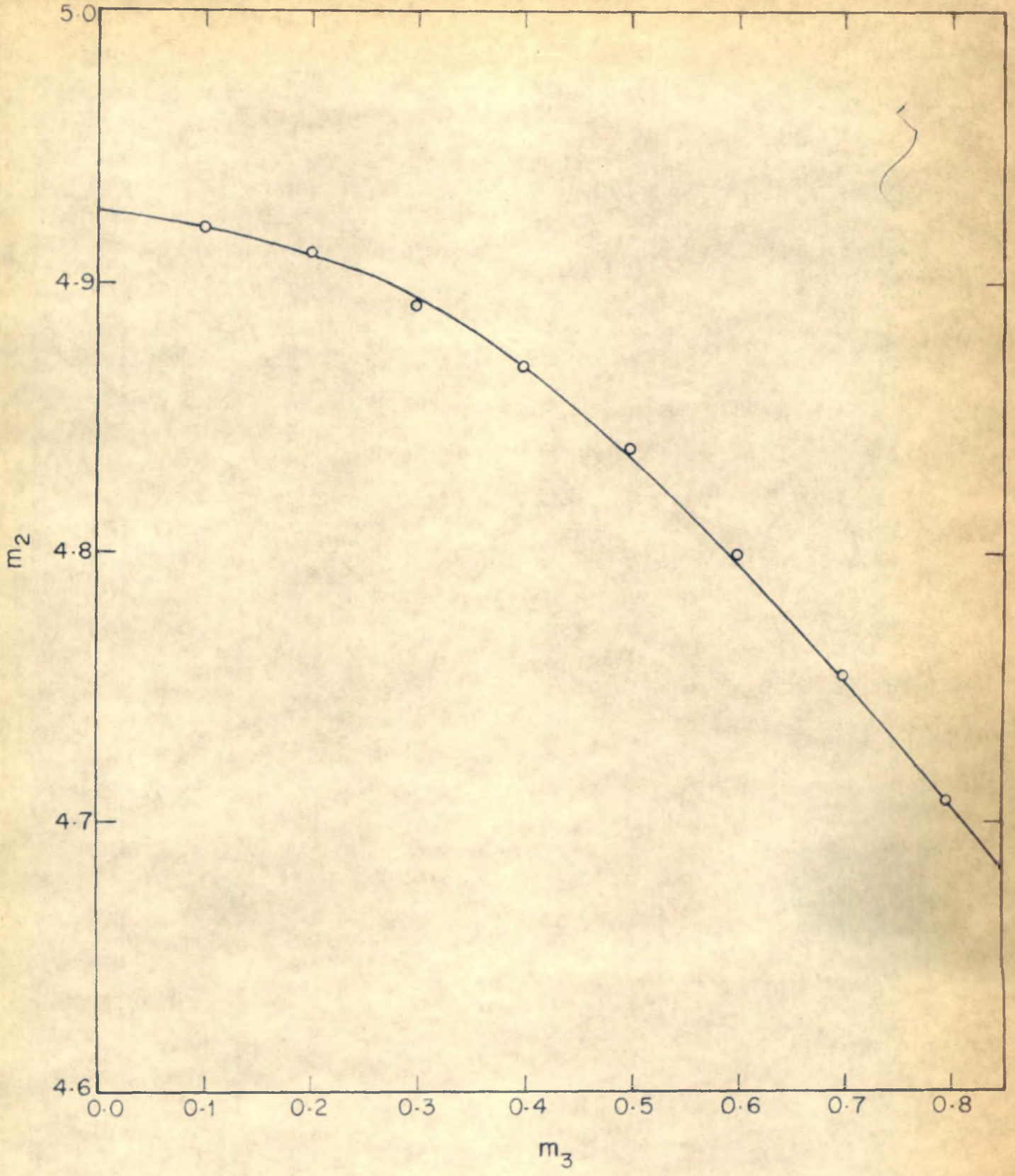

VARIATION OF m_2 WITH m_3 FOR $\omega_m = 1 \times 10^{-3}$

FIGURE 3·2

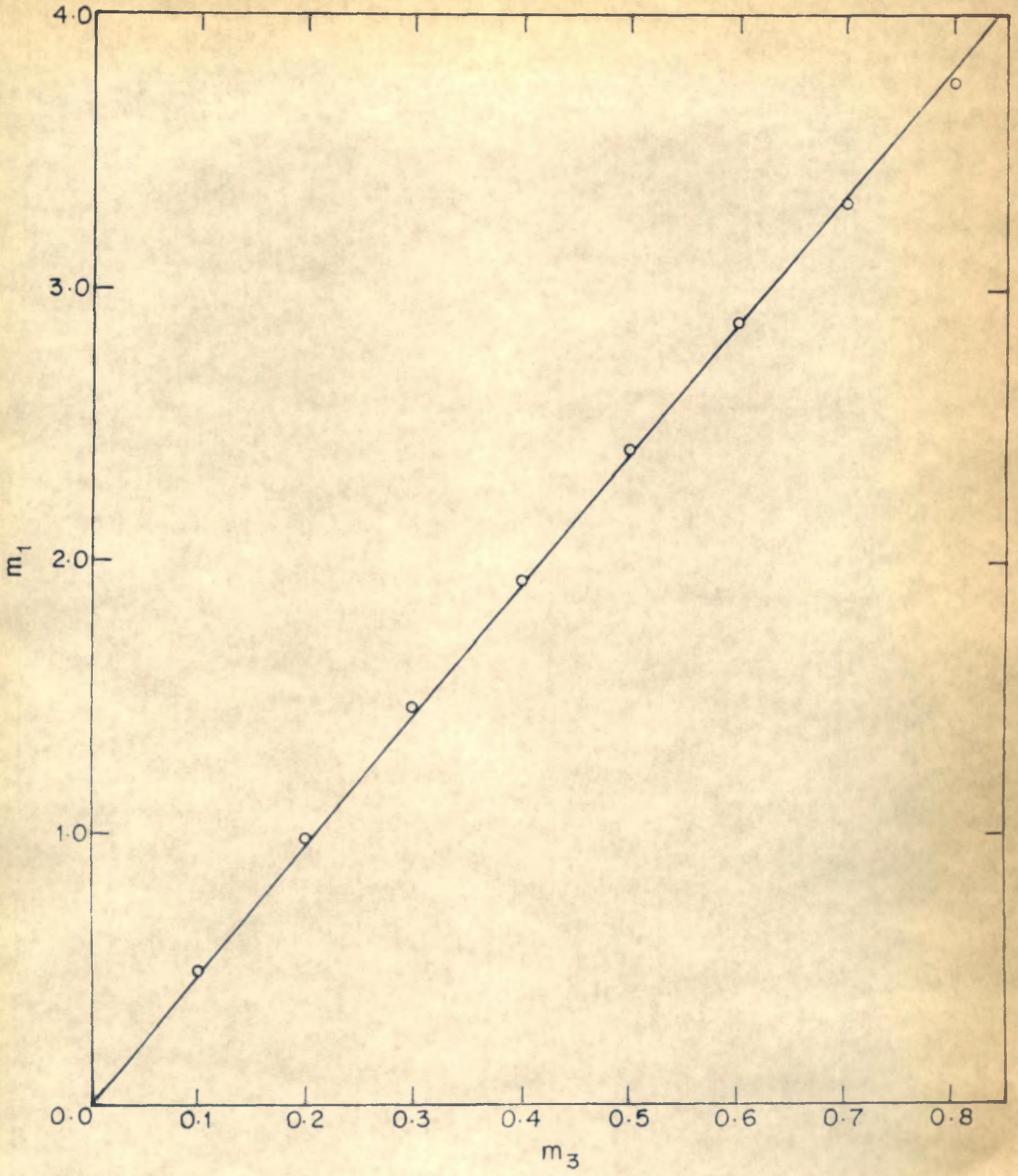

VARIATION OF m_1 WITH m_3 FOR $\omega_m = 1 \times 10^{-3}$

FIGURE 3·3

it can be seen that the straight line plot in Figure 3.3 also indicates parabolic growth of x_r with time. Figure 3.2 however shows a slight variation of m_2 with m_3 and thereby a deviation from the parabolic rate law for x_r.

In the above treatment, the limit of detectability is chosen as the basis. Often the limit is not precisely known for a particular instrument and for a given system. Hence, a slightly different method is proposed as an alternative. Accordingly, any particular concentration may be chosen as the basis. The variation of the corresponding value of x with time may then be followed. This would also give similar results. Thus in Figure 3.4 a plot of m_2 *vs* m_3 for $\omega_m = 0.5$ is presented with a wider range of values of m_3. The plot shows that m_2 is constant for m_3 between 2 and 3. This probably indicates that the parabolic rate law holds in this case more appropriately for higher values of m_3.

3.3 PREDICTION OF DIFFUSIVITY AND RATE CONSTANT VALUES

The plots and some of the facts and observations brought out in the previous section can be utilised for the determination of diffusivity and rate constant values for a given system. This can be done by a trial-and-error method.

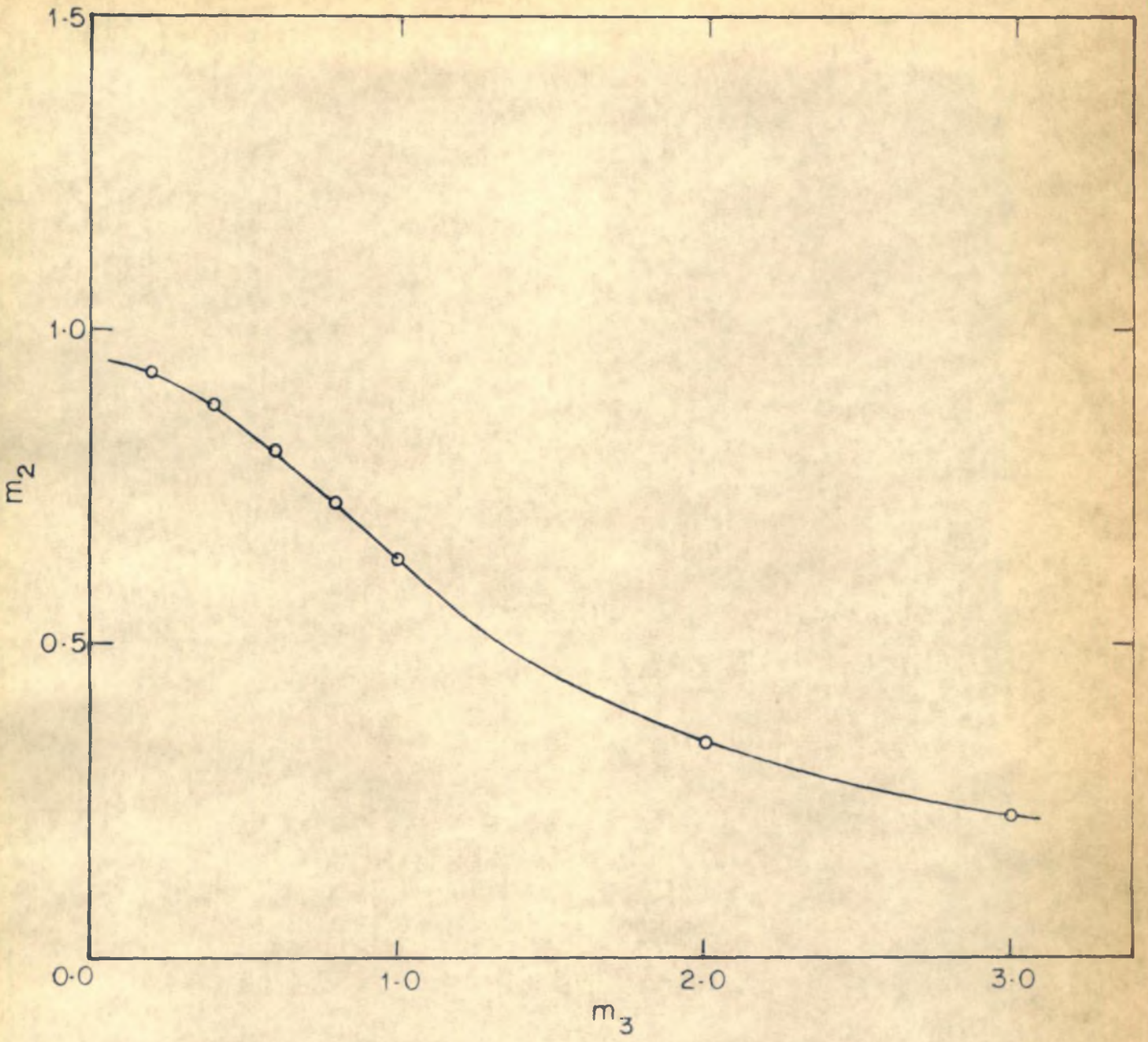

VARIATION OF m_2 WITH m_3 FOR $\omega_m = 0.5$

FIGURE 3.4

The limit of detectability may not always be known precisely, and the calculations are found sensitive to the value. Hence plots for $\omega_m = 0.5$ can more conveniently be used for the purpose.

Thus, for example, a value of k may be assumed and m_3 calculated. Knowing m_3, m_2 can be obtained from a plot of m_2 **vs** m_3 as shown in Figure 3.4. Using this value of m_2, D can be computed knowing $x_{0.5}$ and t from the experimental data. Alternatively a value of D may be assumed and that of k computed. In either case the procedure has to be repeated to get the best values of k and D by, say, least squares analysis. The procedure provides a good estimate of D and k.

Once the D and k values are known for a given system, concentration profiles under a given set of conditions can be predicted. A match of the predicted profile with the experimental profile will indicate the correctness of the estimated D and k values.

The method is not verified here due to lack of reported experimental data satisfying the assumptions made in the above treatment. In a few such systems reported, the data are not in a form accessible to such an analysis.

3.4 ON THE PARABOLIC GROWTH RATE LAW

In studies on solid-solid reactions, the parabolic rate law is often used to determine rate constants, activation energies, etc. The formulation of the parabolic rate law is based on the assumption that diffusion of the reactant species in the product layer is the rate controlling step. Conversely, in all studies where parabolic growth is observed, it is concluded that product layer diffusion is the controlling step. Here it is shown that diffusion-cum-reaction control in a reaction zone formed within one of the reactants can also be consistent with this law under certain conditions. Also it is pointed out that the applicability of parabolic rate law can sometimes be a misinterpretation.

3.4.1 Basic formulation of the law

The parabolic rate law, as proposed originally by Tammann (1920), is basically an empirical expression. In a one-dimensional system (similar to the one considered in the present development), for product layer diffusion control, the rate of growth of the product layer thickness (PLT) $d(\Delta x)/dt$ is considered proportional to the diffusivity D, cross-sectional area A, and the reciprocal of the thickness $1/\Delta x$. Thus,

$$\frac{d(\Delta x)}{dt} = \frac{cAD}{\Delta x} \qquad (3.12)$$

where c is a proportionality constant. On integration this leads to the parabolic rate law:

$$(\Delta x)^2 = Kt \qquad (3.13)$$

where $K = 2cAD$, a constant.

The diffusivity D appearing in Equation 3.12 is considered to be the diffusivity of the species whose transport through the product layer is rate controlling. However, if there is no diffusional resistance in the product layer, and instead the diffusion of the species in the other reactant controls, then the corresponding diffusivity will be involved. The two diffusivities can be quite different, as has already been pointed out in Section 1.2.3.

3.4.2 Experimental observations

Experimentally the rate law is monitored by carrying out reaction between single crystals or pellets of reactants kept in contact, and measuring the thickness of the product layer formed between them as a function of time. Parabolic growth has been observed for a number of systems (see Table 1.2).

In a few such studies the concentration profiles of the reactant species have also been obtained. These studies disclose certain interesting facts. Thus, for a number of important solid-solid systems like $MgO-Fe_2O_3$, $MgO-Al_2O_3$, $MgO-Cr_2O_3$ and $ZnO-Fe_2O_3$, Yamaguchi and Tokuda (1967) obtained concentration profiles in each case using the EPMA technique. The profiles clearly indicate little or no diffusional resistance in the product layer; for the same systems parabolic growth has been observed by others (e.g. Greskovich and Stubican, 1969; Greskovich, 1970; Minford and Stubican, 1974; Pettit *et al*, 1966).

Greskovich and Stubican (1969), in their studies on the system $MgO-Cr_2O_3$, observed parabolic growth of the product layer. However, they have specifically mentioned that no concentration gradient of Cr_2O_3 in the product $MgCr_2O_4$ was observed. Similarly Cerovic *et al* (1969), in their studies on the $NiO-Fe_2O_3$ system, could fit the PLT data well by the parabolic rate law. At the same time, the concentrations of the diffusing species obtained by the EPMA technique at the two boundaries of the product were found to be close and invarient with time and temperature (upto $\sim 1200^{o}C$) indicating an absence of diffusional resistance in the product layer.

As is well known, in any heterogeneous reaction system,

as the temperature is raised the process goes from a kinetic control to a diffusion control regime. This is true for solid-solid reactions also. Cerovic et al (1969), for example, have obtained concentration values at the two boundaries of the product layer. At lower temperatures (up to about 1200°C) almost no concentration gradient exists in the product layer; but at higher temperatures the gradient becomes steeper. The same is brought out more clearly in the studies of Yamaguchi and Tokuda (1967) on the system $MgO-Fe_2O_3$, where actual concentration profiles at two different temperatures have been reported.

The experimental observations, pointed out above, clearly bring out the fact that the parabolic rate law holds even when there is no diffusional resistance in the product layer.

On the other hand, in all the above mentioned studies, concentration gradients of the diffusing species within the other reactant forming a well defined reaction zone have been observed. This calls for a proper interpretation of the parabolic growth rate law.

3.4.3 Mathematical analysis

For a pellet-pellet system, considering no diffusional

resistance in the product layer, the concentration profiles of A in B_2O_3 as obtained by EPMA, are shown schematically in Figure 3.1. Solution to the corresponding mass balance equation has already been obtained in Section 3.2.1 (Equation 3.6).

Now the rate of growth of the product is governed by diffusion and reaction in this zone. Hence, the rate will be given by the flux of the reacting species entering this zone. Since the cross-sectional area is constant,

$$\frac{d(\Delta x)}{dt} = -D \left[\frac{dC_A}{dx}\right]_{x=0} \tag{3.14}$$

Differentiating Equation 3.6 with respect to x,

$$-D \left[\frac{dC_A}{dx}\right]_{x=0} = C_{Ao} (Dk)^{1/2} \left[\text{erf } (kt)^{1/2} + \frac{e^{-kt}}{(\pi kt)^{1/2}}\right] \tag{3.15}$$

If this rate is integrated with respect to time one gets the quantity of the reacting substance (M_t) that has entered the zone in time t. M_t will be directly proportional to the thickness of the product layer (in the one-dimensional case). Thus, on integrating Equation 3.15,

$$M_t = C_{Ao}(D/k)^{1/2}\left[(kt+1/2)\ \mathrm{erf}(kt)^{1/2}+(kt/\pi)^{1/2}\ e^{-kt}\right] \quad (3.16)$$

If the magnitudes of k, D and t commonly encountered in studies on solid-solid reactions are considered, it is noticed that k and D are comparable (so that the reaction term cannot be neglected in the basic equation), and kt is small so that the higher powers of kt can be neglected. Hence, if $\mathrm{erf}(kt)^{1/2}$ and $\exp(-kt)$ are expanded, Equation 3.16 can be approximated to

$$M_t = 2C_{Ao}\ (Dt/\pi)^{1/2}\ \{1+\frac{1}{2}\ kt\} \quad (3.17)$$

Now, if the term kt/2 is negligible in comparison to 1, then (3.17) reduces to

$$M_t = 2C_{Ao}\ (Dt/\pi)^{1/2} \quad (3.18)$$

and since $\Delta x \propto M_t$, we get

$$\Delta x = 2\beta C_{Ao}\ (Dt/\pi)^{1/2} \quad (3.19)$$

or

$$(\Delta x)^2 = Kt$$

where $K = 4\beta^2 C_{Ao}^2 D/\pi$ and β is a proportionality constant.

Equation 3.19 is the parabolic rate law. This, however, indicates a diffusion-controlled mechanism, the term containing k being neglected. Since the fluxes at the interface of the two zones are equal, it would be the same whether the diffusion control takes place in the product zone or in the reaction zone as far as the applicability of the parabolic rate law is concerned. But, the diffusivity (D) in the two cases will be different due to the difference in structure, texture, composition, perfection, etc. in the two zones.

Now consider again the exact expression for M_t, viz. Equation 3.16. Since $\Delta x \propto M_t$ (i.e. $\Delta x = \beta M_t$) it can be rewritten in the form

$$\frac{\Delta x}{\beta C_{Ao}} \left(\frac{k}{D}\right)^{1/2} = \{(kt+1/2)\ \mathrm{erf}(kt)^{1/2} + (kt/\pi)^{1/2}\ e^{-kt}\} \qquad (3.20)$$

Thus, the L.H.S. of (3.20) can be computed by giving values to kt. A plot of $\frac{M_t}{C_{Ao}} \sqrt{K/D}$ **vs** kt has in fact been presented by Crank (1975), where the range 0 to 1 of the values of kt is covered. The plot shows a curve, becoming almost a straight line at higher values of kt.

More interesting results are obtained when

$\left[\frac{\Delta x}{\beta C_{Ao}}\sqrt{k/D}\right]^2$ **vs** kt is plotted. Such a plot is presented in Figure 3.5. It clearly shows a straight line passing through the origin, for values of kt upto 0.3. Thus, for small values of kt parabolic rate law is valid. For the higher values of kt, linear instead of parabolic dependence is obvious from the plot of Crank, indicating kinetic control. In the intermediate region mixed control is operative; as such, it is neither parabolic nor linear. However, a straight line passing through the points for kt = 0.4 and kt = 0.5 and the origin is shown in Figure 3.5 to illustrate that by choosing a particular range of values one can still get a straight line. This is in view of the fact that in most studies where parabolic rate law is shown to be valid for the product layer growth, the $(\Delta x)^2$ **vs** time plots usually show two or three points. A plot of $(\Delta x)^2$ **vs** time over a wide range of times is generally not reported. Moreover in many cases the fit is only approximate. The above analysis shows that it is the value of kt that decides the applicability of the parabolic rate law and not that of the k alone.

Mention must be made at this point of the fact that the product layer in all such studies also contains the diffusing species dissolved in it. As such, the measured

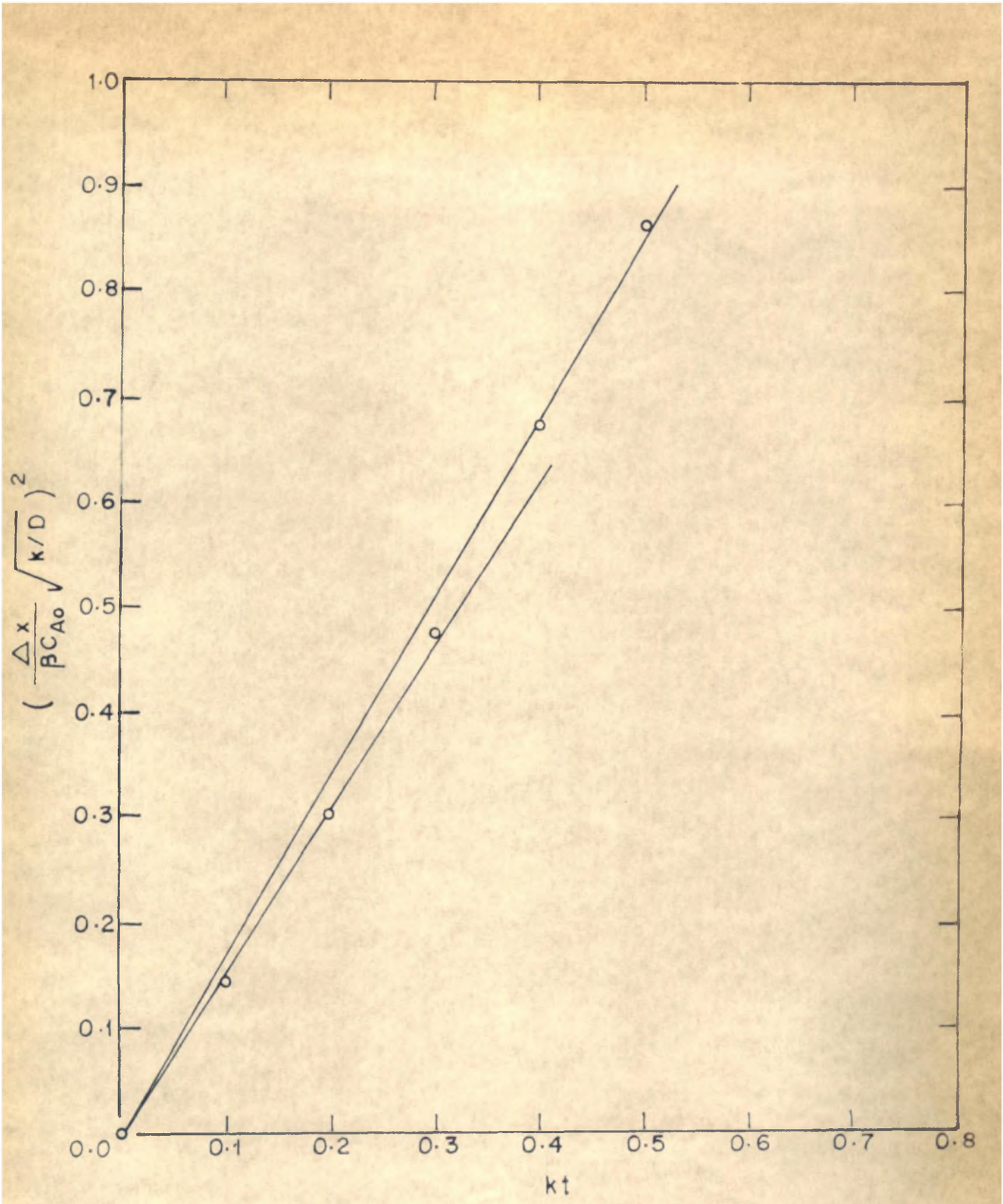

REPRESENTATION OF PARABOLIC RATE LAW WITH DIFFUSION-CUM-REACTION CONTROL IN REACTION ZONE

FIGURE 3·5

thickness is not purely that of the product. This has been rightly pointed out by Cerovic *et al* (1969).

Thus the plot giving a curve in reality (invalidating the applicability of the parabolic rate law) is often approximated by a straight line. This can have more serious effects when the rate constants obtained from the slopes are used in calculating activation energy and the pre-exponential factor. The value of the activation energy estimated from such a treatment can be significantly off.

It may be concluded that the parabolic rate law is a more general law which is not restricted to diffusional control through the product layer only. It would therefore be incorrect to use the parabolic rate law as a test in discerning the controlling mechanism. Moreover, due to the approximation involved in the fitting of the law, it may give erroneous values of the activation energy.

CHAPTER 4

EXPERIMENTAL STUDIES ON THE PELLET-PELLET SYSTEM $CuO-Fe_2O_3$

4.1 INTRODUCTION

In this Chapter the experimental results obtained on the system $CuO-Fe_2O_3$ are reported. To start with, a few experiments were carried out with different systems to examine the feasibility of using these systems for verification of the model developed in Chapters 2 and 3. The systems studied were: succinic anhydride-m-nitroaniline, succinic anhydride-urea, Cu(I)thiocyanate-thiourea, $CuO-Cr_2O_3$, $Bi_2O_3-MoO_3$, $BaSO_4-ZnS$, $CuO-Ni_2O_3$ and $CuO-Fe_2O_3$.

Basically the system should be free of complications like presence of gaseous product, change in weight during reaction, structural changes, appearance of amorphous phases, etc. These factors were examined using differential thermal analysis (DTA), thermogravimetric analysis (TGA), X-ray diffraction, microscopy and electron probe microanalysis (EPMA).

Another important criterion used in the choice of a system was that it should satisfy the assumptions made in the theoretical development. The major assumption is that of one-way diffusion.

Based on the above tests and the information available in the literature, the system $CuO-Fe_2O_3$ was chosen for further analysis. Concentration profiles for the system were obtained by EPMA, and the model developed earlier was tested with these data.

4.2 EXPERIMENTAL

4.2.1 Materials and their properties

(a) Copper oxide

Analytical grade cupric oxide (CuO) powder was obtained from REACHIM (USSR) with maximum impurity percentage of 0.445. The DTA of this powder showed a small exothermic peak at around 400°C; it also showed a slight increase in weight at 600°C. The increase in weight was probably because of the presence of trace quantities of cuprous oxide. The powder was, therefore, calcined at 800°C in atmospheric air for 24 hours. This was then cooled and ball milled for three days using porcelain balls to obtain a very fine powder. The DTA of this powder showed a constant weight up to about 1020°C. The X-ray pattern of the powder showed sharp diffraction lines indicating a purely crystalline material. Absence of cuprous oxide was also confirmed by chemical analysis.

(b) Iron oxide

Ferric oxide (α-Fe_2O_3) powder was obtained from Robert Johnson. The powder was calcined at 1000°C for 24 hours in air, cooled, and ball milled for three days using porcelain balls. The stability and crystallinity of this powder was confirmed by DTA/TGA and X-ray diffraction studies. Absence of ferrous ions in the sample was confirmed by chemical analysis.

4.2.2 The system CuO-Fe_2O_3

The phase diagram of the system CuO-Fe_2O_3 has been presented by Yamaguchi (1966). The diagram shows that up to 1000°C, only the spinel $CuFe_2O_4$ is formed throughout the range of compositions. Above 1015°C, CuO reacts with the spinel to give $CuFeO_2$. Also, at about 1026°C, CuO starts decomposing, giving cuprous oxide Cu_2O. Thus, the reaction between CuO and Fe_2O_3 to give $CuFe_2O_4$ can be safely carried out below 1000°C.

Kinetic studies on the formation of copper ferrite from the reactants in mixed powder form have been reported by Saull *et al* (1970). In these studies, Saull *et al* found that a significant difference exists between calcined and uncalcined ferric oxide. However, pellet-pellet studies on

this system have not been reported hithertofore.

Navrotsky and Kleppa (1968), in their studies on the thermodynamics of formation of simple spinels, have reported data on the system $CuO-Fe_2O_3$. The spinel $CuFe_2O_4$ was prepared by ceramic technique. The recommended conditions are: temperature 900°C and time 90 hours. They obtained the heat of formation of $CuFe_2O_4$ at 970°K as $\Delta H_{970} = +5.05 \pm 0.20$ kcal/mole. This shows that the reaction is slightly endothermic. In fact, from the whole range of spinels investigated, copper spinels in general were found to have typically positive enthalpies of formation. This has been explained on certain structural grounds - copper ferrite has an inverse spinel structure.

In view of the above discussion, actual experiments were carried out at 950°C (isothermal) in air.

4.2.3 EPMA studies

Sample preparation

The fine cupric oxide powder obtained by the procedure described above was pressed in the form of pellets using a hand-operated hydraulic press at a pressure of about 4 tons. The pellets thus obtained were sufficiently hard. They were 11 mm in diameter and 5 mm in height.

Following a similar procedure ferric oxide pellets of the same dimensions were prepared.

The pellets were then sintered at a specified temperature to eliminate the porosity. Thus, the cupric oxide pellets were sintered at just below 1000^{o}C for 3 days in an electric furnace. The ferric oxide pellets were similarly sintered at 1100^{o}C.

The flat faces of the sintered pellets were then polished. The following procedure was adopted for polishing:

(i) Initially, grinding was done on silicon carbide papers, first with 400 and then with 600 paper (the number indicates the mesh size of the coated SiC powder) using a foamless detergent solution as vehicle.

(ii) The grinding was followed by polishing on a polishing machine with a chamois leather base and successively using 600, 900 and 1800 mesh silicon carbide powder. Ethyl alcohol was used as vehicle.

(iii) Further polishing was done using a slurry of alumina powder of 1 micron particle size in water.

(iv) Final polishing was achieved with diamond paste of 0.5 micron size using again ethyl alcohol as vehicle. During the polishing operation, to facilitate a firm grip

on the pellets, they were encapsulated in wax.

The polished faces were observed under a microscope. They had a roughness of less than 1 micron. The pellets were then cleaned in an ultrasonic cleaner using various solvents.

The cleaned pellets were annealed in a tube furnace at 950^{o}C for 12 hours to eliminate any defects introduced due to cold work during polishing. Pairs were prepared for carrying out reaction by placing the polished faces of CuO and Fe_2O_3 pellets in contact in each case. Each pair was held in perfect contact by wedging it tightly into a stainless steel holder, shown in Figure 4.1(a). Pieces of platinum foil were placed on the top and the bottom of the pair to avoid direct contact with the holder.

The holders containing the reactant pairs were then kept one by one in a tube furnace preheated to 950^{o}C. The temperature was monitored by a chromel-alumel thermocouple connected to a calibrated potentiometer through a cold junction. The furnace was maintained at a constant temperature of 950$\pm$5^{o}C with the help of a Sunvic Platinum resistance temperature controller and a voltage stabiliser. The platinum sensing element of the controller was inserted in the furnace along with the thermocouple, so that the

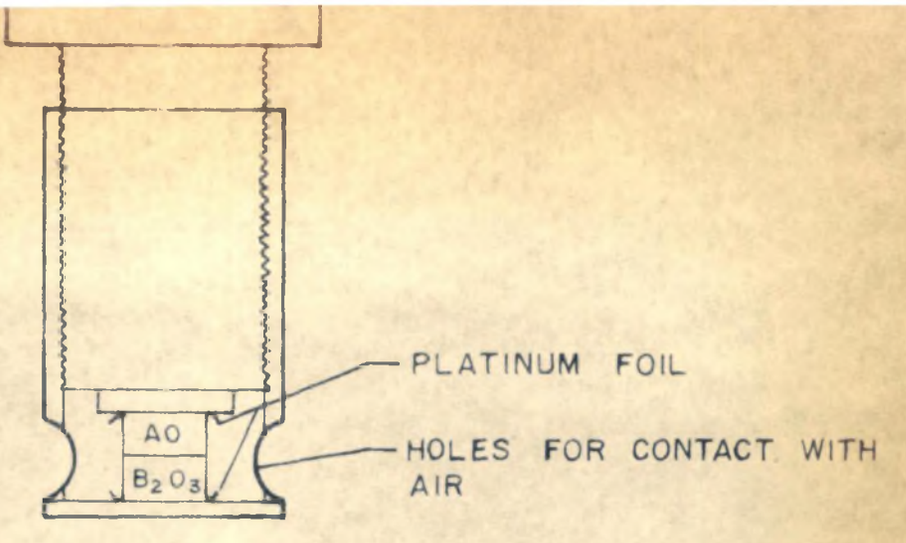

(a) STAINLESS STEEL PELLET HOLDER ASSEMBLY

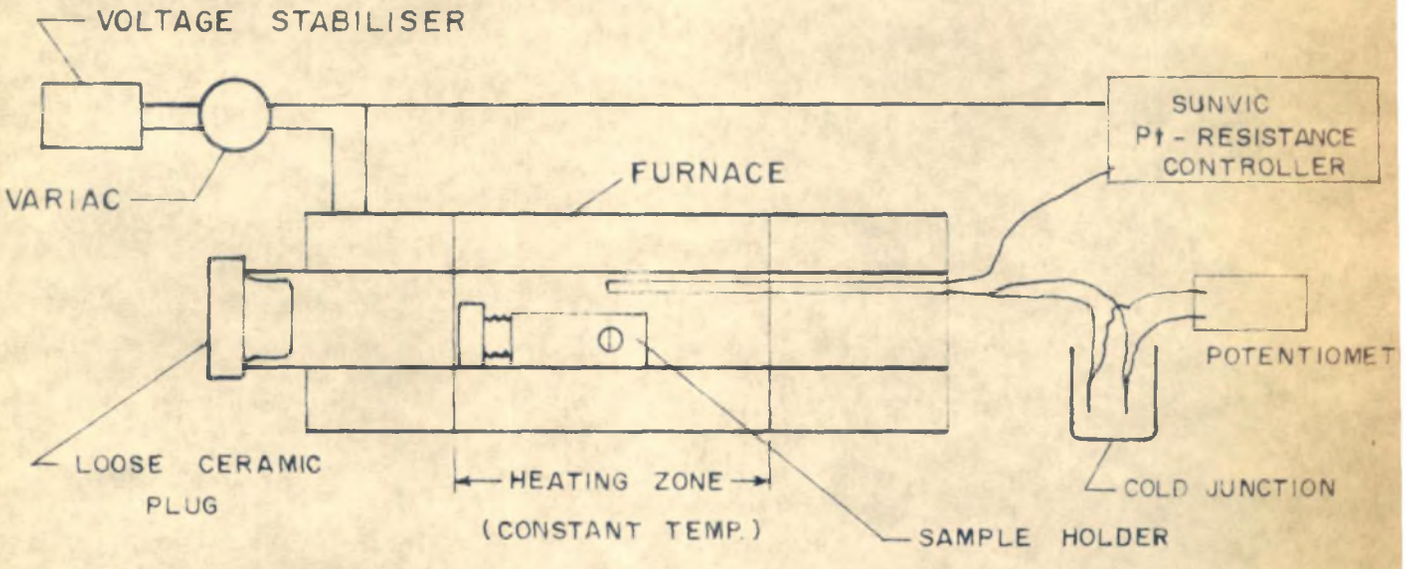

(b) SCHEMATIC DIAGRAM SHOWING THE EXPERIMENTAL SET-UP

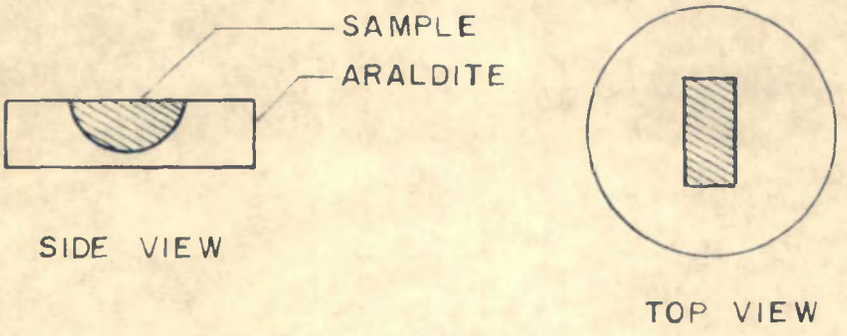

(c) SKETCH OF A SAMPLE ENCAPSULATED IN ARALDITE FOR EPMA ANALYSIS

FIGURE 4·1

temperature at the same position could be sensed by both of them. A constant temperature zone of about 6 inches within the furnace was obtained; hence along the holder length no temperature gradient was present. The complete set-up is shown schematically in Figure 4.1(b).

At the end of the specified time interval the holder was pulled out of the furnace by means of a wire tied to it and was quenched in air.

On cooling, the CuO and Fe_2O_3 pellets easily separated in each case. Product formation could be visually observed on the reacted faces of Fe_2O_3 pellets, but this was not observed in the case of CuO pellets.

The pellets were cut along the axis on a diamond wheel. The cut pieces were then encapsulated in an Araldite mould, with the cut faces exposed on one side of the mould. The moulds were 1 inch in diameter and 5 mm thick; this size was chosen on the basis of the holder size in the EPMA instrument to be used. The exposed faces along with the mould were polished following the procedure described earlier in this section. The sample thus prepared is illustrated in Figure 4.1(c).

Scanning with EPMA

The polished samples were coated with a thin layer of silver paint to get a conducting contact. A CAMECA Electron Probe Micro Analyser, Model MS 46 (at the Defence Metallurgical Research Laboratory, Hyderabad) was used for the analysis. On the silver coated surface a narrow electron beam was scanned perpendicularly to the reaction interface. For both Cu and Fe, Kα intensities were used. The accelerating voltage was 25 KV, the take off angle 18^{o}, and the sample current 50 nA. With a counter and a recorder connected to the analyser, concentration profiles along the width of the sample were obtained.

The concentration profiles of Cu within the Fe_2O_3 pellet after 24 and 48 hours of reaction at $950^{o}C$ are shown in Figure 4.2. A number of trial experiments had to be conducted (to eliminate practical difficulties) before getting the final results. Because of this and particularly due to the nonavailability of the instrument, more results could not be obtained. The model was therefore tested with the data for 24 and 48 hours only.

4.3 RESULTS AND DISCUSSION

In the CuO samples examined no Fe profile could be

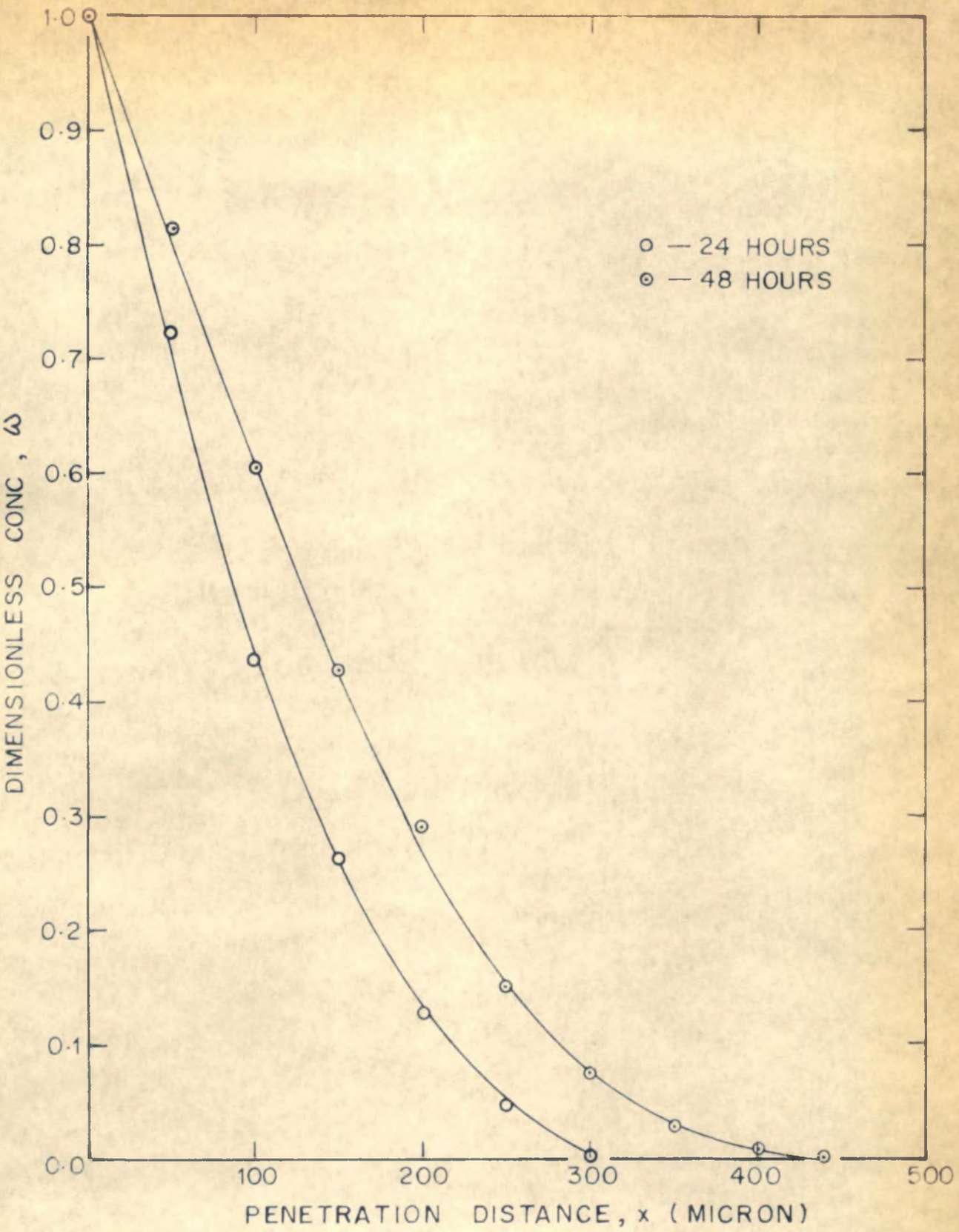

EXPERIMENTAL CONCENTRATION PROFILES OF Cu IN Fe_2O_3 AT 950°C AS OBTAINED FROM EPMA STUDIES

FIGURE 4·2

detected, whereas in the Fe_2O_3 samples Cu profiles were obtained. Within the product layer, no concentration gradient was observed. Thus, the system fulfils the two basic assumptions of the model, viz. (i) absence of diffusional resistance in the product layer, and (ii) one-way diffusion.

4.3.1 Steady state model

The procedure for predicting the concentration profile of the steady state model has already been described in Section 2.3. Now, the apparent reaction zone thickness value corresponding to the concentration profile for 24 hours is $\Delta z = 0.3$. Using Equation 2.17 the value of ϕ_r for $\Delta z = 0.3$ is found: $\phi_r = 10$. Hence, from Equation 2.14, taking $\omega_p = 1$, values of ω for different values of z are computed and plotted in Figure 4.3. The experimental profile is also shown in the figure for comparison. The profiles show a reasonably good match. This is also true for the case of 48 hours (figure not shown).

It may be noted that the agreement between the experimental and predicted profiles is not as good in this case as for some of the reported systems used for testing the model in Chapter 2. This may be because steady state was already established in those cases; here it is obviously not so.

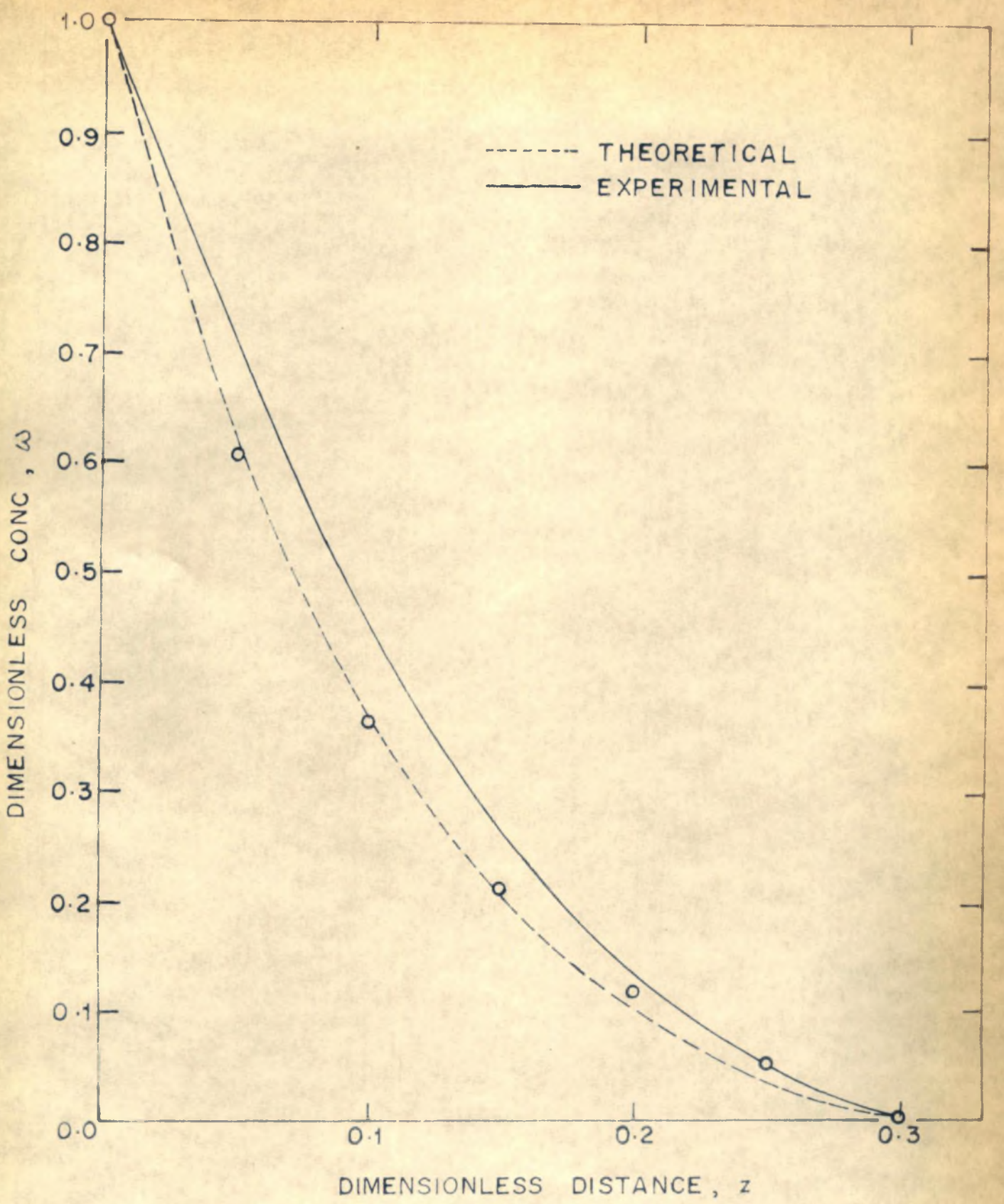

COMPARISON OF THE THEORETICAL PROFILE CALCULATED FROM THE STEADY STATE MODEL WITH THE EXPERIMENTAL PROFILE OBTAINED FROM EPMA STUDIES

(FOR THE SAMPLE OF 24 HOURS)

FIGURE 4·3

4.3.2 Unsteady state model

A method has been described in Section 3.3 for obtaining the diffusivity (D) and rate constant (k) values from the concentration profiles obtained by EPMA. The D and k values thus obtained can be used to predict concentration profiles.

Since the limit of detectability in the present case could not be determined precisely, the alternative method suggested in Section 3.3 was used here. Accordingly the plot for $\omega_m = 0.5$ shown in Figure 3.4 was used. The method can be summarised as follows:

(1) A rate constant value was assumed. Hence for the two times, m_3 values were computed, since $m_3 = \sqrt{kt}$.

(2) From the plot in Figure 3.4, the corresponding values of m_2 were obtained.

(3) From the m_2 values thus obtained, D values in the two cases were computed using the relation

$$D = \frac{x_{0.5}}{m_2 \sqrt{t}}$$

where $x_{0.5}$ is the distance at which $\omega_m = 0.5$.

The difference between the D values thus obtained for two times was minimised by trials at several values of k. The procedure was programmed on a MOSCAL 1080 PS programmable calculator. The best values of k and D thus obtained are: $k = 1 \times 10^{-7}$ sec^{-1} and $D = 1.0689 \times 10^{-9}$ cm^2 sec^{-1}.

Using these values of k and D, concentration profiles were predicted. These are shown in Figure 4.4 along with the experimental profiles. The plots show remarkably good match. The deviation towards the end is likely to be due to the limit of detectability of the instrument for the system studied. In fact, from the theoretical plot, the limit of detectability value can be determined.

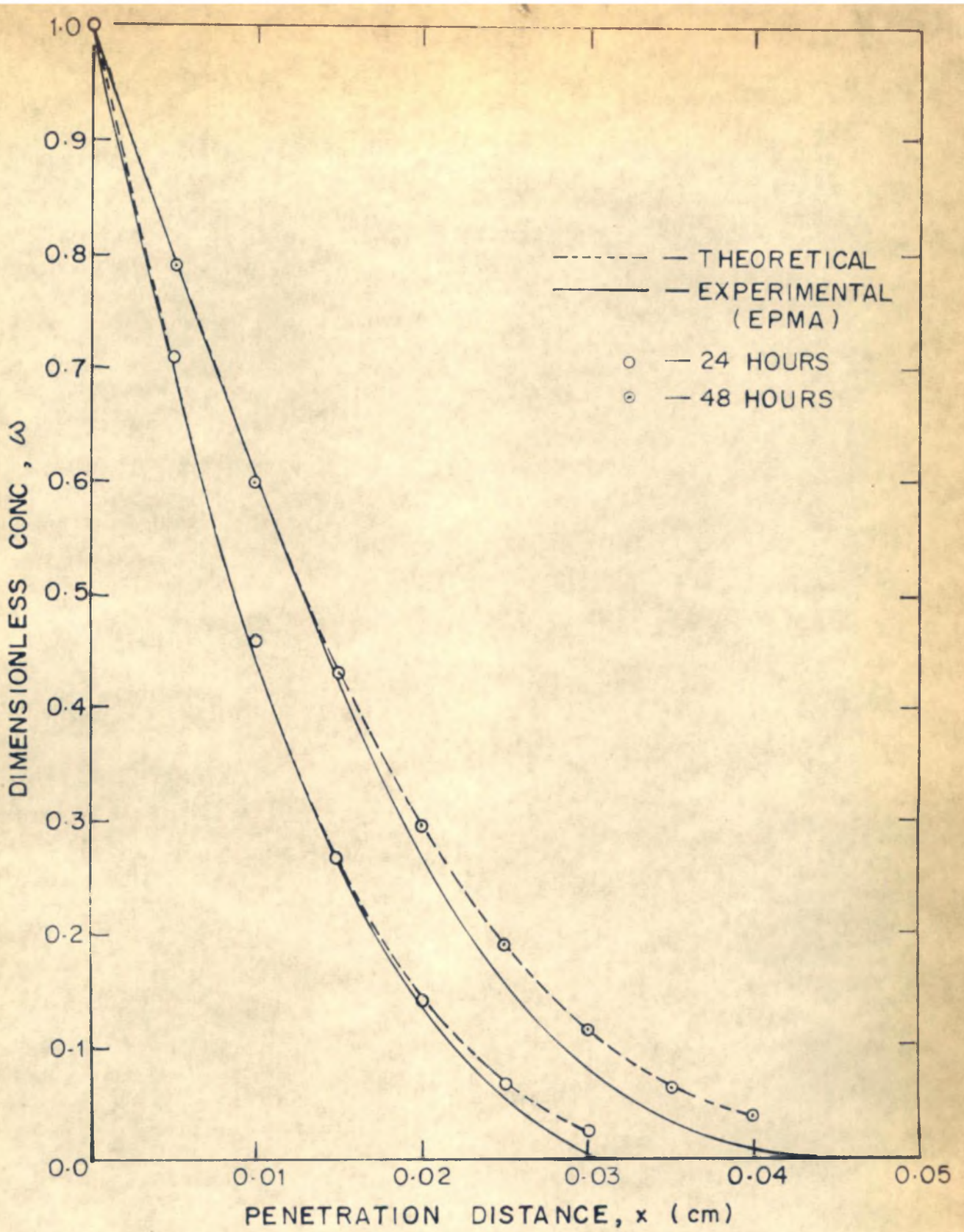

COMPARISON OF THE THEORETICAL PROFILES COMPUTED FROM THE UNSTEADY STATE MODEL WITH THE EXPERIMENTAL PROFILES OBTAINED FROM EPMA STUDIES

FIGURE 4·4

CHAPTER 5

ANALYSIS OF MIXED POWDER REACTIONS

5.1 INTRODUCTION

Mixed powder solid-solid reactions, in view of their industrial importance, have received greater attention than the pellet-pellet systems. Thus a number of models have been developed for mixed powder reactions, which provide conversion-time relationships. However, no firm strategy has yet emerged for a complete analysis of kinetic data on mixed powder systems.

Jander (1927) for the first time formulated a mathematical model for diffusion-controlled mixed powder reactions. Since then a number of models have evolved, all of which follow basically the same treatment. Expressions have also been derived for other controlling mechanisms. Hulbert and Klawitter (1967) have classified the different models proposed based on the controlling mechanism involved, while Sharp *et al* (1966) have prepared numerical tables for all of them.

The various models and the general features of analysis of mixed powder reactions have already been discussed in Section 1.5. A major drawback of most of the earlier

studies is that a single controlling mechanism is considered to be operative throughout the course of reaction. Diffusion control being predominant in many cases, the data are fitted using one of the expressions for diffusion-control. The fact that chemical reaction can also be a controlling step, especially at relatively lower temperatures, is mostly neglected. Moreover, a number of expressions exist even for diffusion control mechanism; some are theoretical and some empirical. As such, in most of the cases, a trial-and-error fit is employed.

In the present chapter a more general treatment of mixed powder systems is attempted. Thus, different controlling regimes are considered and a unique expression in each case is suggested to eliminate the tria-and-error procedure. A procedure is then proposed which is tested with a few reported experimental data.

The analysis is based on an analogy between solid-solid and gas-solid (noncatalytic) reactions. While such an analogy has been considered in some earlier studies, it has not been brought out clearly and established from theoretical and experimental considerations. For this purpose a new concept is introduced here first, and then the consequent development presented.

5.2 THE HYPOTHETICAL PARTICLE CONCEPT

Consider a solid-solid reaction

$$A(s) + B(s) \longrightarrow C(s)$$

In practice such reactions are usually carried out by the so-called "ceramic technique" described in Section 1.7. Accordingly the steps involved in the overall process are: (1) sizing of the powders of individual component oxides, (2) mixing of these powders in proper proportions (usually in a ball mill), (3) compacting the powder mixture to a suitable size and shape, and (4) heating the compacts at the desired temperature in a furnace. Thus the reaction proceeds inside a compact amongst the individual grains of reactants that are randomly distributed.

Now the particles of A and B within a compact will be of different shapes and sizes, and variously distributed. As such, initially the reaction will start only in certain discrete areas where A and B are effectively in contact. If a representative B particle is considered, it will initially have a nonuniform product core due to reaction only at contacts between A and B. This will eventually be smoothened due to consequent diffusion and reaction, and a spherical shell of product

enclosing the unreacted spherical core of B will appear. These different stages are represented in Figure 5.1(a).

The situation described above is however difficult to analyse mathematically. Hence, a hypothetical particle of B is postulated which is completely surrounded by the reactant A. The product growth will now be uniform resulting in a spherical product shell enclosing the unreacted particle of B. This situation is identical to that in a gas-solid (noncatalytic) reaction system, which has been extensively studied.

Even in practice, such a situation is not difficult to visualise for solid-solid reactions. First, there is the possibility of participation of almost the whole surface of a particle of B due to vapour phase diffusion and surface diffusion. The contribution of vapour phase diffusion in solid-solid reactions has already been discussed in Section 1.6.1. Fast surface diffusion (and grain boundary diffusion) of one of the reactants over the surface of the other would also achieve the same results. In fact, the contribution of surface diffusion in solid-solid reactions has recently been mathematically treated by Komatsu and coworkers (Moon and Komatsu, 1974; Maruyama *et al*, 1976; Yamashita *et al*, 1977) who have attempted to estimate the surface layer thickness values in various

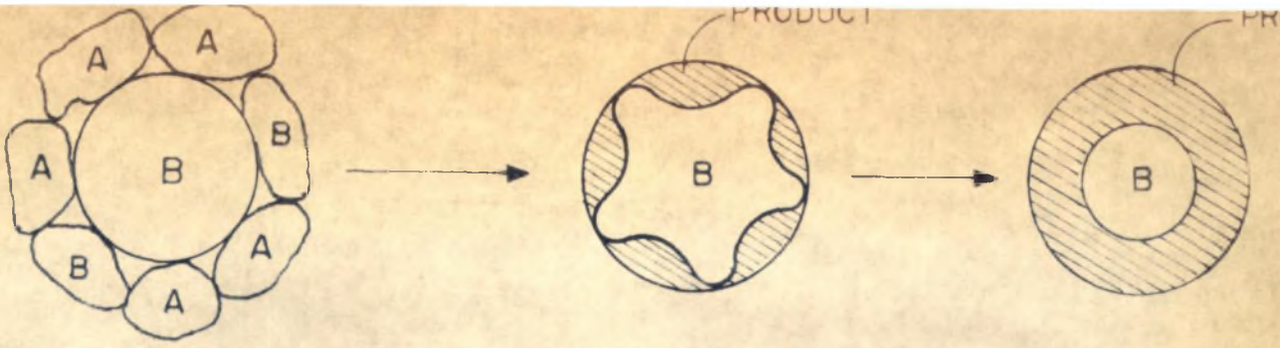

(a) SCHEMATIC REPRESENTATION OF THE PLAUSIBLE COURSE OF REACTION OF THE CENTRAL B PARTICLE WITH THE SURROUNDING A PARTICLES

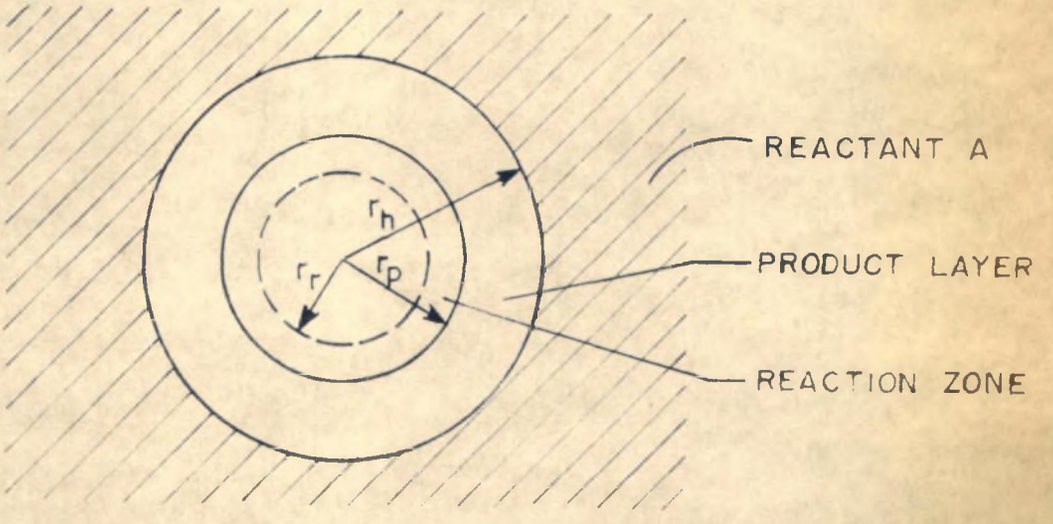

(b) THE HYPOTHETICAL PARTICLE

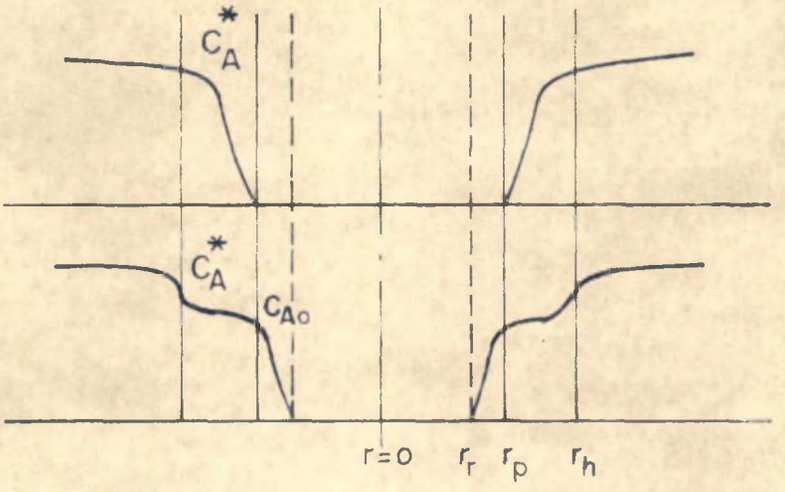

(c) CONCENTRATION PROFILES FOR DIFFUSION IN THE PRODUCT LAYER AND DIFFUSION-CUM-REACTION IN A REACTION ZONE

FIGURE 5.1

systems. Secondly, in the absence of vapour phase or surface diffusion, the concept of hypothetical particle to be presented now will help in realising such a situation.

Considering again the random spatial arrangement of particles of A and B around a central B particle as illustrated in Figure 5.1(a), it is obvious that only a part of the total surface area of the central B particle is effectively in contact with the other reactant A. From a knowledge of the average particle radius of B, the total surface area S_B of a particle of B can be calculated:

$$S_B = 4\pi r_B^2 \tag{5.1}$$

Now, the effective contact area S_{Be} is a fraction of the total surface area S_B. Thus,

$$S_{Be} = f\, S_B \tag{5.2}$$

The factor f can be obtained by a simple geometrical consideration. For an ideal packing of equisized spheres, f is given by

$$f = \frac{N_A}{N_A + N_B} \tag{5.3}$$

N_A and N_B being the number of particles of A and B respectively in a given mixture. N_A and N_B can be calculated knowing the densities (ρ_i), the particle radii (r_i) and the weights (W_i) of A and B. The resulting expression is:

$$f = \frac{\bar{sw}}{1 + \bar{sw}} \tag{5.4}$$

where $s = r_B^3 \rho_B / r_A^3 \rho_A$ and $\bar{w} = W_A/W_B$, the weight ratio. However, Equation 5.4 is for an ideal situation, wherein perfect mixing is assumed; also it does not take into account the voidage between the particles, which reduces the contact area further. Hence, the factor f is modified by introducing a parameter g, either as a multiplying factor (in which case, $g < 1$) or as an exponent ($g > 1$, since $f < 1$). The two forms are:

$$f_e = gf = g\left[\frac{\bar{sw}}{1 + \bar{sw}}\right], \quad g < 1 \tag{5.5}$$

and

$$f_e = (f)^g = \left[\frac{\bar{sw}}{1 + \bar{sw}}\right]^g, \quad g > 1 \tag{5.6}$$

where f_e denotes the effective value of the factor.

The form given by Equation 5.6 is identical to a factor used by Komatsu (1965) for calculating the number of contact points between the particles of A and B (see Equation 1.59). It may be inferred from the above discussion, however, that it is more logical to consider contact surface area rather than contact points.

Knowing the effective contact area S_{Be} of a single representative B particle, one can now define a hypothetical spherical particle of B with radius $r_{Bh} = \sqrt{S_{Be}/4\pi}$. This hypothetical particle can be assumed to be completely surrounded by the component A, so that reaction proceeds inwards forming an immobile product shell surrounding the unreacted core of B. Such a particle is represented in Figure 5.1(b). The situation is identical to that encountered in gas-solid (noncatalytic) reactions.

Different modes of reaction can now be treated on a common basis. Thus, when vapour phase or surface diffusion contributes to the mass transfer phenomenon, r_{Bh} will apporach r_B, the actual particle radius. Also, if the particles of A are extremely small compared to those of B, i.e. $r_A << r_B$, then s will become large, so that 1 can be neglected in comparison to the term $s\bar{w}$ in (5.4), and f approaches unity. This results in $S_{Be} \approx S_B$ or

$r_{Bh} \approx r_B$. It may be noted that the designation of the given two components as A and B is arbitrary. However, from the mechanistic point of view, the component whose particle size affects the overall rate is treated as the component B.

With the hypothetical particle concept described above, the analogy between solid-solid and the gas-solid (noncatalytic) reactions becomes clearer. Yet a basic difference between the two remains, viz. in gas-solid systems one of the reactants (the gas phase) is in continuous flow, while such is not the case in solid-solid systems. As a consequence, the bulk concentration of the gas can always be maintained constant; the bulk phase concentration of the corresponding component (i.e. A) in the latter, on the other hand, cannot remain constant as it is consumed. However, for the purpose of analysis one is concerned with the interface concentration rather than the bulk concentration; and the interface concentration is maintained constant for the major part of the reaction as evidenced by the studies of Cerovic *et al* (1969). Hence, the possible complication due to a varying concentration is eliminated.

5.3 CONTROLLING MECHANISMS

Considering the hypothetical particle, the various resistances offered in series would be: (1) self-diffusion of A, (2) diffusion of A through the product layer, and (3) diffusion and reaction within the unreacted B. Of these, the resistance due to self-diffusion is never found to be controlling in solid-solid addition reactions considered here.

5.3.1 Product layer diffusion control

For this case the well known rate expression derived for gas-solid (noncatalytic) reactions in the shrinking core model can be directly used (see Levenspiel, 1974). Thus,

$$t/\bar{t} = 1 - 3(1-\alpha)^{2/3} + 2(1-\alpha) \qquad (5.7)$$

where α is the fractional conversion, t the time, and $\bar{t}$ the time required for complete conversion. $\bar{t}$ is given by the expression

$$\bar{t} = \frac{\rho_B r_h^2}{6 D_{ep} C_A^*} \qquad (5.8)$$

The apparent rate constant $1/\bar{t}$ and the corresponding activation energy can thus be calculated. If the other quantities in Equation 5.8 are known, the radius of the hypothetical particle r_h and consequently the effective surface area S_{Be} can be determined. Of the quantities involved, ρ_B is always known (or can be easily determined) and C_A^* can be found experimentally by EPMA studies; D_{ep} has, however, to be determined separately.

The expression for gas-solid reactions given by (5.7) is a mathematically derived one and not an empirical equation. It might therefore be used in preference to any empirical expression developed specifically for solid-solid reactions. Whether the reaction under consideration is controlled by this mechanism or not can be easily verified by studying the effect of particle size, since $\bar{t} \propto r_B^2$ for product layer diffusion control.

In the above treatment, the size of the reacting particle is assumed unchanging during reaction. However, if the molar volumes of the product and the reactant (B) are different, a change in size has to be expected. A rate expression accounting for such a volume change in the shrinking core model has been derived by Carter (1961b), wherein a parameter Z is introduced representing the volume

of the product formed per unit volume of the reactant B consumed. The resulting rate expression is:

$$Kt = \frac{Z-\{1+(Z-1)\alpha\}^{2/3} - (Z-1)\ (1-\alpha)^{2/3}}{(Z-1)} \qquad (5.9)$$

5.3.2 Chemical reaction control

In the shrinking core model, reaction is considered to be occurring at the surface of the unreacted core. A more general treatment results following the zone model developed in the earlier chapters. The surface reaction then becomes a limiting case.

The zone model developed in Chapter 2 can be readily adapted to a spherical particle. In fact, Mantri et al (1976) have developed equations for a spherical particle under similar conditions in gas-solid (noncatalytic) reactions. Thus referring to Figure 5.1(c) the dimensionless concentration in the reaction zone can be expressed as

$$\omega = \omega_p \frac{\text{Sinh } \{\phi_r(z-z_r)\}}{\text{Sinh } (\phi_r\ \Delta z)} \qquad (5.10)$$

where

$$\Delta z = z_p - z_r \qquad (5.11)$$

The dimensionless quantities are now $\omega = C_A/C_{Ao}$, $z = r/r_h$, and $\phi_r = r_h \sqrt{k/D_{er}}$ the Thiele modulus.

The rate of reaction can be written as

$$-\frac{1}{4\pi r_p^2}\frac{dn_A}{dt} = -\frac{1}{4\pi r_p^2}\frac{dn_B}{dt} = -\rho_B \frac{dr_p}{dt} \qquad (5.12)$$

since

$$-dn_B = -\rho_B dV \simeq -\rho_B d\left(\frac{4}{3}\pi r_p^3\right) = -4\pi \rho_B r_p^2 dr_p \qquad (5.13)$$

The rate of reaction can also be expressed in terms of the flux of the reactant species entering the reaction zone. Thus,

$$-\rho_B \frac{dr_p}{dt} = M D_{er} \left[\frac{dC_A}{dr}\right]_{r=r_p} \qquad (5.14)$$

Obtaining the flux from Equation 5.10 and combining with (5.14) the rate becomes

$$-\frac{dr_p}{dt} = \frac{MC_{Ao} D_{er}}{\rho_B r_h} \omega_p \phi_r \coth(\phi_r \Delta z) \qquad (5.15)$$

All the quantities on the R.H.S. being constant (here, the zone thickness Δz is assumed constant), integration of (5.15) for r between r_h and r_p and t between o and t gives

$$(r_h - r_p) = k't \tag{5.16}$$

When expressed in terms of conversion $\alpha\{=1-(r_p/r_h)^3\}$ this becomes

$$1 - (1 - \alpha)^{1/3} = k_o t \tag{5.17}$$

In these equations

$$k_o = \frac{MC_{Ao}D_{er}}{\rho_B r_h^2} \omega_p \phi_r \coth(\phi_r \Delta z) \tag{5.18}$$

and

$$k' = r_h k_o$$

The final form of the expression obtained is thus identical to that obtained for the shrinking core model. This also explains why often the simple shrinking core model is adequate even for gas-solid (noncatalytic) reactions.

Now, if the reaction zone thickness is too small, i.e. $\Delta z \longrightarrow o$, then ϕ_r becomes large so that (5.18) reduces to

$$k_o = \frac{MC_{Ao}(kD_{er})^{1/2}}{\rho_B r_h}$$

$$= \frac{MC_{Ao}k_s}{\rho_B r_h} \qquad (5.19)$$

since $(kD_{er})^{1/2} = k_s$, the surface reaction rate constant.

The rate constant k_o appearing in Equation 5.17 is now the same as $1/\bar{t}$ appearing in the corresponding expression in the shrinking core model. Here again, knowing the other quantities and using the experimental value of $\bar{t}$, r_h can be estimated. However, evaluation of r_h is unimportant from the practical view-point, since the overall constant and activation energy can be obtained from Equation 5.17.

It should be noted that Equation 5.17 is a predictive expression, and the rigorous form may be quite complicated, especially if an unsteady state process is considered.

For discerning the controlling mechanism experimentally in gas-solid reactions, usually the effect of particle size

on rate (or on $\bar{t}$) is examined: for product layer diffusion control rate is proportional to $1/r^2$ and for chemical reaction control to $1/r$. In the present case, the particle size involved is that of the hypothetical particle, i.e. r_h, which is related to r_B, the actual particle radius, in a complex manner. The procedure for determining the controlling regime is outlined below.

5.4 TEST OF EXPERIMENTAL DATA FOR THE CONTROLLING REGIME

Once the analogy between solid-solid and gas-solid (noncatalytic) reactions is established, the same predictive equations for conversion-time relationship can be used. This eliminates trial-and-error method involved, as mentioned earlier.

Thus for diffusion control, Equation 5.7 or 5.9 can be used, as the case may be; for chemical reaction control Equation 5.17 should be used. Here again, as pointed out earlier in Section 3.4, it should be noted that the diffusion control may be in the product layer or in the unreacted core. In both the cases, the fluxes being the same, the same expression will be applicable.

A few reported data on mixed powder systems will now be used for demonstrating the procedure. Krishnamurthy *et al* (1974), in their studies on the mixed powder reaction

between ZnO and Fe_2O_3, have fitted the data with Jander's equation. When the data points are replotted according to Equation 5.7, a remarkable fit is obtained as shown in Figure 5.2. In this case, possible reaction control at shorter times cannot be tested due to lack of data points for time less than 2 hours.

Branson (1965), in his studies on the system ZnO-Al_2O_3, found that Equation 5.9 could correlate the data well for most part of the reaction. In the earlier stages, however, a marked deviation is observed. This has been explained on the basis of initial phase boundary control mechanism. If the data points are plotted according to Equation 5.17, linear plots are obtained as shown in Figure 5.3. The corresponding Arrhenius plot is shown in Figure 5.4.

An organic solid-solid system has been studied by Ramachandran *et al* (1974). Their data can also be similarly analysed. The analysis shows chemical reaction control for shorter times and diffusion control for the rest, as is illustrated in Figure 5.5.

Finally, mention should be made of the deviation appearing invariably at longer times. This is primarily due to the fact that when most of A is consumed, the interface concentration may drop considerably. Probably a more

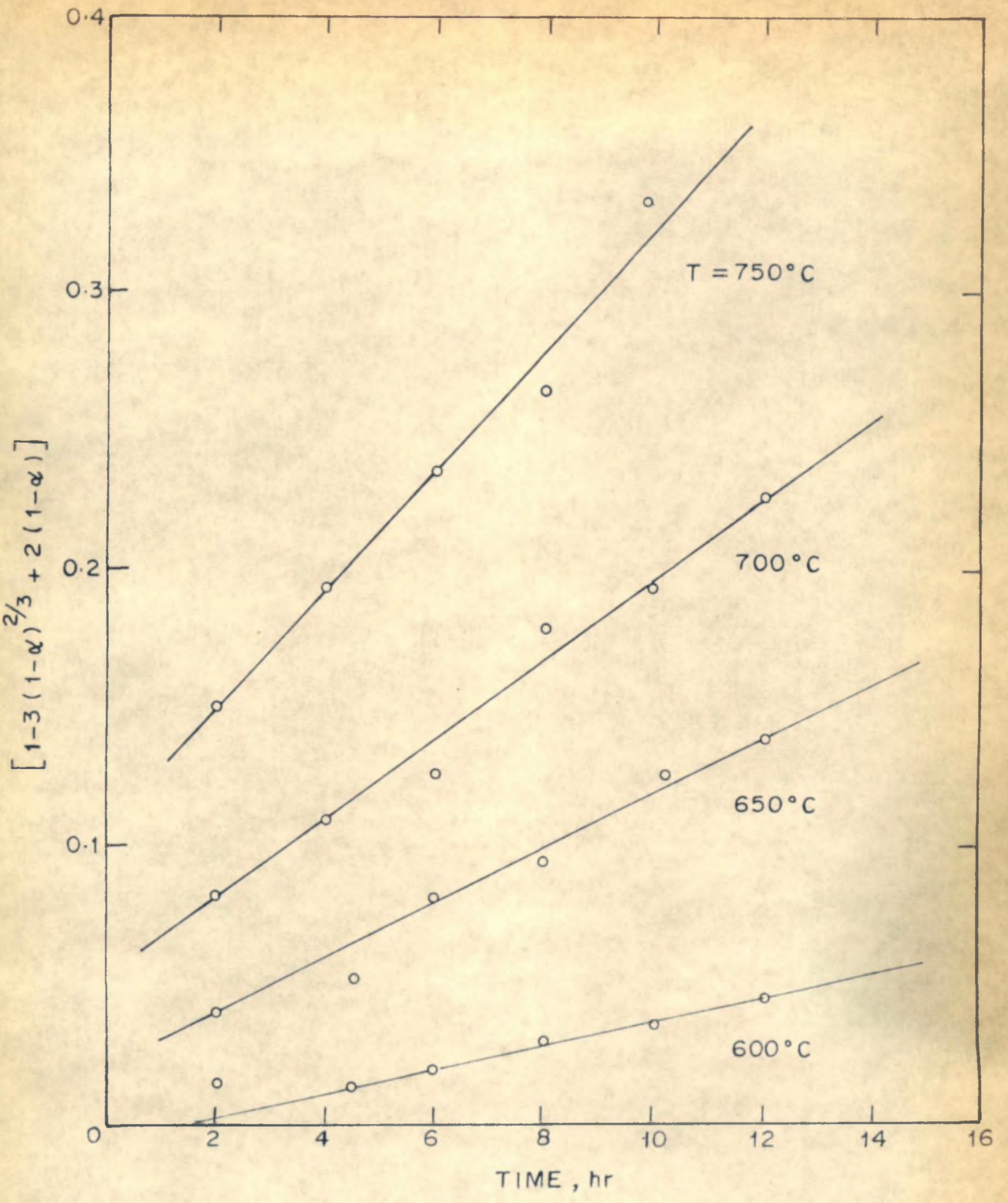

DATA OF KRISHNAMURTHY *et al* (1974) PLOTTED ACCORDING TO EQUATION 5·7

FIGURE 5·2

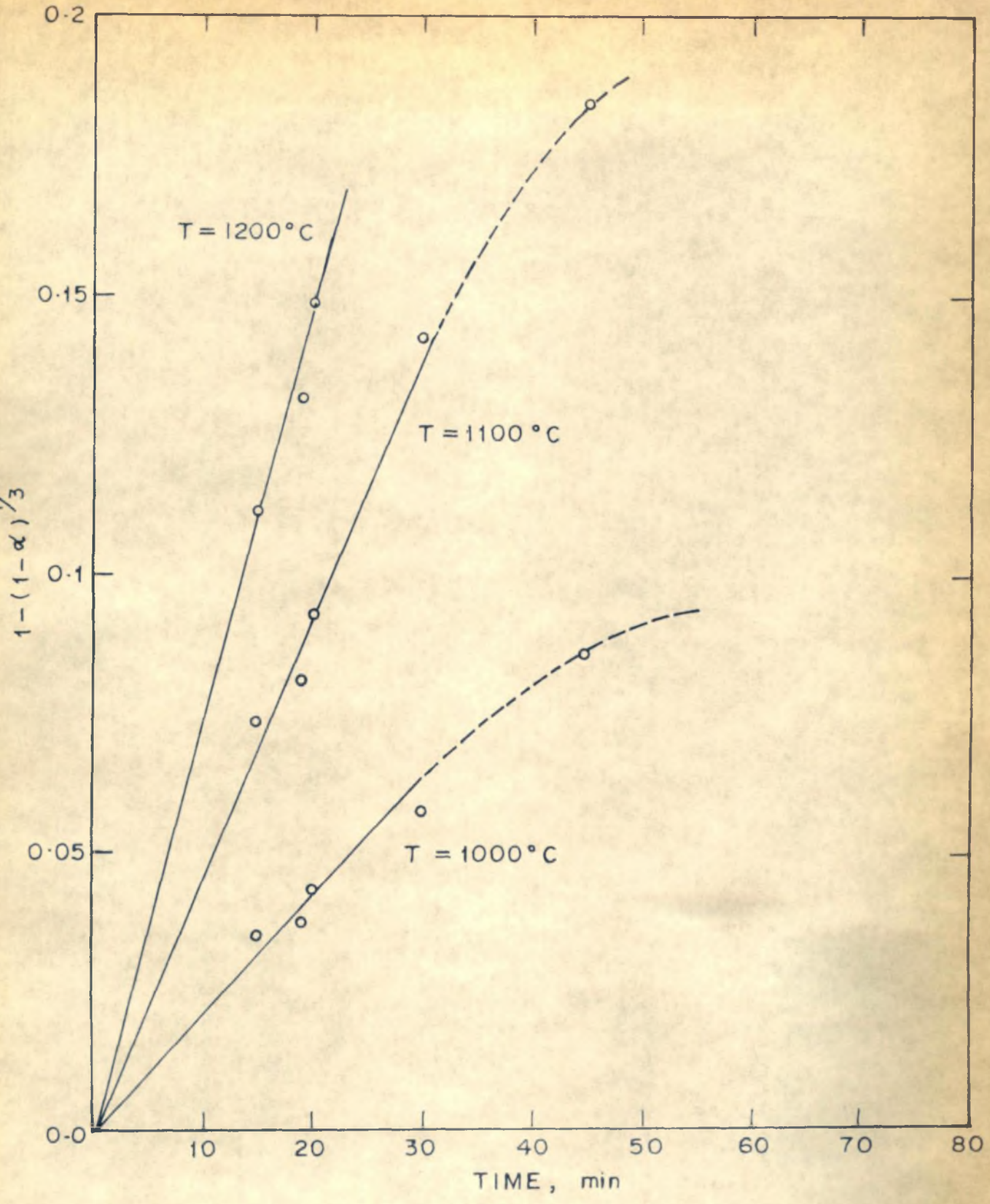

DATA OF BRANSON (1965) FOR THE INITIAL PERIOD PLOTTED ACCORDING TO EQUATION 5·17

FIGURE 5·3

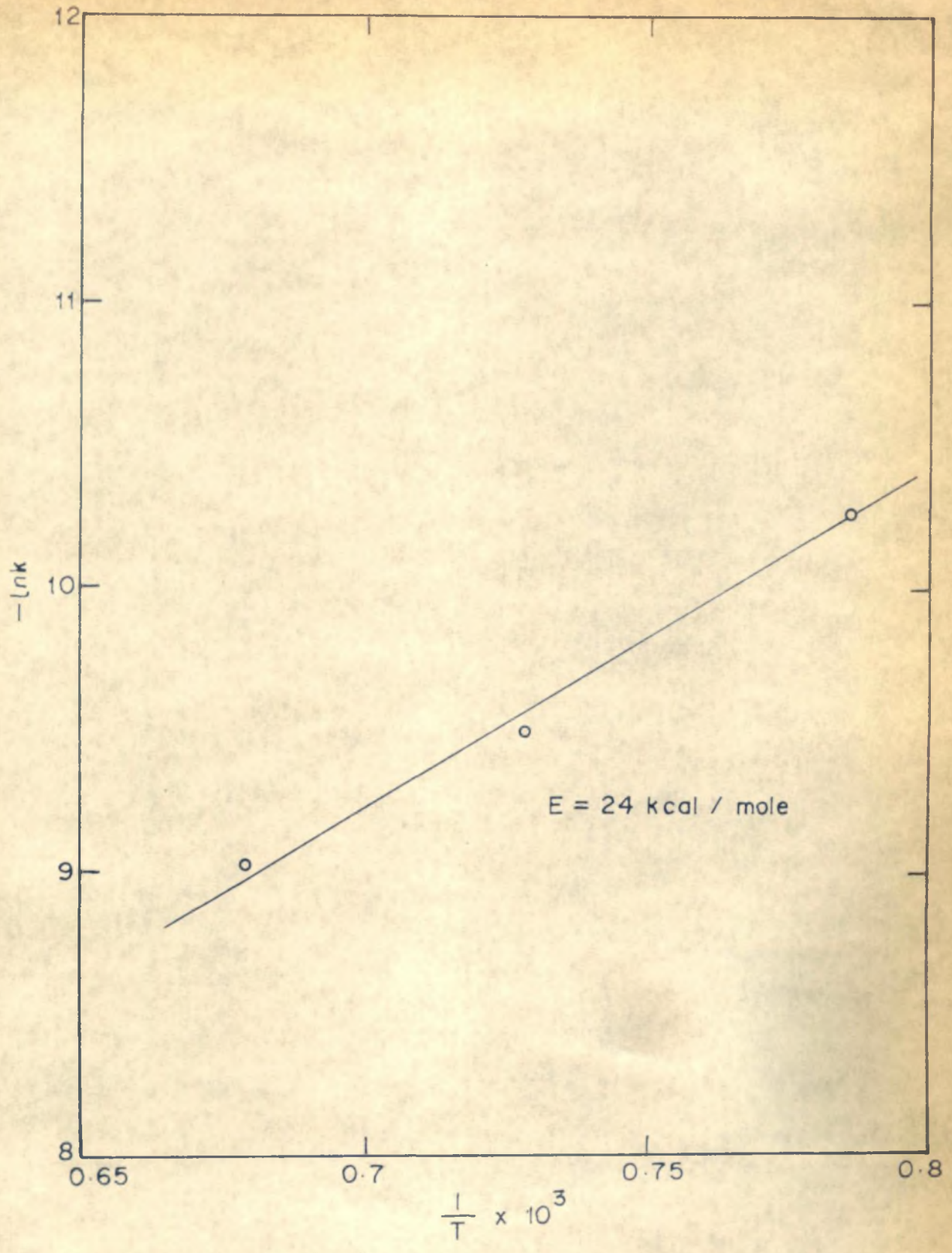

ARRHENIUS PLOT CORRESPONDING TO FIGURE 5.3

FIGURE 5.4

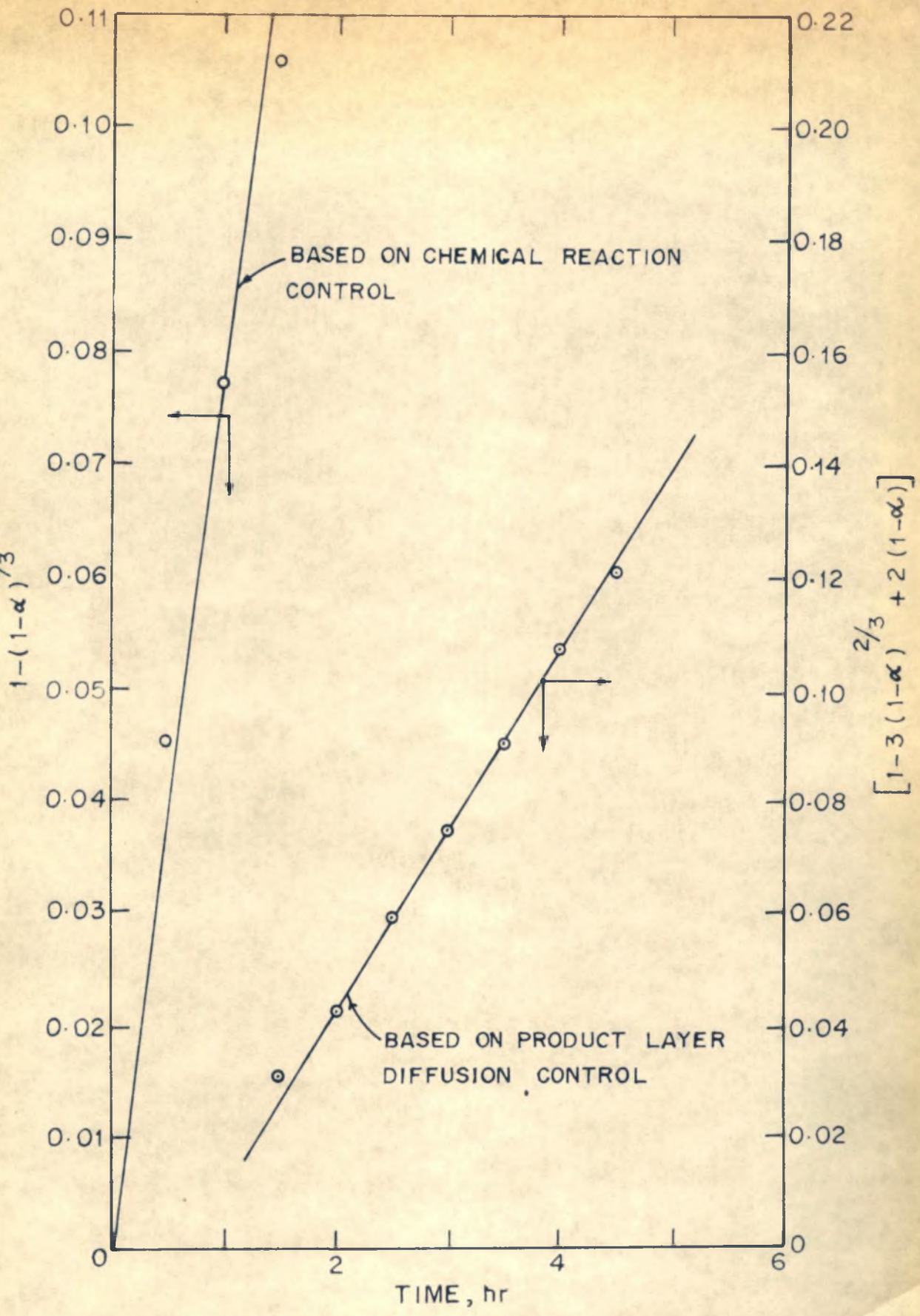

CONVERSION DATA OF RAMACHANDRAN *et al* (1974) PLOTTED ACCORDING TO EQUATIONS 5·7 AND 5·17

FIGURE 5·5

practical reason is the lack of contact between still unreacted components which are separated by a large distance due to improper mixing. Effectively in both the cases the rate falls tremendously. This usually happens only after 80-90% conversion.

5.5 CONCLUSION

Mixed powder systems are far more important industrially than pellet-pellet systems whose usefulness is restricted to a theoretical understanding of solid-solid reactions. On the other hand, mixed powder systems by their very nature are difficult to analyse. Thus the general approach so far has been to fit the data for each system according to a specific empirical equation (Jander's equation, Carter's equation, etc.). In addition to being empirical this approach assumes a single controlling mechanism throughout the reaction.

In this chapter an attempt has been made to extend the methods of analysis of gas-solid reactions to mixed powder systems. While in the case of pellet-pellet reactions the geometrical considerations involved did not pose any problems, in the case of mixed powder systems the concept of a hypothetical particle has been introduced to facilitate analysis. With this concept the theory of gas-solid reactions

has been extended to mixed powder systems and a procedure suggested for analysing the controlling regimes throughout the course of the reaction. It has been shown that a reaction can exhibit different regimes of control and that unique equations are possible for representing any specific regime, such as product layer diffusion or chemical reaction in a zone.

Much more work needs to be done on mixed powder systems before any claim can be made that a satisfactory approach is available. The approach suggested in this chapter should be regarded as no more than a first attempt towards analysing mixed powder reactions, and several improvements and changes would be necessary if a more rigorous and sophisticated model is eventually to emerge.

CHAPTER 6

STUDIES ON AN INDUSTRIALLY IMPORTANT SOLID-SOLID SYSTEM Si-CuCl

6.1 INTRODUCTION

A number of studies on solid-solid reactions amongst oxides have so far been reported in the literature, but comparatively few studies have been attempted on other systems of practical interest. In view of this, an industrially important system Si-CuCl is chosen here for study.

The preparation of the alloy Cu_3Si from the system Si-CuCl appears as an important step in the manufacture of chlorosilanes which are the starting materials in the manufacture of a variety of silicones such as silicone fluids, oils, emulsions, elastomers, insulating resins, textile finishing agents, paints, varnishes, etc. Chlorosilanes are prepared by reaction of silicon (s) with aliphatic halides (g) in the presence of the alloy Cu_3Si (the so-called η-phase) as catalyst. The first step is therefore the preparation of the η-phase which is accomplished by the reaction between Si (s) and CuCl (s):

$$nSi + 4CuCl \longrightarrow (n-1)Si^{*} + 4Cu^{*} + SiCl_4 \qquad I$$

$$3Cu^{*} + Si^{*} \longrightarrow Cu_3Si(\eta) \qquad II$$

(The asterisks denote that the corresponding components are in an activated state.)

In actual practice a large quantity of silicon is reacted in the solid phase with a small quantity of cuprous chloride (8-16%) to provide the contact mass for the main reaction containing mostly silicon and catalytic quantities of the η-phase. This silicon is then reacted with, say, methyl chloride in a suitable reactor in the presence of the η-phase to give various methyl chlorosilanes:

$$Si + 2MeCl \xrightarrow{Si-Cu} Me_2SiCl_2 \text{ (main product)}$$

$$2Si + 4MeCl \xrightarrow{Si-Cu} Me_3SiCl + MeSiCl_3$$

$$Si + 3MeCl \xrightarrow{Si-Cu} MeSiCl_3 + 2Me^{\cdot} \qquad III$$

$$Si + HCl + MeCl \xrightarrow{Si-Cu} MeHSiCl_2$$

$$Si + 2Cl_2 \longrightarrow SiCl_4$$

(Me = CH_3, Si-Cu = η-phase catalyst)

The reactions mentioned above are the overall reactions and one of the elementary steps involved is the

reaction between copper and methyl chloride to give CuCl which in turn reacts with silicon (s) to regenerate the η-phase according to reaction I.

In spite of the importance of reaction I, kinetics of this reaction have not been studied in detail; Komatsu (1954) has reported probably the only attempt wherein the data have been interpreted based on a modified form of Jander's equation discussed in Section 1.5.4.

Instead of pure silicon, which is costly, leached ferrosilicon is normally used in the above process. In fact, presence of iron (4-5%) is reported (Lobusevich *et al*, 1976) to have an added advantage in that it stabilises the catalyst by binding part of the impurities (Ti, Mn, V and P) which otherwise have unfavourable effects on the catalytic properties. Moreover, in the present studies on the reaction between leached ferrosilicon (with ~ 5% Fe) and CuCl, it has been confirmed that the iron present has no adverse effect on the reaction.

In the following, results of the experimental work on this system are reported. They reveal a typical autocatalytic system. The kinetics are evaluated in this light, and effects of various parameters discussed subsequently.

6.2 EXPERIMENTAL PROCEDURE

6.2.1 Materials used

Ferrosilicon

Ferrosilicon in the form of lumps with 80-85% purity was obtained from M/s Indian Metals & Ferroalloys Ltd., Orissa. The material was enriched to ~95% Si by leaching with dilute HCl. On leaching, the lumps crumbled to powder. The powder was thoroughly washed with distilled water and dried by keeping in an oven at ~150°C for 24 hours. Various sieve fractions from -50+70 mesh to -300 mesh were then collected. These were again dried and stored in a dessicator before actual use.

Cuprous chloride

Cuprous chloride was freshly prepared from chemically pure copper sulphate by reaction of the latter with sodium chloride in aqueous medium. Sulphur dioxide was used as a reducing agent. The product obtained was in the form of a fine powder; different particle sizes could not be obtained. The purity of the sample was checked by chemical analysis. The filtered product was carefully dried under vacuum to avoid any oxidation. The dried powder was stored in a dessicator.

6.2.2 Chemical analysis

As the reaction indicates, one of the products, silicon tetrachloride ($SiCl_4$), is a gas. During reaction, a continuous flow of an inert gas (UHP Argon) was maintained, so that the $SiCl_4$ gas was carried away. The outcoming gas was absorbed in distilled water, where it reacted instantaneously according to the reaction

$$SiCl_4 + 2H_2O \longrightarrow SiO_2 + 4HCl \qquad \text{IV}$$

The resulting solution was simultaneously titrated against a standard NaOH solution, using phenolphthalein as indicator. To ensure complete reaction of $SiCl_4$, a well stirred, baffled vessel was used; also the flow rate of Argon was kept moderate.

The amount of NaOH required corresponding to complete conversion was calculated knowing its normality and the weight of CuCl taken. Hence, conversion as a function of time could be obtained in each case.

6.2.3 Kinetic studies

As mentioned earlier, the reaction under study is important from the view-point of catalyst development in the manufacture of chlorosilanes. The amount of copper

required in the form of catalyst is usually 5-10% by weight. The corresponding amount of CuCl initially required is 8-16% by weight. In view of this, in the present studies, all the kinetic runs were carried out with ~ 15% by weight of cuprous chloride.

The reactor

A few initial experiments were conducted to decide the type of reactor, weight of sample, etc. Thus a glass tube (diameter 30 mm, length 450 mm) was used as reactor. One end of the tube was provided with a gas inlet and a thermocouple jacket reaching the centre of the tube, while the other end was closed by a cap containing an outlet tube. The reactor was placed within an electrically heated horizontal tubular furnace. Proper insulation was provided to avoid heat losses. Temperature was monitored through a calibrated millivoltmeter using a Chromel-Alumel thermocouple. The complete reactor assembly is schematically represented in Figure 6.1.

For carrying out an experiment, ferrosilicon (2g) and cuprous chloride (0.3 g) were intimately mixed in a glass mortar and pestle. The mixture was carefully transferred to a glass boat of adequate size, which was placed in the reactor at the outlet end. A glass rod with a

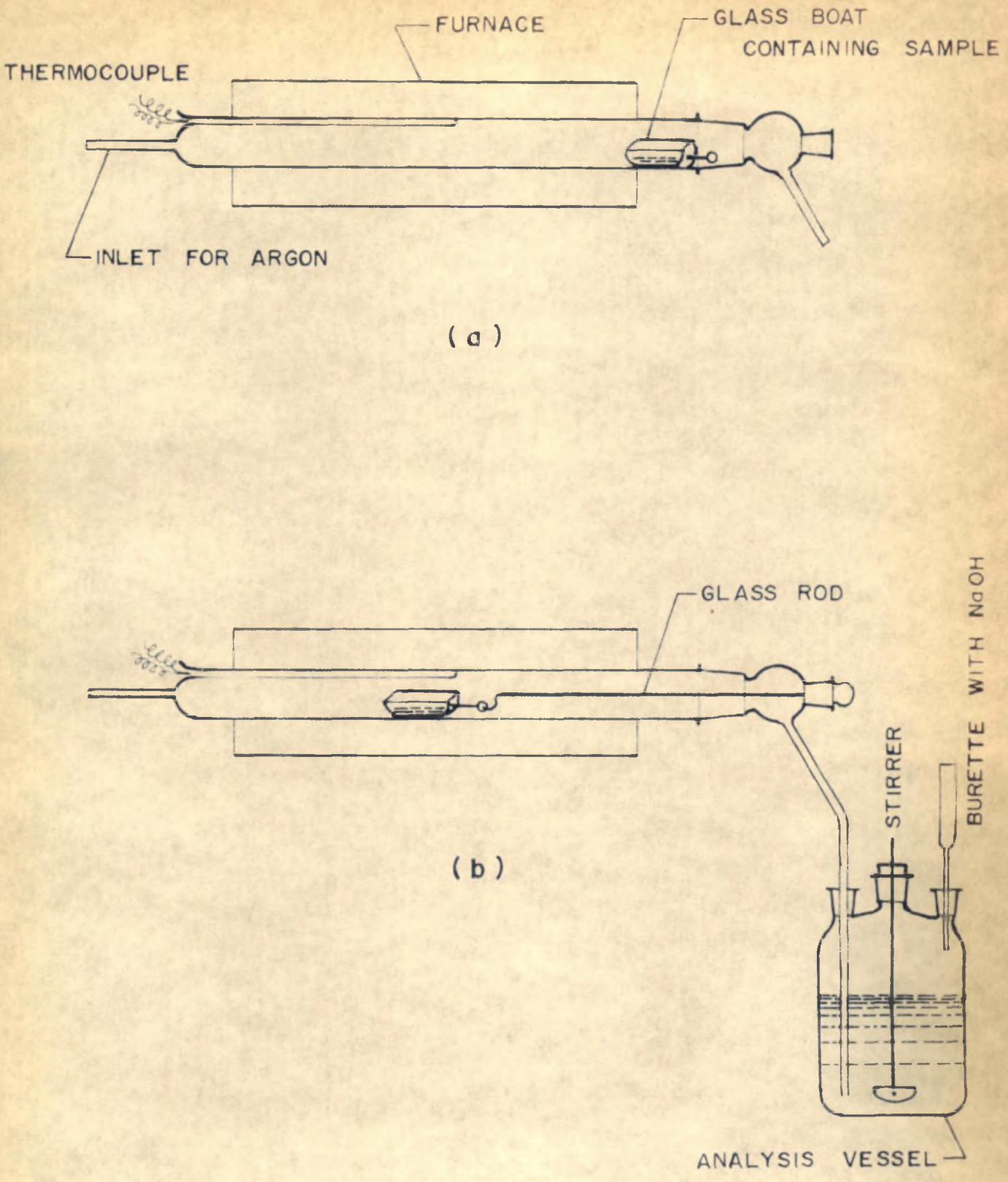

SCHEMATIC DIAGRAM SHOWING THE EXPERIMENTAL SET-UP FOR STUDIES ON THE SYSTEM Si-CuCl

FIGURE 6·1

ground joint at one end (fitting in the female joint of the cap) was provided to push the boat to the central heating zone of the reactor.

The part of the reactor where the boat was initially placed was just outside the furnace and acted as a preheater for the sample. This arrangement helped in two ways: (1) if some moisture was present in the sample, it was removed due to the moderate heating and carried away by the Argon gas; (2) the time required for the sample to reach the reaction temperature was shortened and a drastic temperature drop in the central zone when the boat was pushed, was avoided.

Argon flow rate

The object of using an inert gas here was first to remove the air and to keep an inert atmosphere throughout, and secondly to drive away the product gases. Argon was used for this purpose. The flow rate had to be adjusted so as to eliminate any possible resistance due to diffusion of the product gas; at the same time it had to be moderate enough to ensure complete reaction in the analytical vessel as mentioned earlier.

A few runs were carried out with different flow rates of Argon to test the criteria mentioned above. Based on

these a flow rate of 180 ml/min was found optimum. Therefore in all the kinetic runs the same flow rate was maintained.

Temperature

De Cooker *et al* (1975) studied the effect of temperature on this reaction by thermal analysis techniques, and have also reported the thermodynamics of the reaction. For this type of reaction threshold temperature has been found to exist above which the reaction proceeds rapidly. The threshold temperature is the temperature at which a notable rate of reaction can be observed. This may depend on a number of factors like impurity, history, etc. For the reaction Si+CuCl the threshold temperature is reported to be between 180° and 400°C, but usually it is 300°C. In the present studies also, this temperature was found to be about 300°C. The lower limit is thus automatically fixed. The upper temperature limit was fixed with respect to the melting point of CuCl, which is 422°C. Thus kinetic runs were carried out at 300°, 330°, and 360°C.

6.2.4 Other parameters

Particle size:

As mentioned earlier, cuprous chloride was obtained

as a fine powder; hence different particle sizes could not be used. Experiments with different particle sizes of ferrosilicon were carried out. However, with too coarse particles, mixing of powders could not be achieved. Such fractions were therefore discarded. All the runs were carried out at 360°C. For studying other parameters in all the cases the smallest particle size corresponding to -300 mesh sieve fraction was used.

Reactant ratio:

A few experiments were carried out to examine the effect of reactant ratio by varying the percentage of cuprous chloride in the reaction mixture. These runs were conducted at 330°C.

Additives:

Certain substances, when added in minute quantities, are known to accelerate such reactions; they are therefore known as promoters. Similarly certain substances called inhibitors retard the progress of a reaction. Thus zinc, antimony, cadmium, etc. are used as promoters in the chlorosilanes reaction; their exact role is however not known. With this in view, the effect of zinc and antimony on the present reaction was studied.

An experiment was carried out with pure silicon (99.9%) to see if iron present in ferrosilicon has any adverse effect.

All the experiments carried out are tabulated in Table 6.1. Each experiment was repeated to check reproducibility of the results.

6.3 RESULTS AND DISCUSSION

6.3.1 Kinetics and mechanism

Rate expression

Reaction I as written is not an elementary reaction, but proceeds through steps (Andrianov et al, 1970) as follows:

$$Si \xrightarrow{CuCl} SiCl \xrightarrow{CuCl} SiCl_2 \xrightarrow{CuCl} SiCl_3 \xrightarrow{CuCl} SiCl_4 \qquad V$$

However, the intermediate steps being fast, the only product detected is $SiCl_4$, and the rate is controlled by the first step alone. If the reaction is written as

$$A + B \longrightarrow P + Q \qquad VI$$

where A = CuCl, B = Si, P = $SiCl_4$, and Q = Cu, then the rate of reaction can be written as

$$\frac{-dC_A}{dt} = \frac{dC_P}{dt} = k''C_AC_B \qquad (6.1)$$

TABLE 6.1

EXPERIMENTAL DATA

Run No.	Composition of reaction mixture			Particle size of ferrosilicon mesh	Argon flow rate ml/min	Temperature ^{o}C
	Ferrosilicon g	CuCl g	X (=Zn, Sb) mg			
1	2	3	4	5	6	7
PS1	2	0.3	-	-120+150	180	360
PS2	2	0.3	-	-150+170	180	360
PS3	2	0.3	-	-170+200	180	360
PS4	2	0.3	-	-200+240	180	360
PS5	2	0.3	-	-240+300	180	360
PS6	2	0.3	-	-300	180	360
T1	2	0.3	-	-300	180	300
T2	2	0.3	-	-300	180	330
R1	2	0.1	-	-300	180	330

TABLE 6.1 (Continued)

1	2	3	4	5	6	7
R2	2	0.2	-	-300	180	330
R3	2	0.4	-	-300	180	330
F1	2	0.3	-	-300	105	360
F2	2	0.3	-	-300	155	360
F3	2	0.3	-	-300	210	360
A1	2	0.3	Zn-4	-300	180	300
A2	2	0.3	Zn-4	-300	180	330
A3	2	0.3	Zn-4	-300	180	360
A4	2	0.3	Zn-4, Sb-1	-300	180	300

Since B is used in excess, C_B can be assumed constant and the rate expressed as

$$\frac{-dC_A}{dt} = k_o C_A \qquad (6.2)$$

In the present studies all the conversion (α) *vs* time (t) plots revealed a typical S-shape (see Figure 6.2), i.e. the rate initially increased, reached a maximum, and then decreased. A typical rate curve (for run T2) is shown in Figure 6.3. This suggests autocatalysis, the plausibility of which is supported by the fact that finely divided copper is known to be a catalyst for reduction reactions. Moreover, reactions where *in situ* formation of metallic copper is involved are known to be autocatalytic in nature. Thus reduction of CuO by H_2 as well as by formaldehyde are both autocatalytic reactions.

The autocatalytic step in the present case can be represented as

$$A + B + Q \longrightarrow P + 2Q \qquad \text{VII}$$

and the corresponding rate expressed as

$$\frac{-dC_A}{dt} = k''_{ac} C_A C_Q \qquad (6.3)$$

The total rate of reaction will therefore be

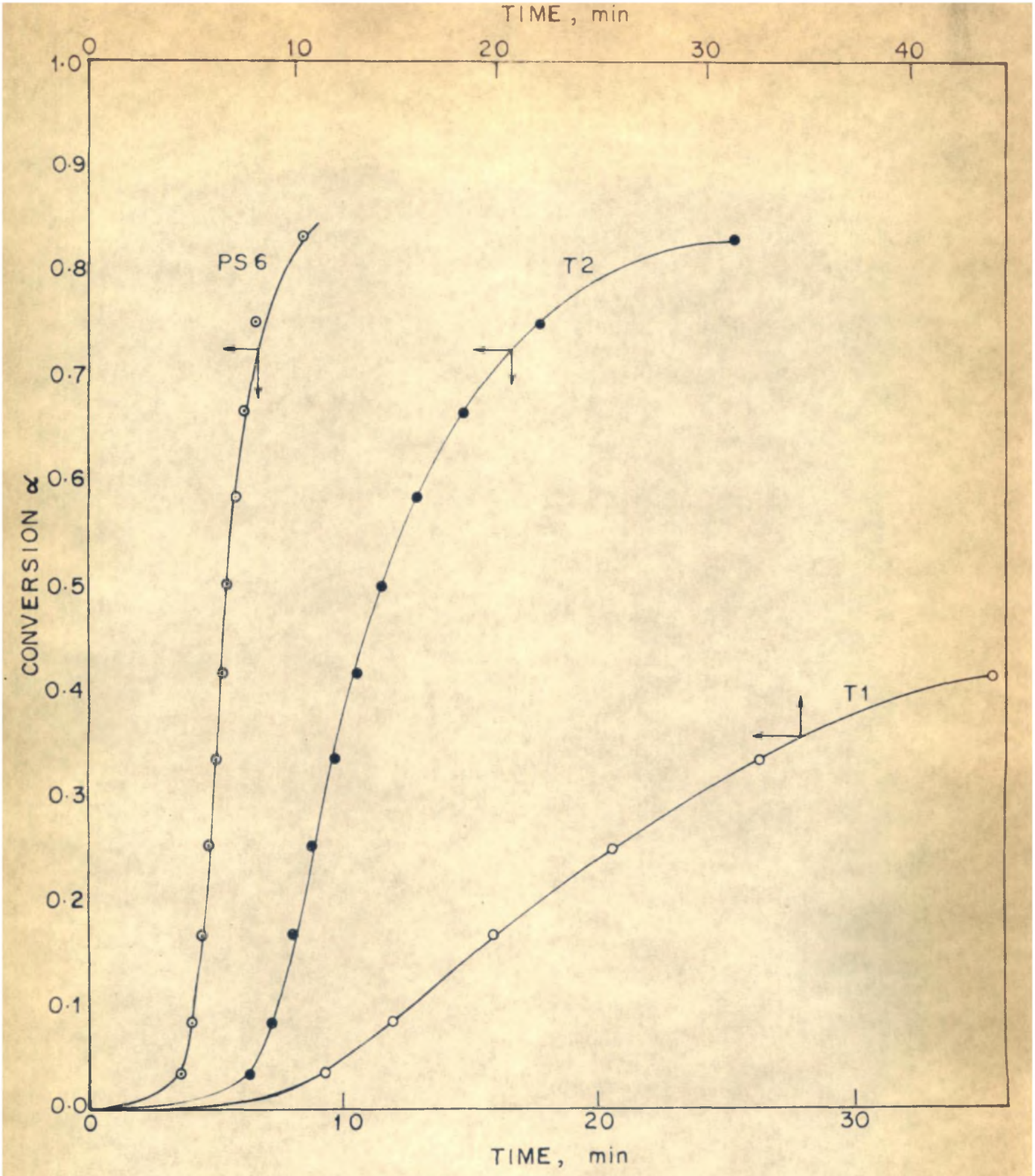

FRACTIONAL CONVERSION WITH
TIME AS A FUNCTION OF TEMPERATURE

FIGURE 6·2

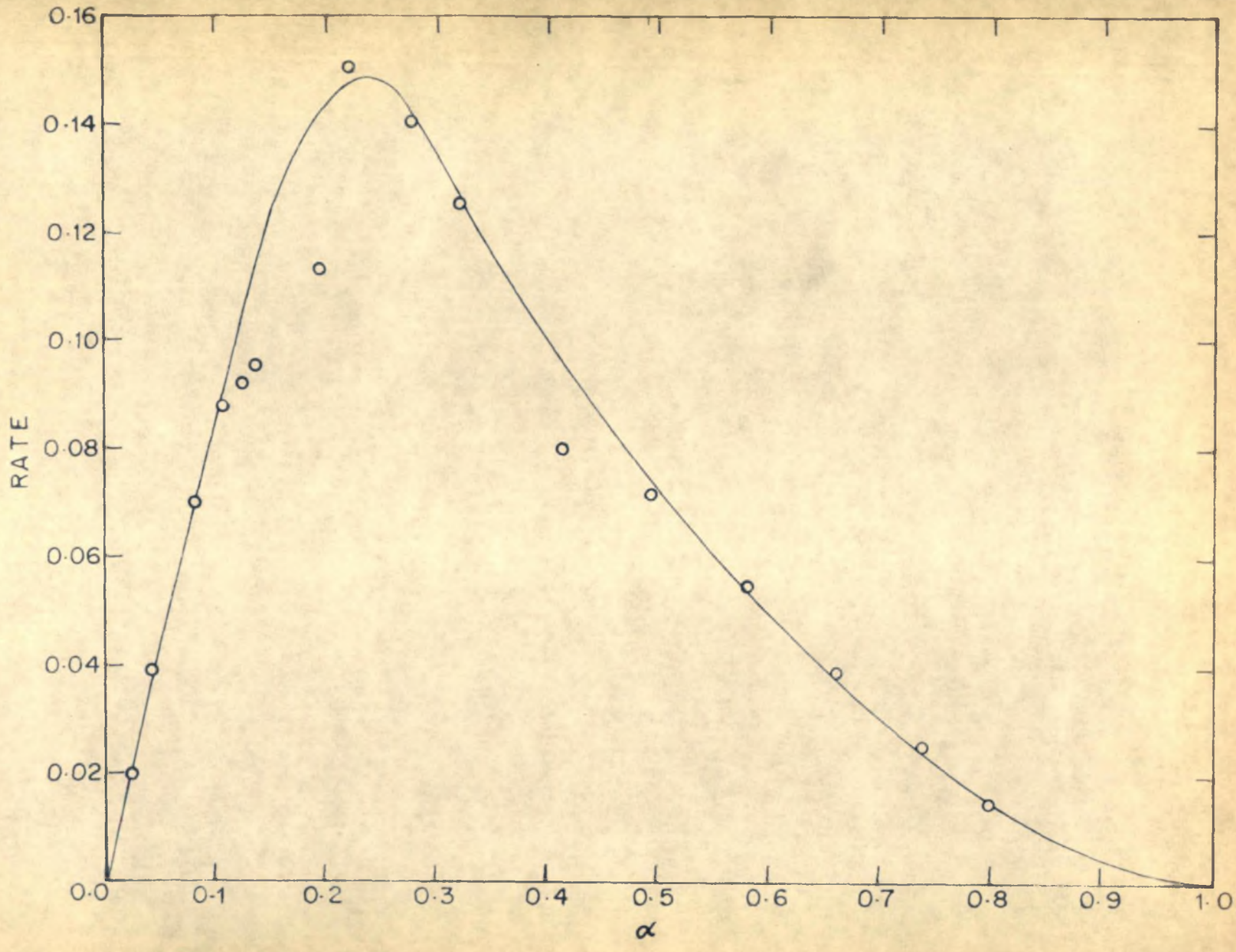

RATE AS A FUNCTION OF CONVERSION FOR RUN T 2

FIGURE 6·3

$$\frac{-dC_A}{dt} = k_o C_A + k''_{ac} C_A C_Q \qquad (6.4)$$

When expressed in terms of conversion (α) Equation 6.4 becomes

$$\frac{d\alpha}{dt} = k_o(1-\alpha) + k''_{ac} C_{Ao} \alpha(1-\alpha) \qquad (6.5)$$

Accordingly a plot of rate/$(1-\alpha)$ *vs* α should give a straight line. This method has been used by Bandrowski *et al* (1962) for NiO reduction.

We shall now develop the conversion-time relationship for the autocatalytic reaction scheme postulated above. The resulting expression can then be used to fit the data. Thus, Equation 6.5 may be rewritten in the form:

$$\frac{d\alpha}{dt} = k_o + (C_{Ao} k''_{ac} - k_o)\alpha + (-C_{Ao} k''_{ac})\alpha^2 \qquad (6.6)$$

which on integration gives

$$\ln \frac{\alpha + \hat{k}_1}{1-\alpha} = k_2(t-t_i) \qquad (6.7)$$

where $\hat{k}_1 = k_o / C_{Ao} k''_{ac}$, $k_2 = k_o + C_{Ao} k''_{ac}$, and t_i = time at which the reaction starts, called induction period.

Plots of L.H.S. of (6.7) vs t can be prepared to obtain k_2, if $\hat{k}_1$ is known independently. Determination of $\hat{k}_1$ is accomplished by considering the rate maximum, which can be obtained by writing d(rate)/dt = 0. Differentiating Equation 6.6 and equating to zero, we get

$$\frac{d(\text{rate})}{dt} = C_{Ao}k''_{ac} - k_o - 2C_{Ao}k''_{ac}\alpha_m = 0 \qquad (6.8)$$

so that

$$k_o/C_{Ao}k''_{ac} = \hat{k}_1 = (1-2\alpha_m) \qquad (6.9)$$

where α_m represents the value of α at which the maximum rate is obtained. Once $\hat{k}_1$ and k_2 are known, the rate constants k_o and k''_{ac} can be calculated using the relations:

$$k_o = \frac{\hat{k}_1 k_2}{(\hat{k}_1+1)}$$

and (6.10)

$$k''_{ac} = \frac{k_2}{C_{Ao}(\hat{k}_1+1)}$$

Equation 6.7 with $\hat{k}_1 = 0$ represents the well known Prout-Tompkin equation which is widely used for decomposition reactions and also some autocatalytic reactions.

In the light of the above development, $\hat{k}_1 = 0$ indicates $\alpha_m = 0.5$ (from Equation 6.9). However, this may not always be the case; values of α_m other than 0.5 are also possible. Bond (1962) in his studies on the reduction of CuO (which is autocatalytic) has in fact used a modified form of the Prout-Tompkin equation with $\hat{k}_1 = 0.3$ (i.e. $\alpha_m = 0.35$). The present analysis leading to Equation 6.10 provides a more general treatment of autocatalytic reactions.

Analysis of data

Preliminary experiments were carried out and operating conditions were chosen so that reaction was confined to the kinetic regime. The rate expression for homogeneous reactions derived above could therefore be used to analyse the data.

For applying the procedure outlined above $\hat{k}_1$ value should be known in each case. α_m for various runs were obtained from plots of the type shown in Figure 6.3 (for run T2) and $\hat{k}_1$ calculated using Equation 6.9. Plots of $\ln\{(\alpha+\hat{k}_1)/(1-\alpha)\}$ *vs* t were then prepared. Figure 6.4 shows such plots for the three temperatures studied, 300, 330 and 360°C. From these plots, values of k_2 were determined and then from Equation 6.10 the noncatalytic rate constant k_o and the autocatalytic rate constant k''_{ac} were calculated.

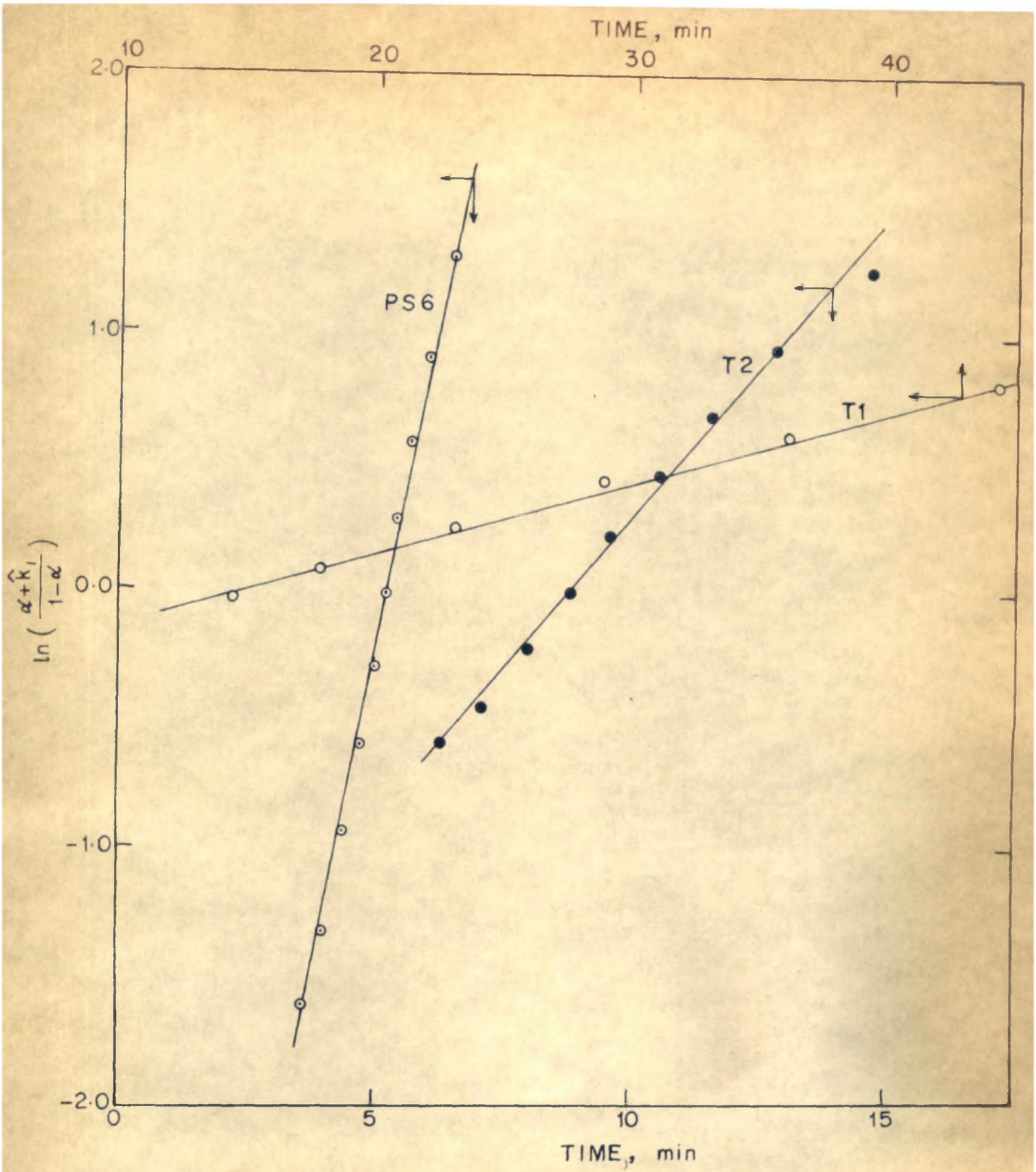

CONVERSION–TIME DATA PLOTTED ACCORDING TO EQUATION 6·7

FIGURE 6·4

The results of the calculation are presented in Table 6.2 below.

TABLE 6.2

Run	$\hat{k}_1$	k_o sec^{-1}	k''_{ac} $cm^3\ gmole^{-1}\ sec^{-1}$
T1	0.90	2.368×10^{-4}	0.175
T2	0.50	1.333×10^{-3}	1.778
PS6	0.16	2.345×10^{-3}	9.770

Arrhenius plots for the two rate constants are shown in Figure 6.5, from which the activation energies were calculated. The catalytic step VII has an activation energy (E) of 49.6 kcal/mole indicating a temperature sensitive reaction. For the noncatalytic step VI, however, the activation energy (E) is found to decrease with temperature. A change in E with temperature indicates a shift in the controlling mechanism of reaction: a drop in E is attributed to a shift in controlling mechanism from one to the other of the successive elementary steps (Levenspiel, 1974). The present reaction being a consecutive reaction as shown by scheme V, such a shift in controlling mechanism is possible. Also, in this reaction decomposition

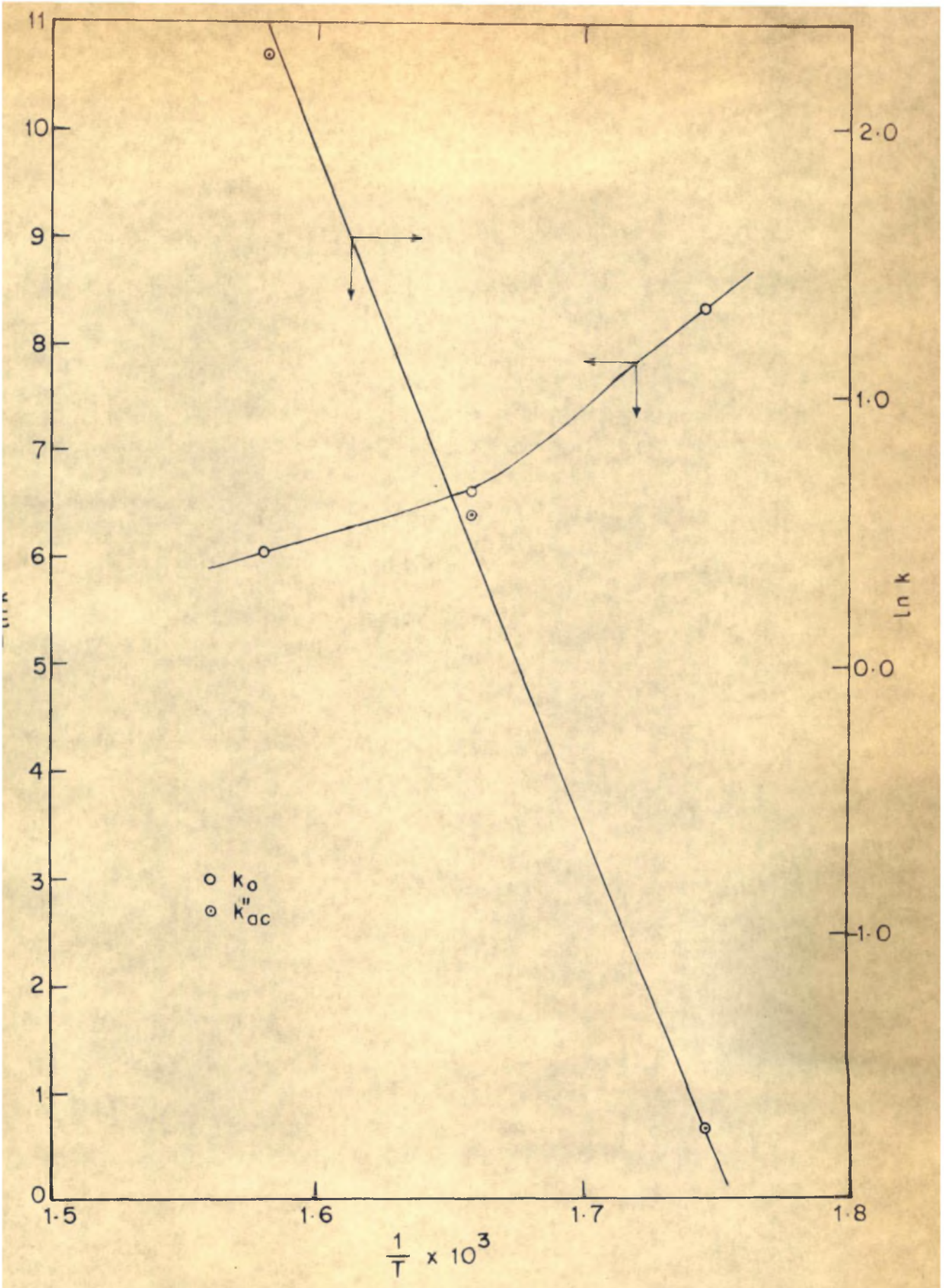

ARRHENIUS PLOT FOR THE RATE CONSTANTS k_o AND k''_{ac} FOR THE RUNS T1, T2 AND PS6

FIGURE 6·5

or polarisation (and hence activation) of CuCl may be involved as an elementary step, whose rate may be controlling at lower temperatures. Consequent shift in controlling mechanism may be from this step to the next in which this activated CuCl reacts with silicon. However, no firm conclusion can be drawn due to lack of data on decomposition of CuCl for comparison.

6.3.2 Effect of other parameters

In the course of the study some observations were made regarding certain operating parameters such as particle size, reactant ratio and additives on the reaction. Such studies also helped in determining operating regimes. A qualitative description of these is given below.

Particle size

Variation of particle size of ferrosilicon is not expected to have any effect on the intrinsic rate constants k_o and k''_{ac}. $\hat{k}_1$ ($=k_o/C_{Ao}k''_{ac}$) was in fact found to be the same for reaction with various particle sizes of ferrosilicon. When the corresponding data were plotted according to Equation 6.7 the slope was found to increase in general with decreasing particle size; however, the variation was irregular. The reason for this can be sought in the degree

of mixing initially achieved, which is less for coarser particles of ferrosilicon. Therefore, for all the other runs, a size range was chosen such that $\hat{k}_1$ and k_2 are unaffected. Thus, -300 mesh particles were used.

Reactant ratio

The reactant ratio was varied by changing the cuprous chloride percentage, while the weight of ferrosilicon was kept constant (resulting in a variation of C_{Ao}). This would change $\hat{k}_1$ and k_2, but the rate constants k_o and k''_{ac} would remain unaffected. Thus, using the values of k_o and k''_{ac} obtained for run T2, α_m and k_2 were predicted. The predicted values were found to match well (to within 10%) with the actual values (see Table 6.3).

TABLE 6.3

Run	α_m predicted	α_m actual	k_2 (sec^{-1}) predicted	k_2 (sec^{-1}) actual
R2	0.125	0.125	0.0031	0.00275
R3	0.3125	0.33	0.0048	0.0042

In plotting the data according to Equation 6.7 for runs with 0.3 g CuCl it was noticed that for $\alpha > 0.8$ the

data points deviated significantly. This is considered to be due to a diffusional resistance offered by the product (copper) which covers the ferrosilicon particles, and thereby renders contact between the reactants impossible. This was supported by the results obtained with higher percentages of CuCl, wherein such deviations appeared at conversions corresponding to the same weight of copper formed (other conditions remaining the same).

Additives

Results of the experiment with 99.9% pure silicon were identical with those obtained with ferrosilicon under identical conditions. This confirmed that the iron present in ferrosilicon had no bad effects on the present reaction.

Addition of small quantities of zinc was found to modify the kinetics at lower temperatures; the same at higher temperatures had adverse effects. This will be evident from a comparison of the values of k_o and k''_{ac} given in Table 6.4 below with those in Table 6.2.

TABLE 6.4

Expt. No.	$\hat{k}_1$	k_o (sec^{-1})	k''_{ac} (cm^3 $gmole^{-1}$ sec^{-1})
A1	0.75	6.428×10^{-4}	0.5714
A2	0.6	1.999×10^{-3}	2.2208
A3	0.57	2.966×10^{-3}	3.4692

No explanation can be given for this apparent anomaly.

Acceleration of rates due to addition of small quantities of other catalysts has been observed in earlier studies on autocatalytic reactions. Thus, in the reduction of CuO by H_2, addition of Ni and Pt (well known reduction catalysts) was found to increase the rates (Delmon, 1972).

Addition of 1 mg of antimony along with 4 mg of zinc to the reaction mixture lowered the rates indicating an inhibitory effect. Voorhoeve (1967) has in fact reported that the quantity of antimony is critical: up to a certain optimum quantity it acts as a promoter, but beyond that it acts as an inhibitor.

In view of the above results it appears that promoters are added to accelerate the catalyst preparation

step rather than the main reaction resulting in chlorosilanes. However, more detailed studies on the main reaction are needed before drawing any firm conclusions.

Commercial fine copper powder when added to the reaction mixture, had no effect on the rate of reaction, while copper formed in the reaction when added, significantly increased the rate. Similar results were obtained by Bond (1962) in his studies on the reduction of CuO by H_2.